Astrofizyka cząstek

prof. dr hab. A.F.Żarnecki
Zakład Cząstek i Oddziaływań Fundamentalnych IFD

Wykład VIII

- promieniowanie kosmiczne: przypomnienie
- kaskady atmosferyczne
- eksperymenty naziemne, Pierre Auger Observatory
- wybrane wyniki

Spectrum and origin of CRs

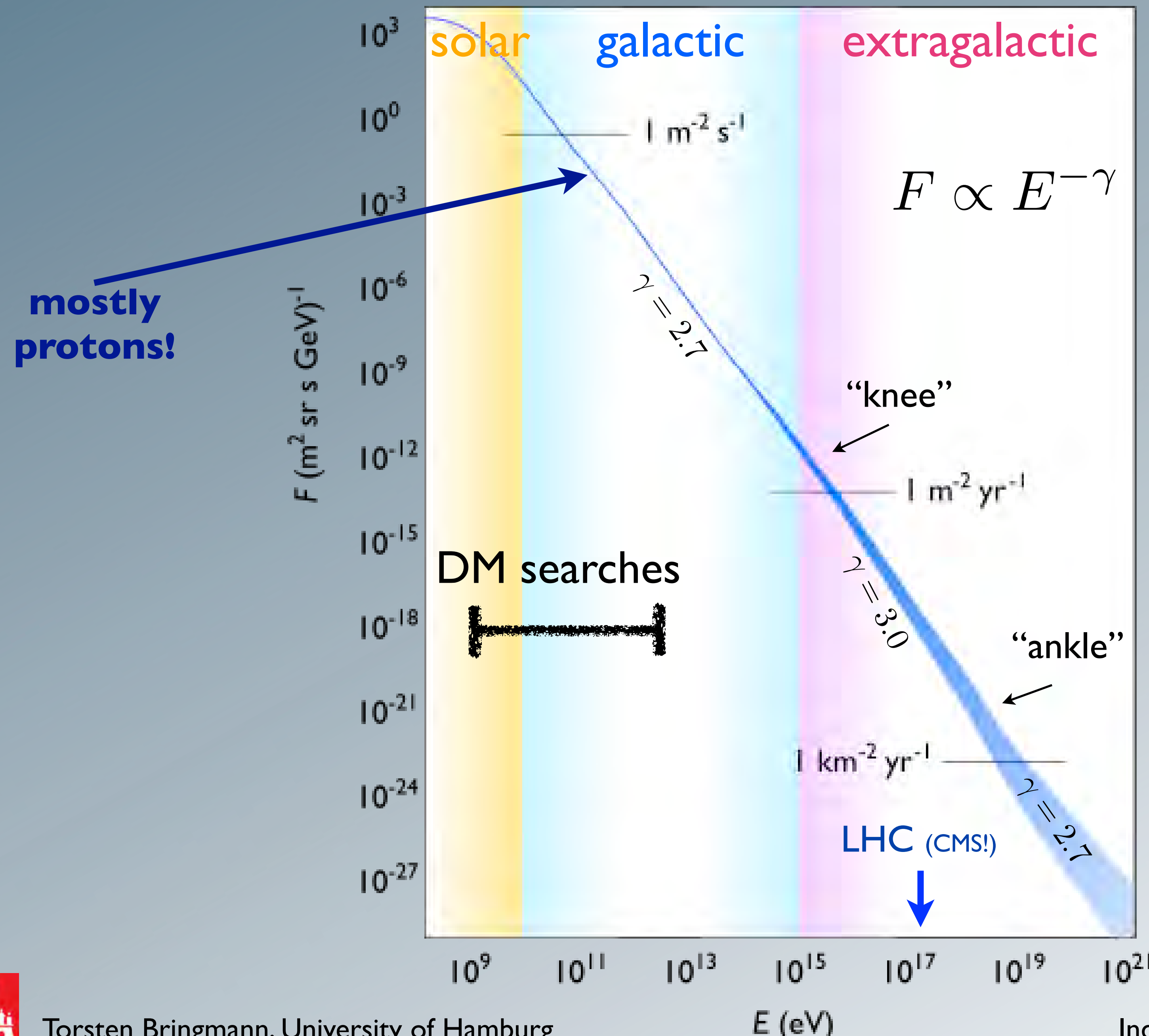

Summarizing:

SNRs are good candidate sources for CRs because:

- they can provide the right amount of energy in form of CRs (if **~10% efficiency**)
- they inject CRs in the ISM with (roughly) the spectrum needed to explain CR observations (**~ $E^{-2.1...2.4}$**)
- they can accelerate CRs (at least) up to the energy of the CR knee (**~5 x 10^{15} eV**)

CR energy balance

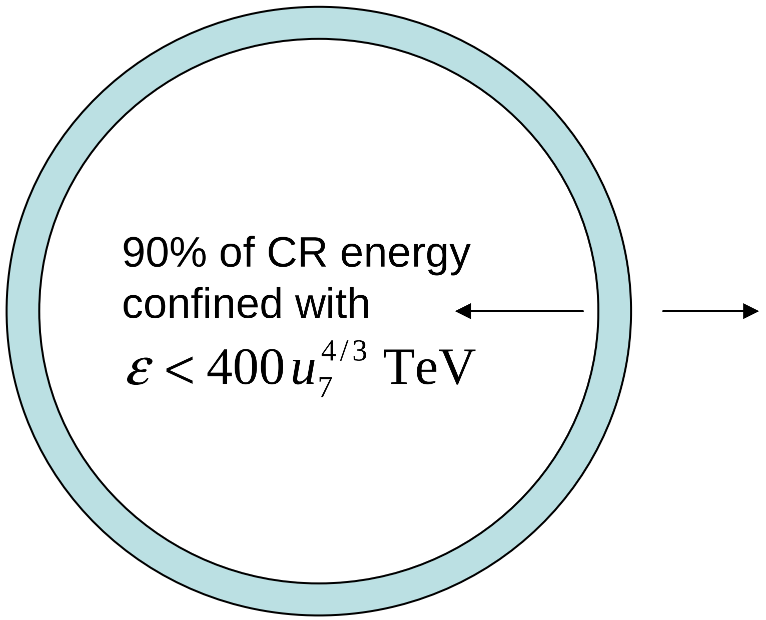

10% of CR energy escapes with $\varepsilon_{escape} \approx 400\, u_7^{4/3}$ TeV

Low energy CR cool adiabatically as SNR expands

Energy drives blast wave

Given to new generation of CR

Source of $\ln(\varepsilon_{max}/\varepsilon_{min})$

$$E_{total} = 0.05 \ln\left(\frac{\varepsilon_{max}}{\varepsilon_{min}}\right)\left(\frac{4\pi R_0^3}{3}\right)\rho_0 u_0^2$$

Energy spectrum of escaping CR

Integrate over Sedov lifetime

$$N(\varepsilon) = \frac{2\pi\rho_0 R_0^3 u_0^2 \eta}{e\varepsilon_0^2}\left(\frac{\varepsilon}{\varepsilon_0}\right)^{-2}$$

Same as test particle spectrum

Follows from Sedov: $R \propto t^{2/5}$

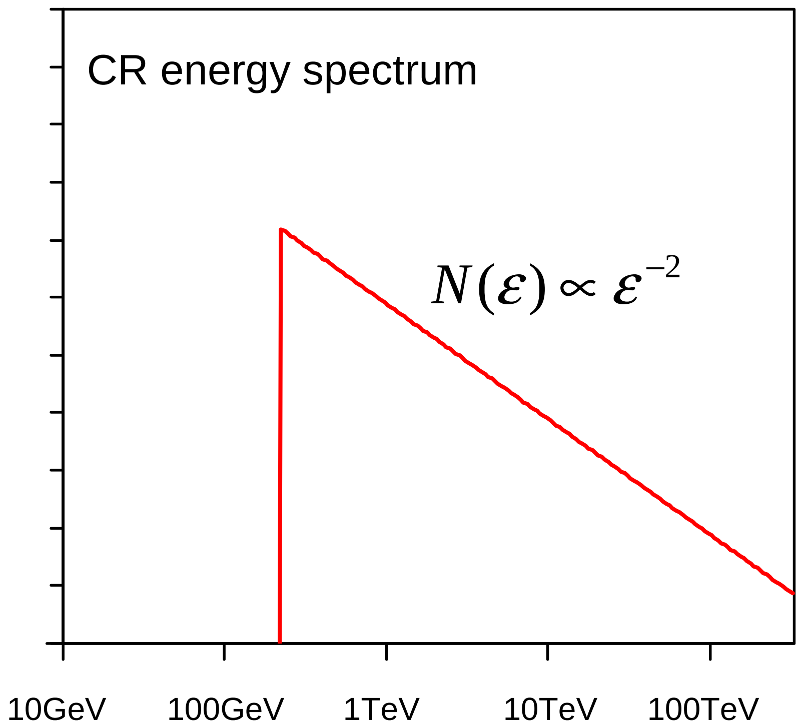

What about CR in SNR interior?

Sedov SNR as 'CR bubble' (Chevalier 1983)

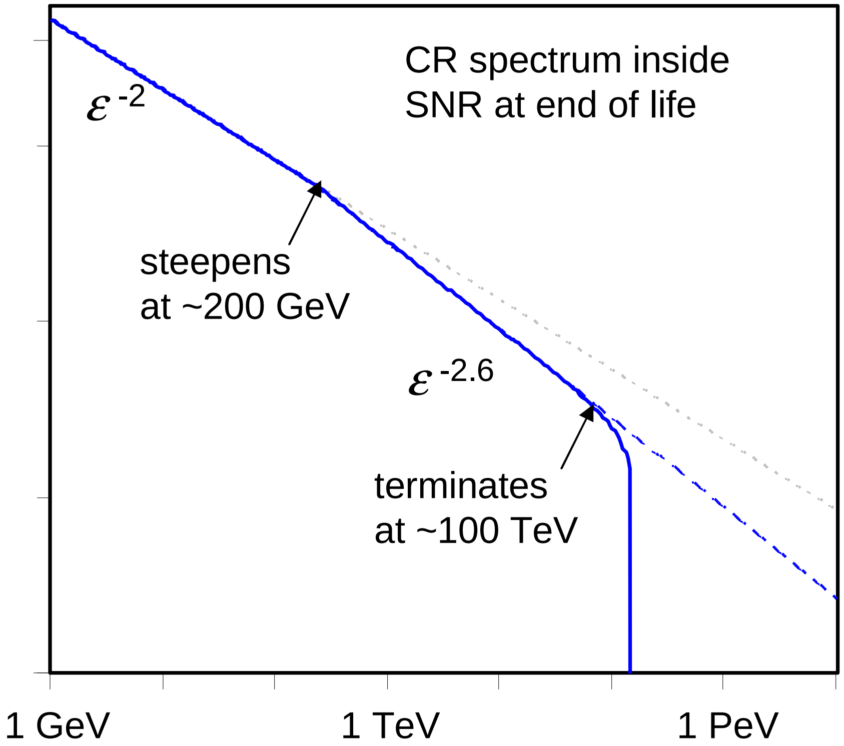

CR initially accelerated to 1 PeV
cool adiabatically to ~100 TeV

Cygnus Loop

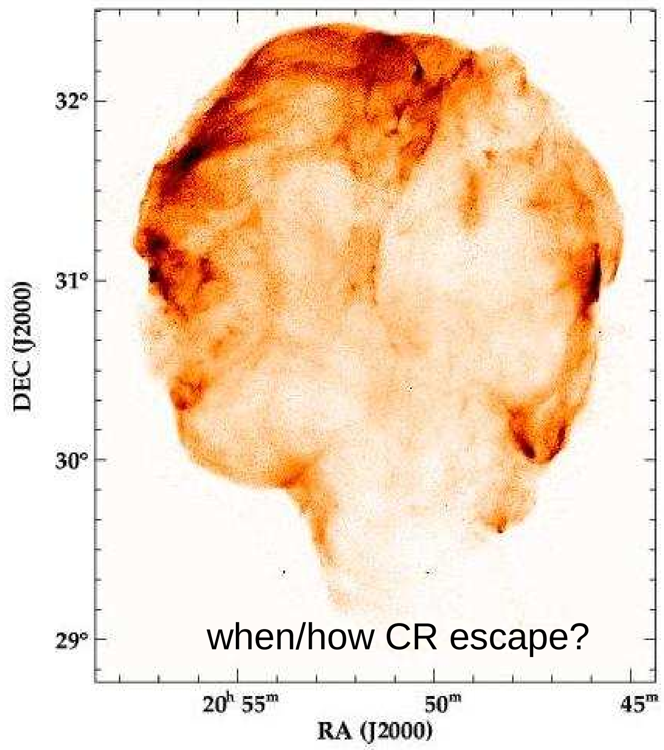

ROSAT HRI, *Credit:*
N. Levenson (Johns Hopkins), S. Snowden (USRA/GSFC)

http://heasarc.gsfc.nasa.gov/docs/objects/heapow/archive/nebulae/snr_cygl_comp.html

Two CR escape routes

? Spectral join correlate with the PAMELA feature at 200GeV ?

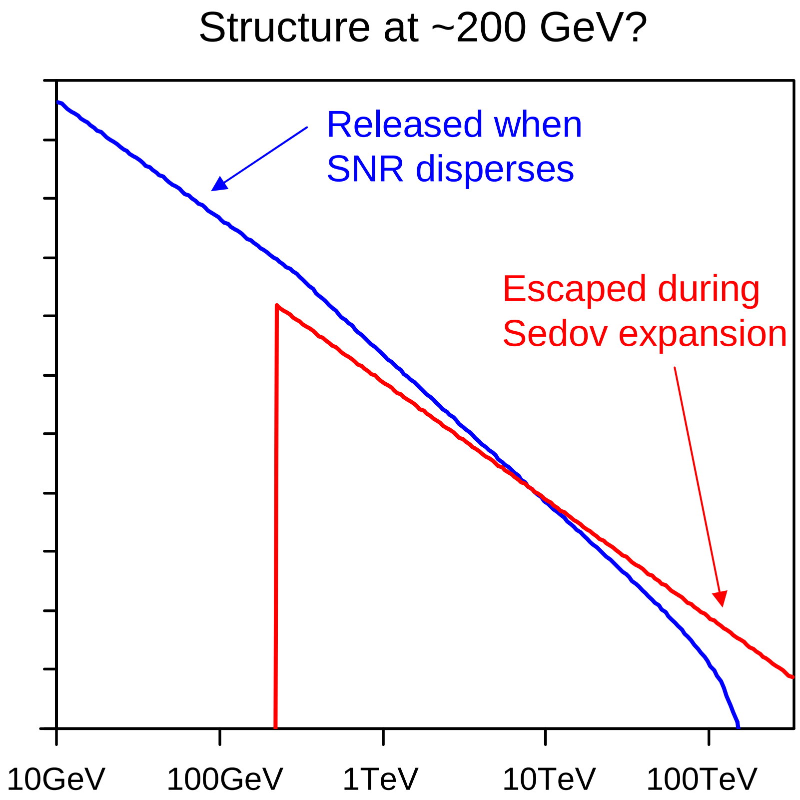

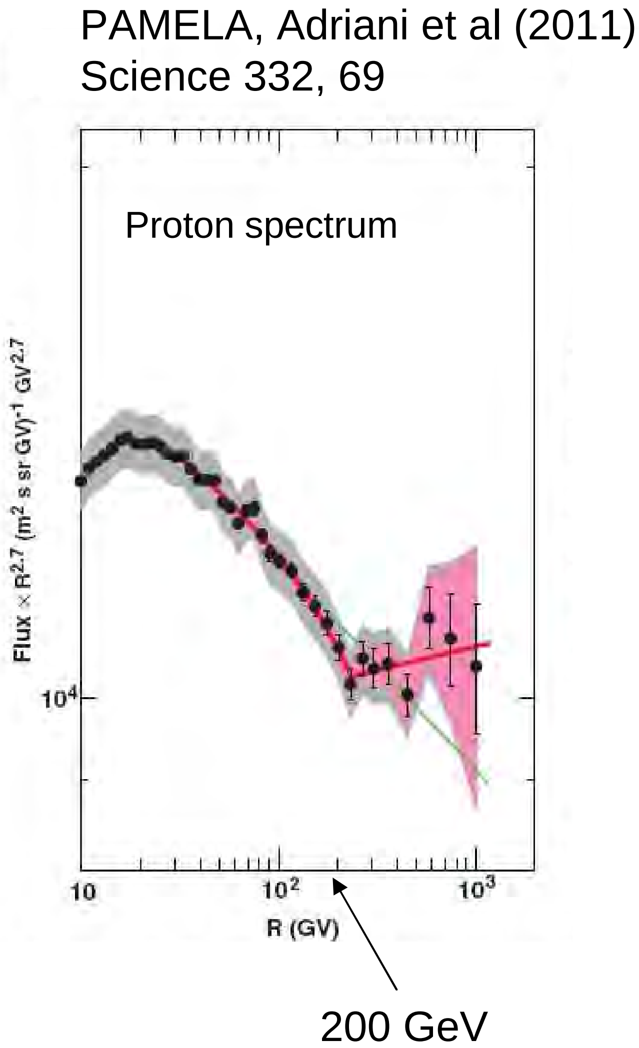

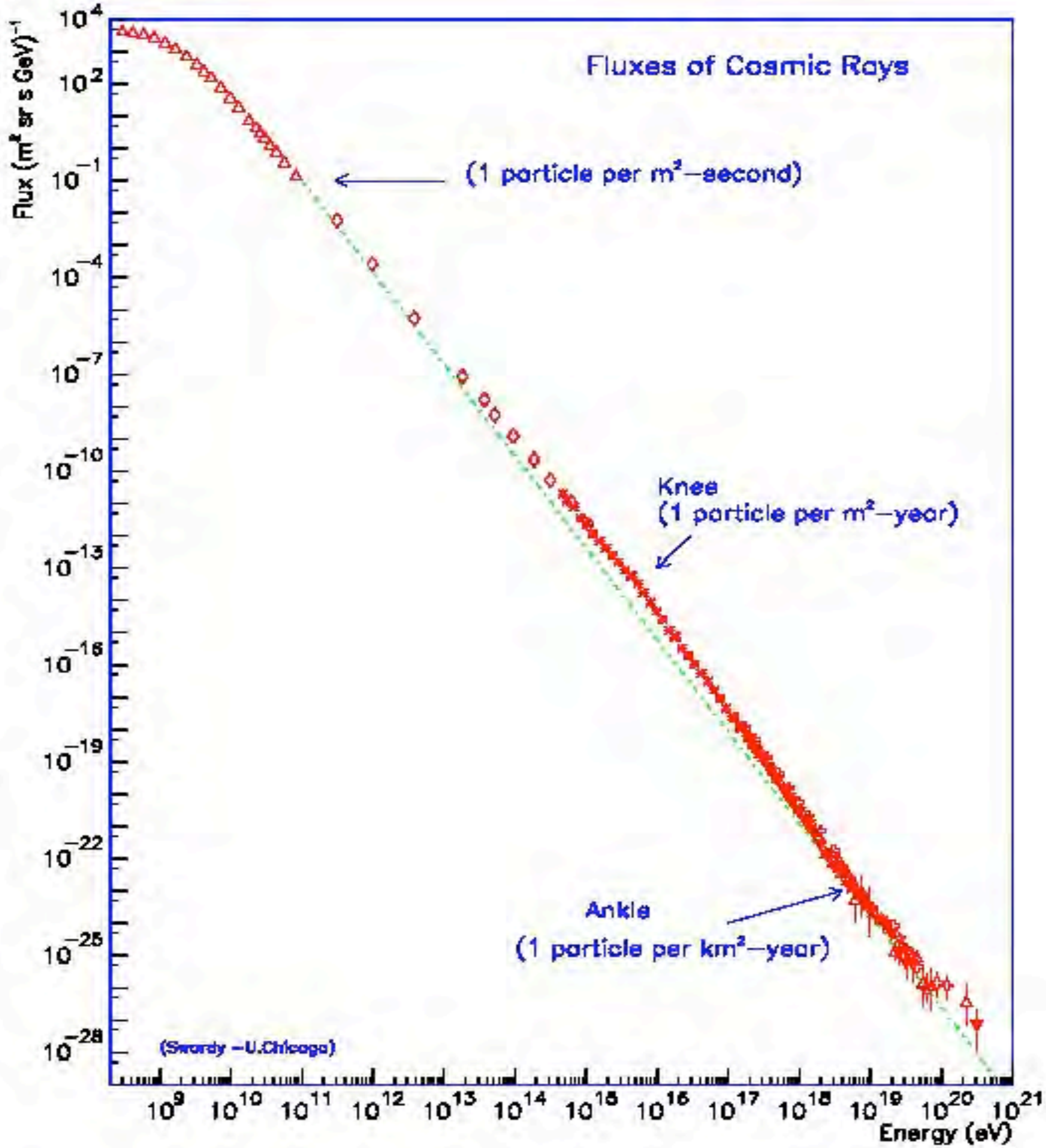

Fluxes of Cosmic Rays
(1 particle per m²–second)
Knee
(1 particle per m²–year)
Ankle
(1 particle per km²–year)
(Swordy – U.Chicago)
Flux (m² sr s GeV)⁻¹
Energy (eV)

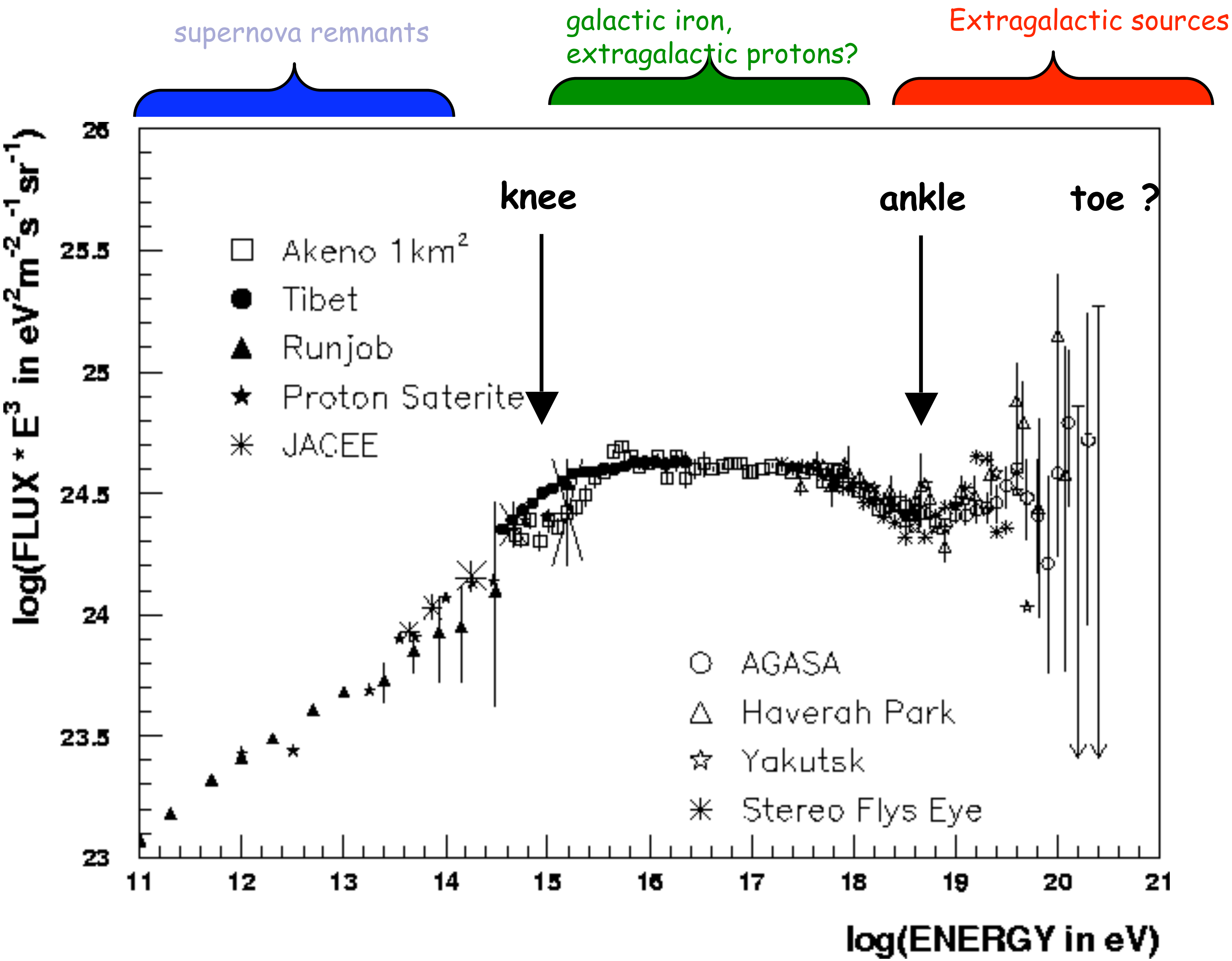
supernova remnants
galactic iron,
extragalactic protons?
Extragalactic sources
knee
ankle
toe ?
Akeno 1km²
Tibet
Runjob
Proton Saterite
JACEE
AGASA
Haverah Park
Yakutsk
Stereo Flys Eye
log(FLUX * E³ in eV²m⁻²s⁻¹sr⁻¹)
26
25.5
25
24.5
24
23.5
23
11
12
13
14
15
16
17
18
19
20
21
log(ENERGY in eV)

The Highest Energy Cosmic Rays

Events above 10^20 eV may have been detected

- Acceleration mechanism ???
- GZK cutoff ??? (Greisen Zatsepin Kuzmin 1966)
  Protons: pion photo-production for $E > 5 \times 10^{19}$ eV
  Limits distance to < 50-100 Mpc.
  Nuclei: photo-disintegration with infrared background
  Photons: e+e- pair production with radio background
- No apparent sources (arrival directions)

The Greisen-Zatsepin-Kuzmin (GZK) effect

Nucleons can produce pions on the cosmic microwave background

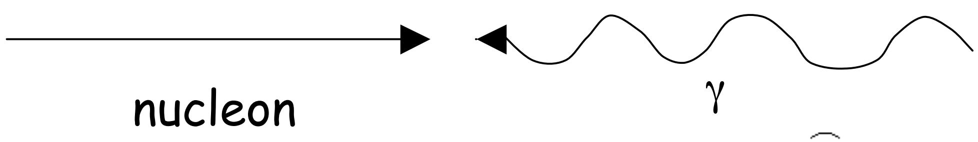

$$E_{th} = \frac{2m_N m_\pi + m_\pi^{\ 2}}{4\varepsilon} \approx 4 \cdot 10^{19}\,\mathrm{eV}$$

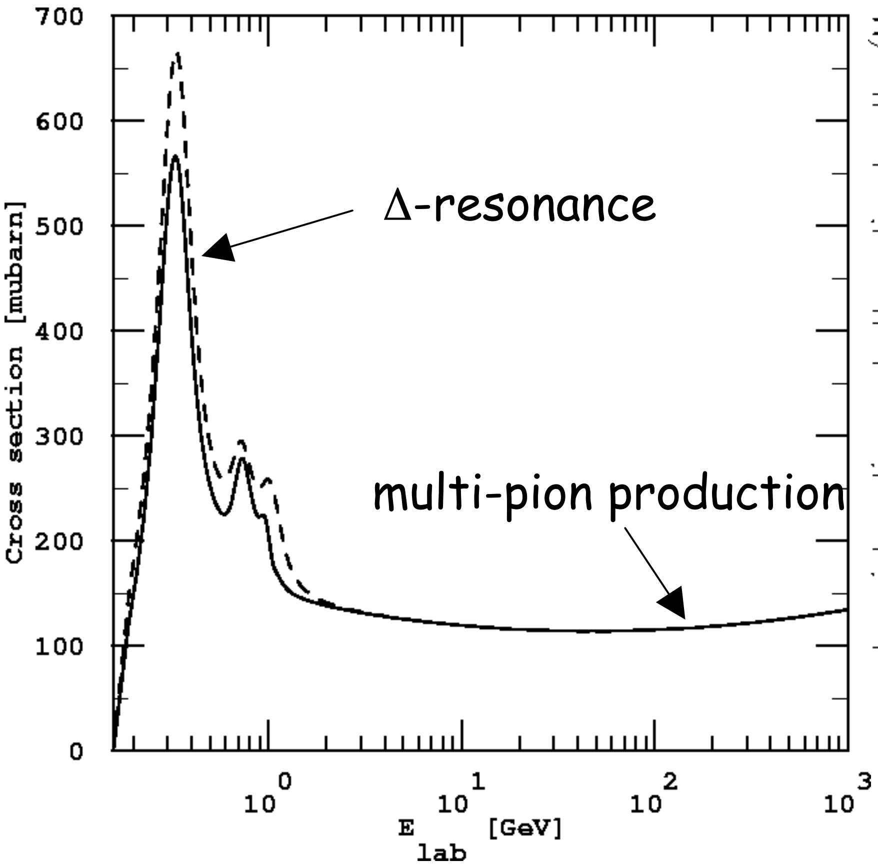

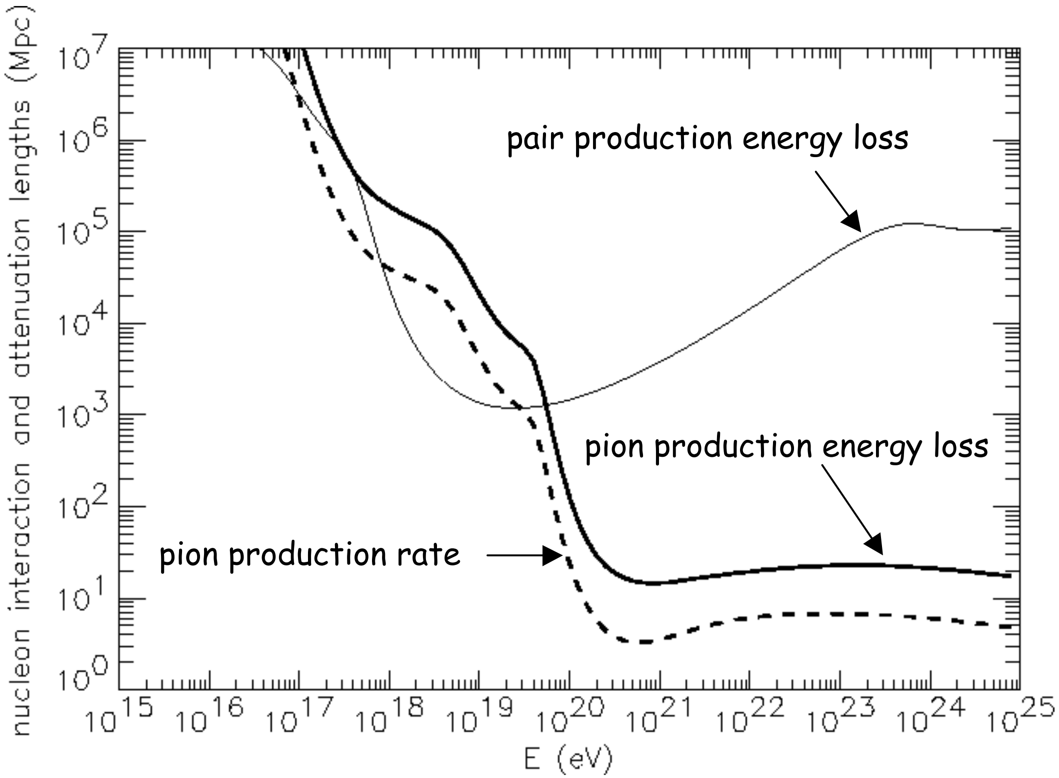

⇒sources must be in cosmological backyard within 50-100 Mpc from Earth
(compare to the Universe size ~ 5000 Mpc)

Same true for heavy nuclei: Fe

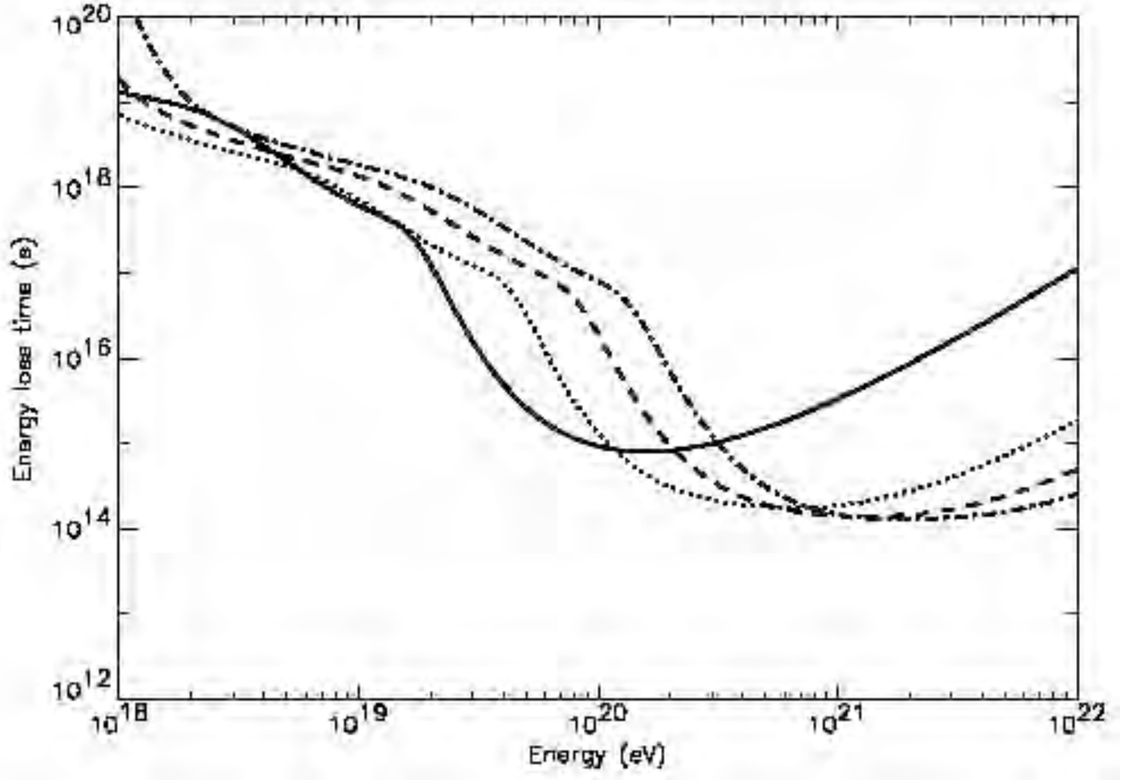

Simulation by D.Allard

Extragalactic UHECRs

- Protons, nuclei and photons lose energy in intergalactic space due to interactions with the CMB

Problem with propagation

sources < 50 Mpc

Proton energy vs. distance
(J. Cronin)

Auger Project: GZK

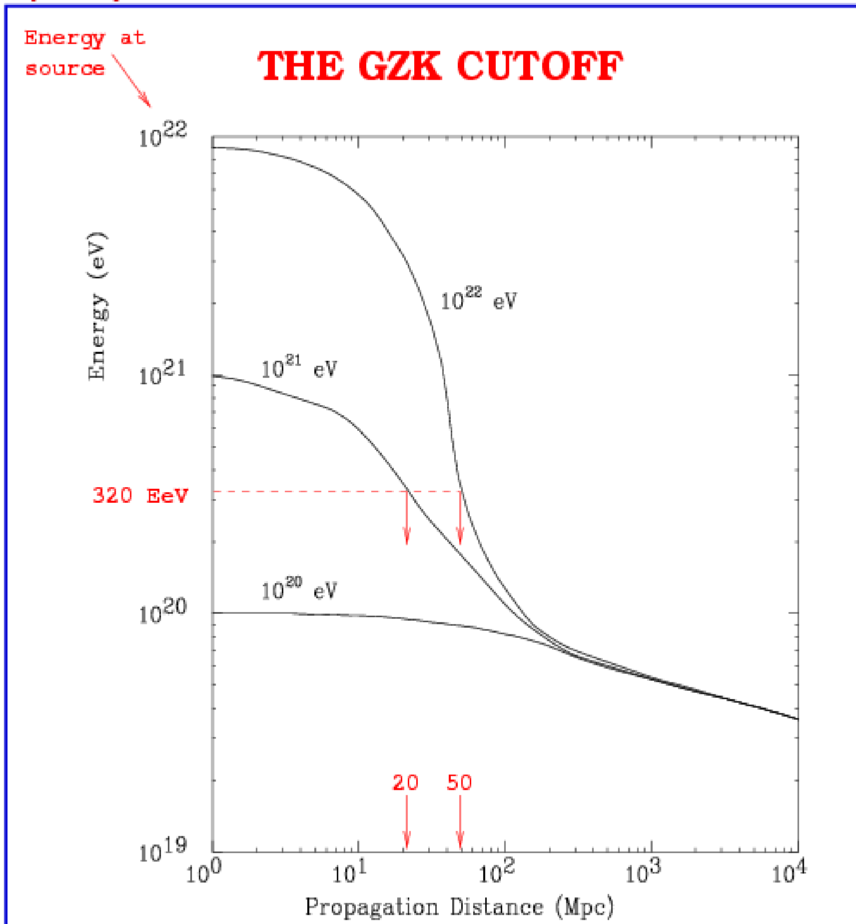

Energy attenuation of protons

Protons: photopion threshold @ ~50 EeV

Photons: pair production threshold @ ~200 TeV

Nuclei: photodisintegration above 50 EeV

Neutrinos: no problem!

For E>100 EeV, the source must be within ~50 Mpc

UHECR propagation in Milky Way

- Deflection angle ~ 1-2 degrees at 10^{20}eV for protons
  - Astronomy by hadronic particles?

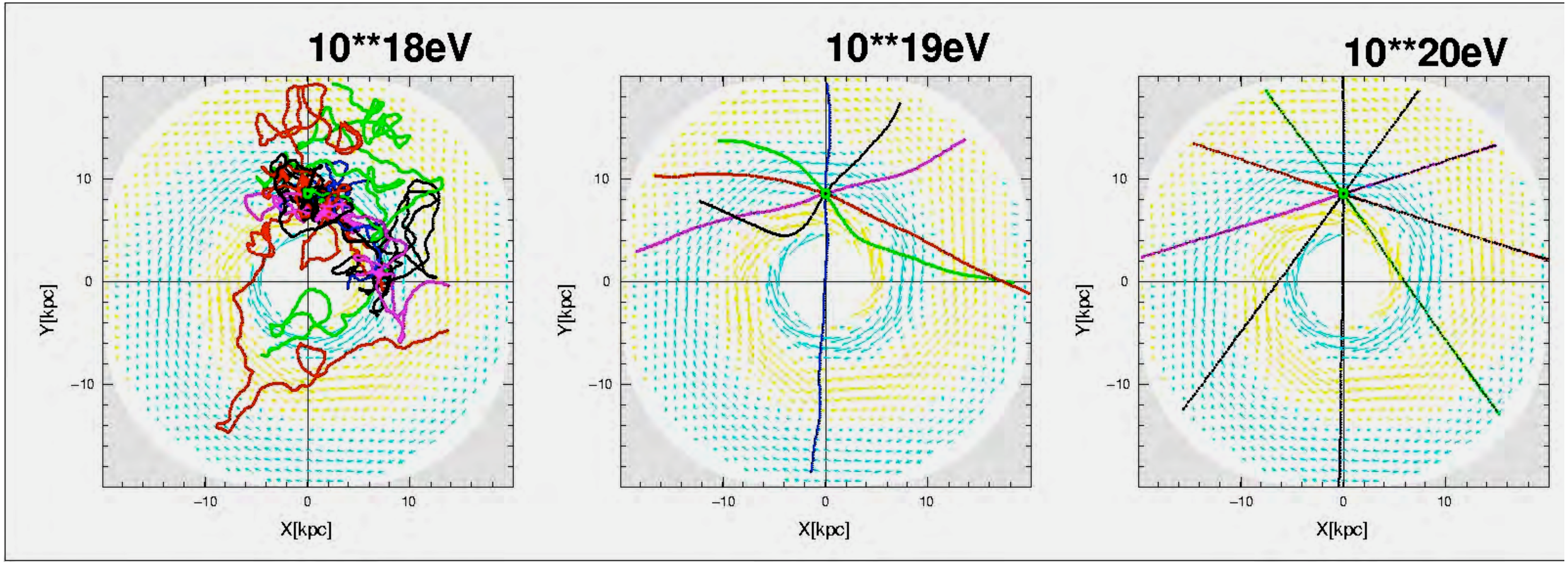

...WHOSE LOCATION IS DICTATED BY THE CR FLUX

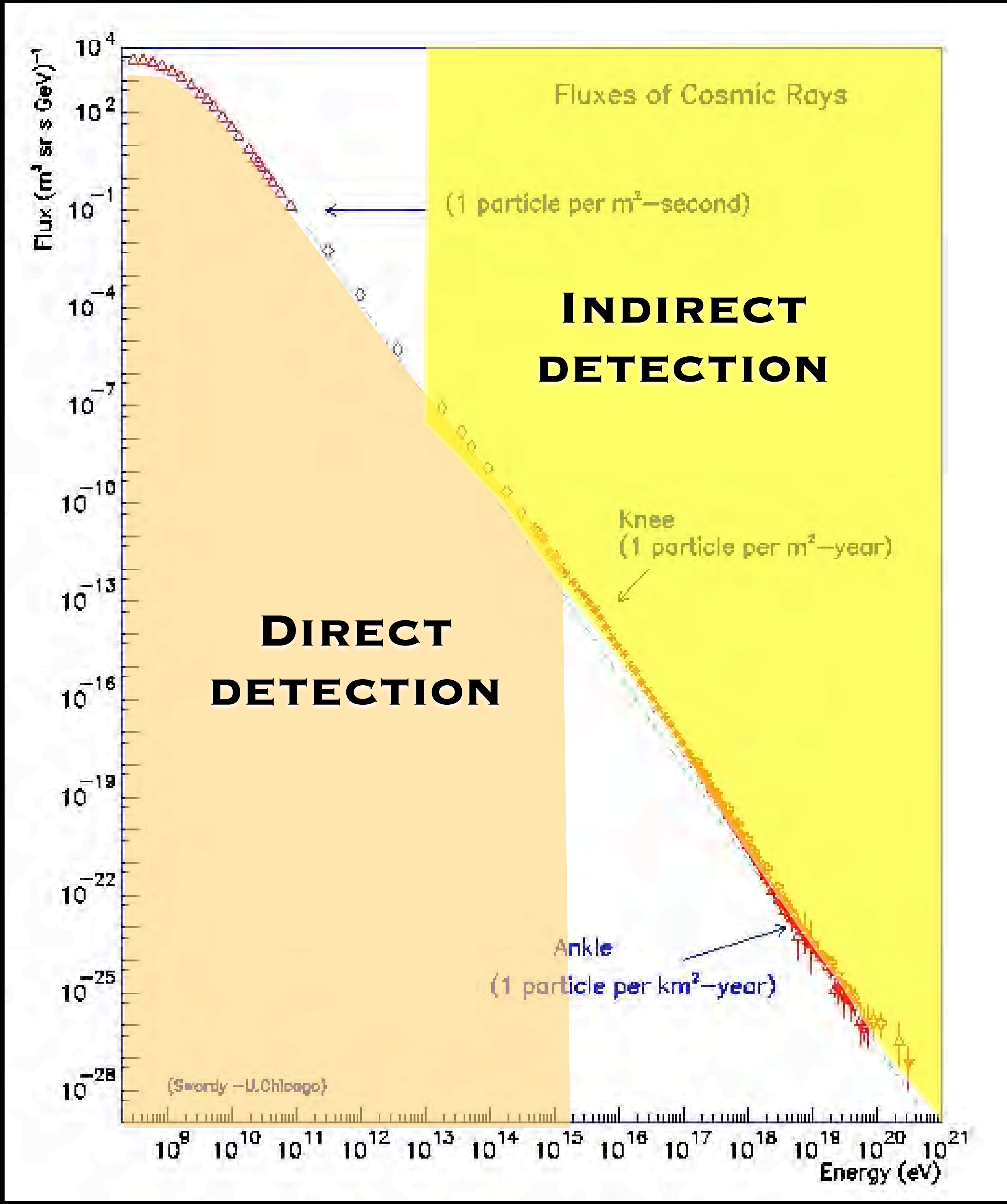

Low-energy CRs: rather high flux (1/ m^2 s) but absorbed in the upper atmosphere.
Direct detection (top of the atmosphere or in space)

Balloons
Rockets
Satellites

High energy cosmic rays: very rare (1/km^2 y), but "penetrating" up to ground (atmospheric air-showers).
Indirect detection: long-lived large arrays (ground level)

Large telescopes
Extensive Air showers arrays

HOW DO WE DETECT RARE HIGH-ENERGY COSMIC RAYS?

As usual, a few steps back in time...

At the beginning of 1930s, Rossi already suspected the production of secondary particles by cosmic rays in matter, and saw the first hints of atmospheric showers

Rossi placed three G-M counters in a triangular array. The three counters could not be discharged by a single particle travelling in straight line. Yet, even when completely surrounded by lead the array recorded coincidences. The coincidence rate fell ALMOST to zero when the upper lead was removed. The coincidences could only have been the result of two or more ionizing particles emerging simultaneously from the lead. Coincidences were present also without lead: it later turned out that this effect was due to the production of secondary CRs in atmosphere

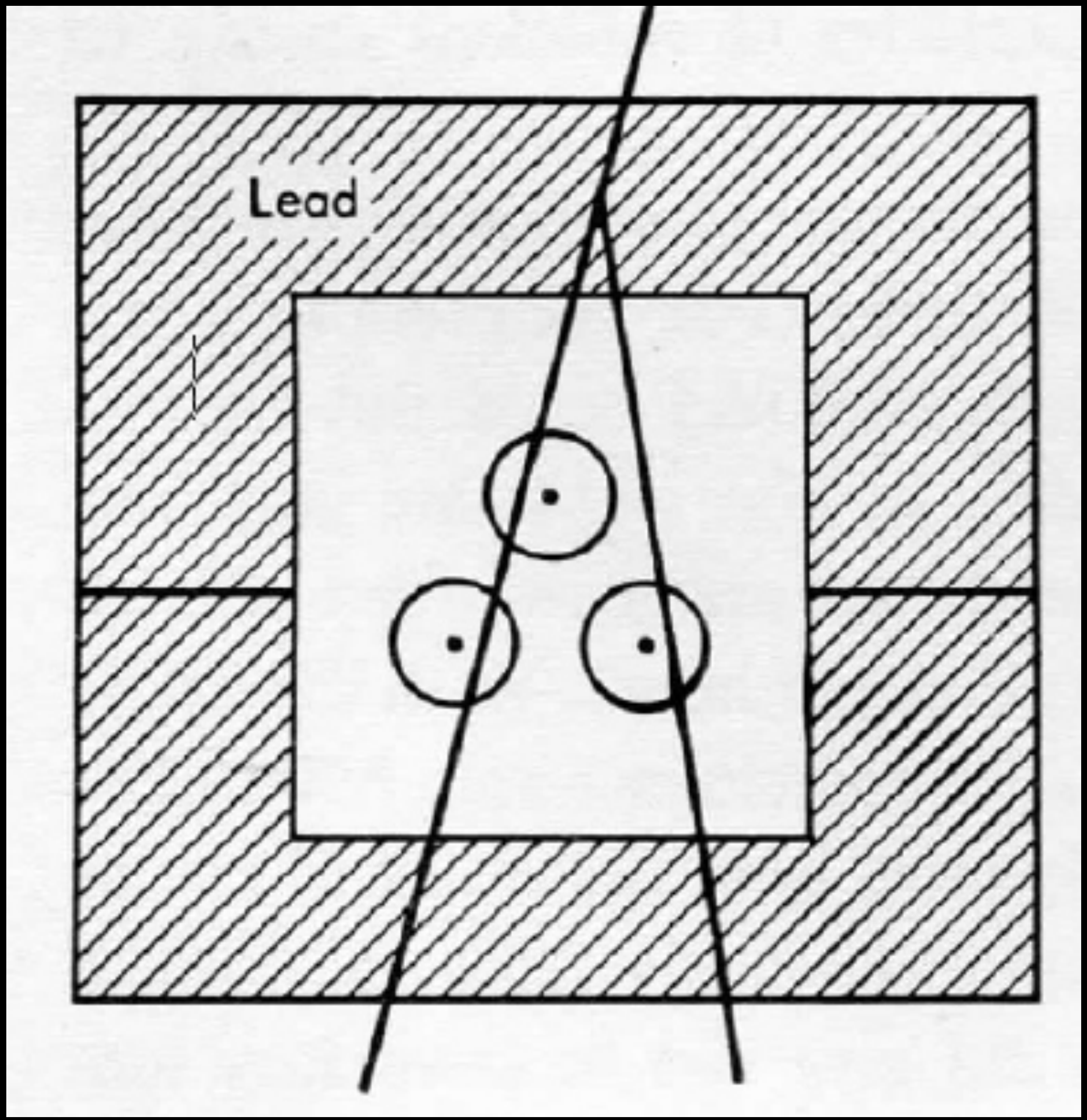

Pierre Auger

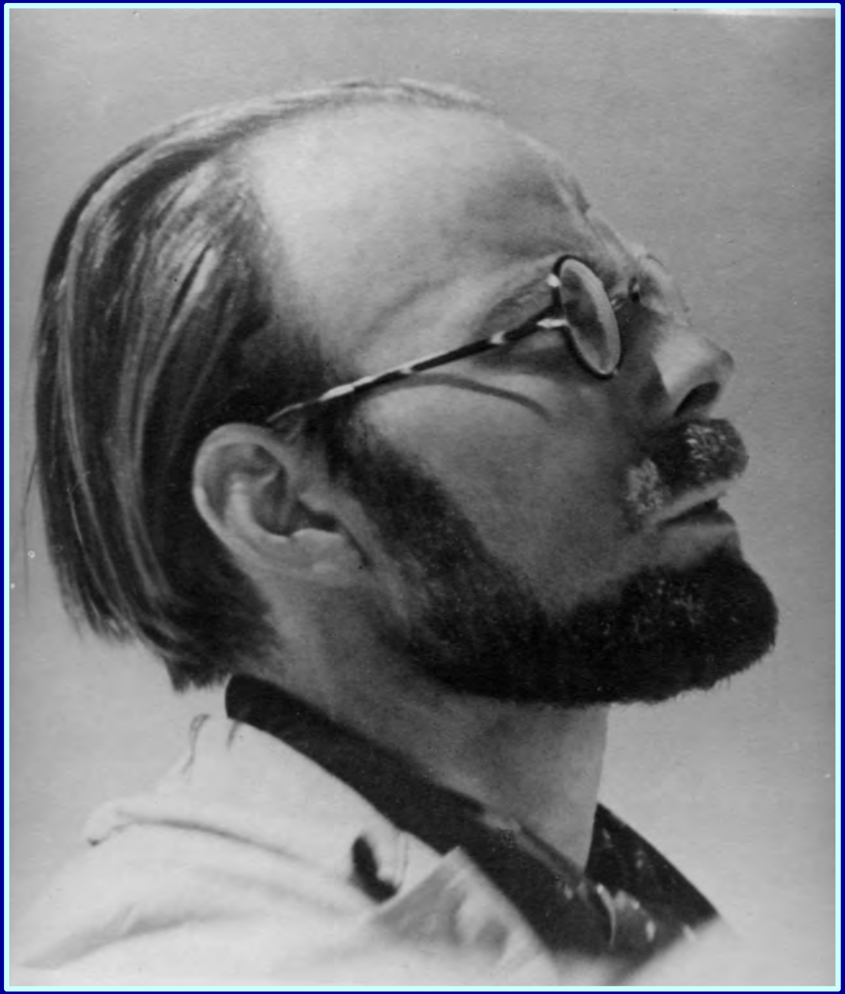

In the 1930s, the French physicist Pierre Auger (1899-1993) devoted his research activities to cosmic rays with arrangements of Geiger counter in coincidence installed in the Curie Institute in Paris.

Involving very efficient electronic circuits for the time, the array of Geiger counters developed by Auger could be deployed on more than 100 m along the roofs of the buildings of the Curie street.

Discovery of the extensive air showers

Auger, Maze (1938), C. R. Académie des Sciences, vol. 206, p. 1721.

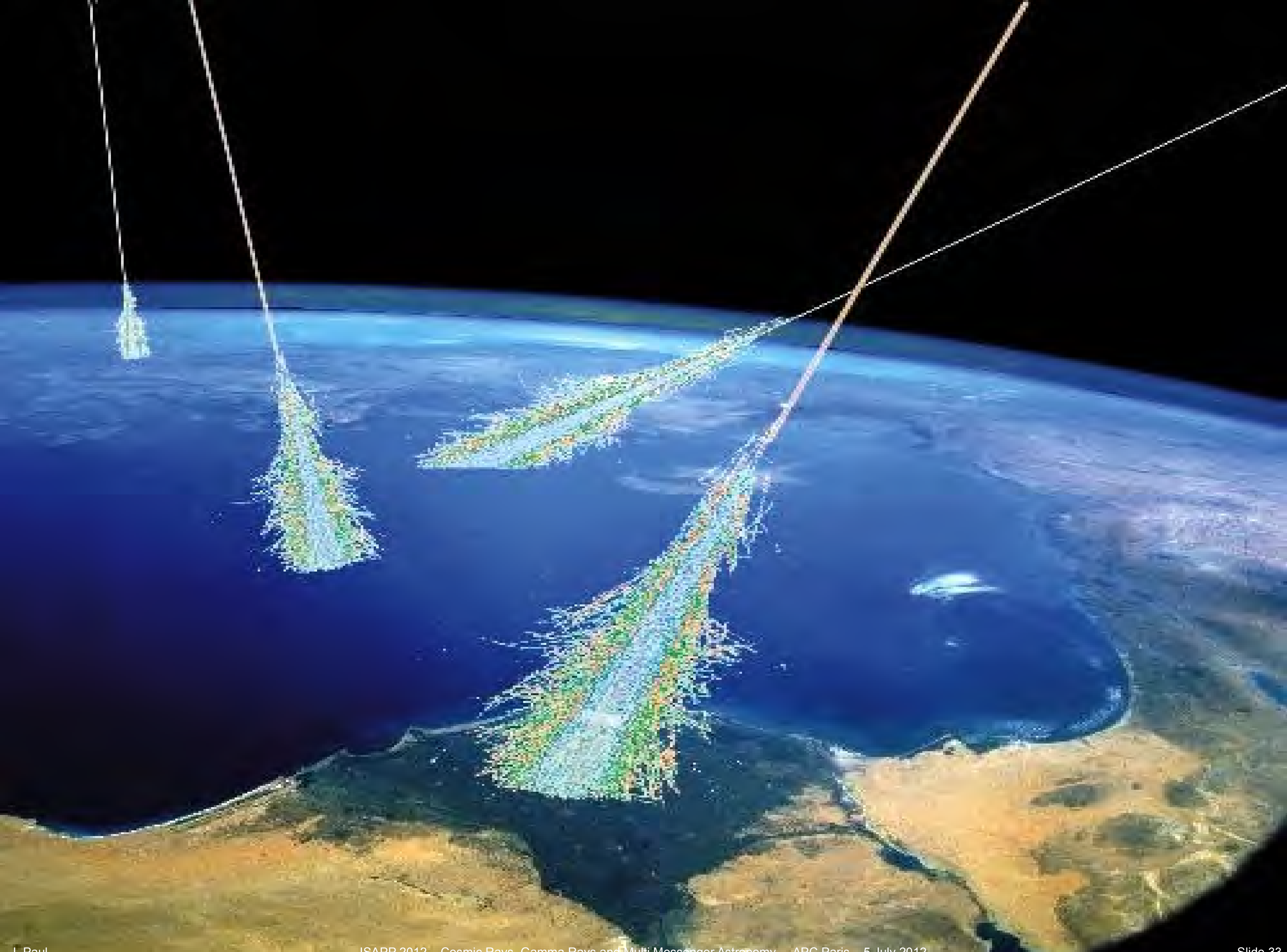

EXTENSIVE AIR SHOWERS

A high energy primary particle, upon entering the atmosphere, initiates a chain of nuclear interactions

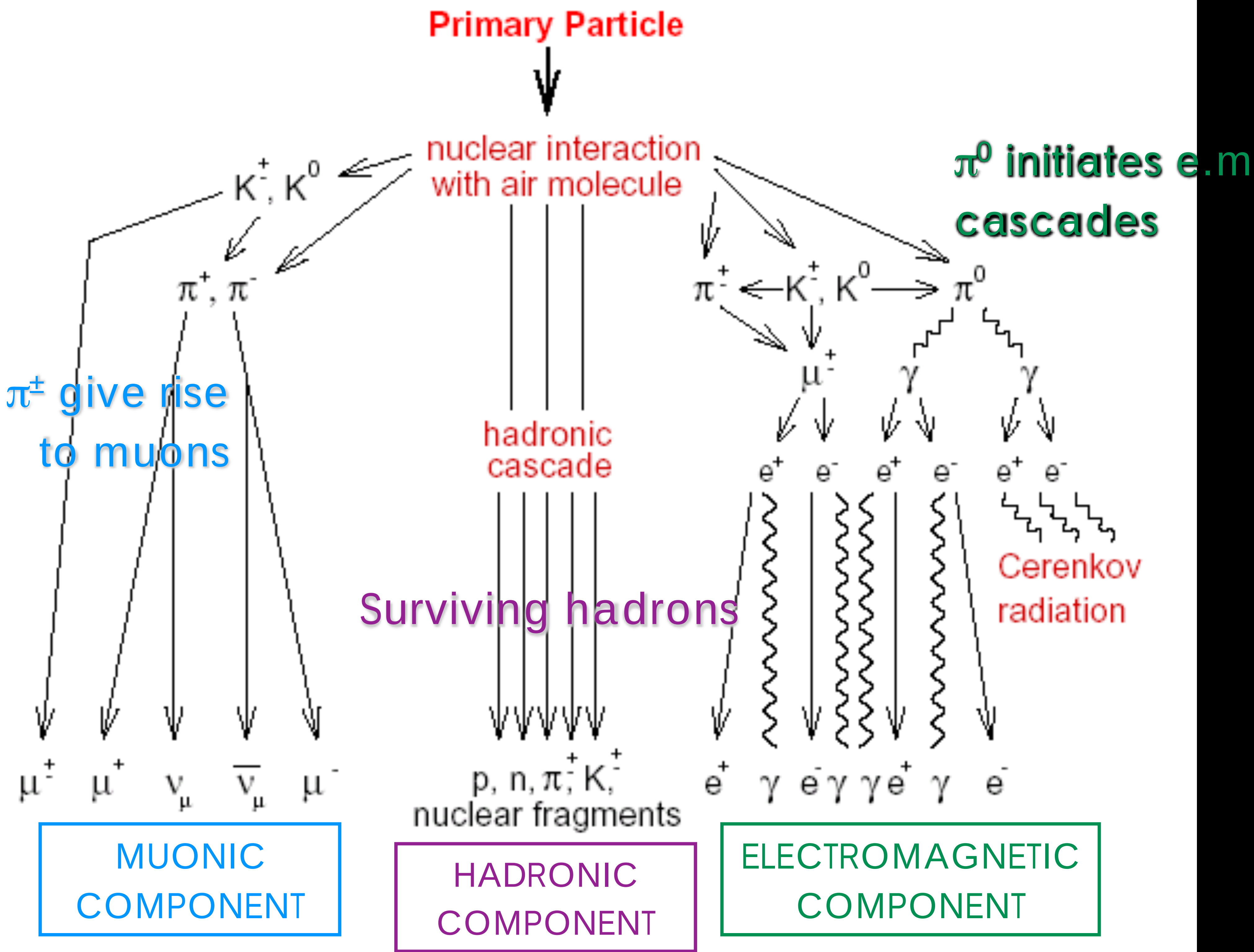

EAS LATERAL DEVELOPMENT

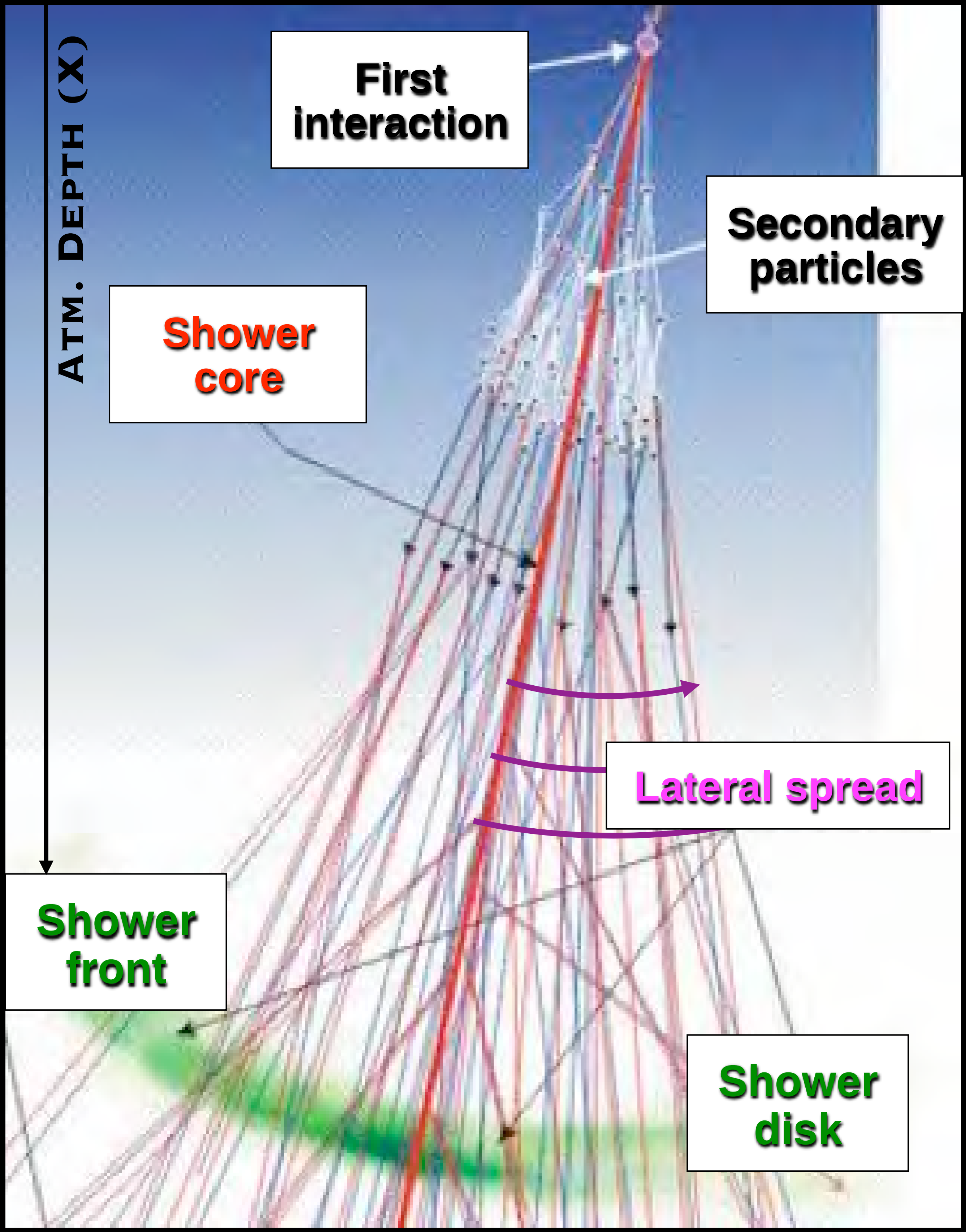

Secondary particles form a narrow "bundle": the shower core

Initial transverse momentum and multiple scattering in atmosphere causes particles to spread out laterally from the core -> lateral distribution: particle density is greatest at the core and it decreases with increasing distance from it

Due to different path lengths and velocities across the atmosphere shower particles are distributed over a wide area in a thin curved disk

EAS LONGITUDINAL DEVELOPMENT

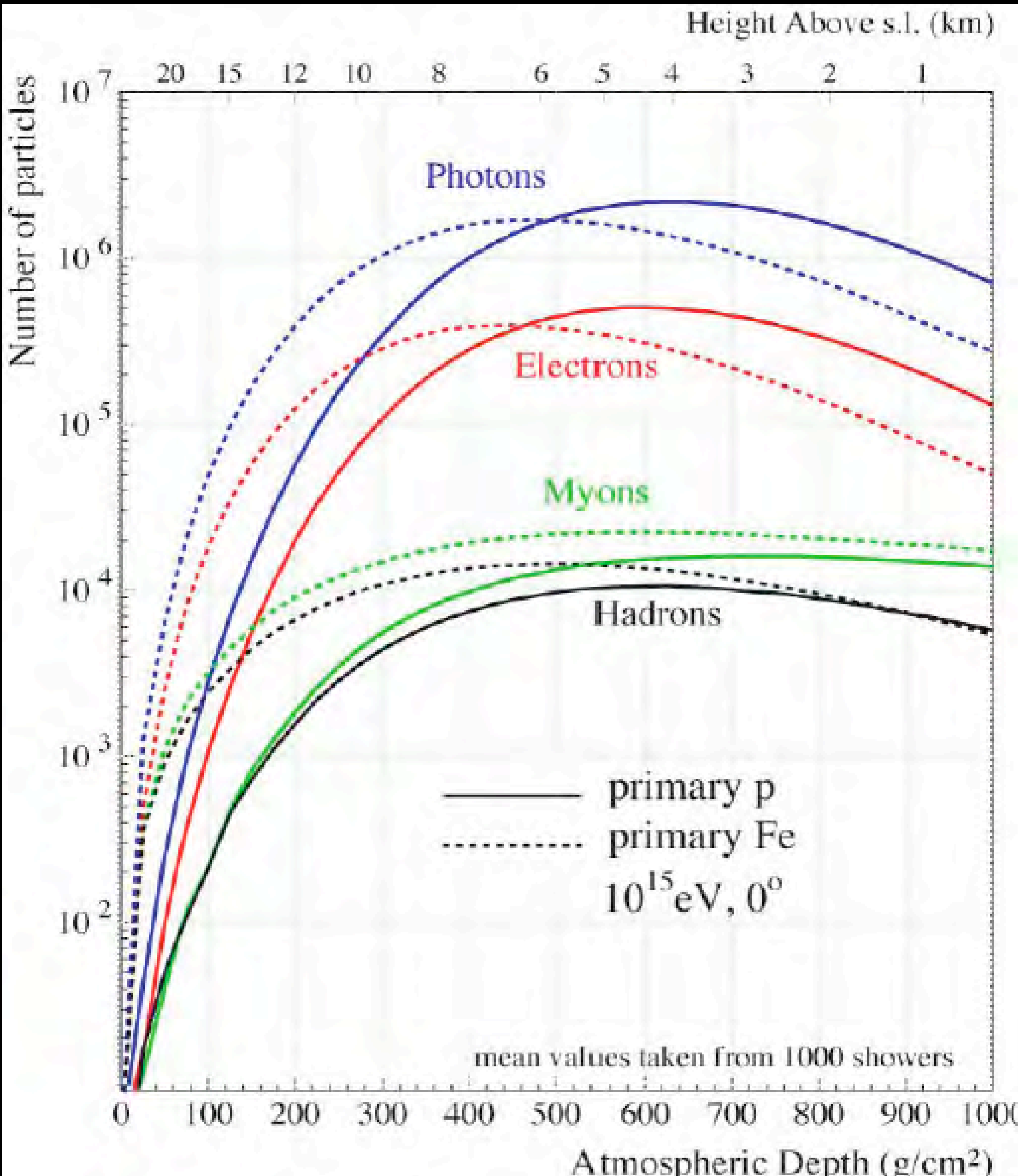

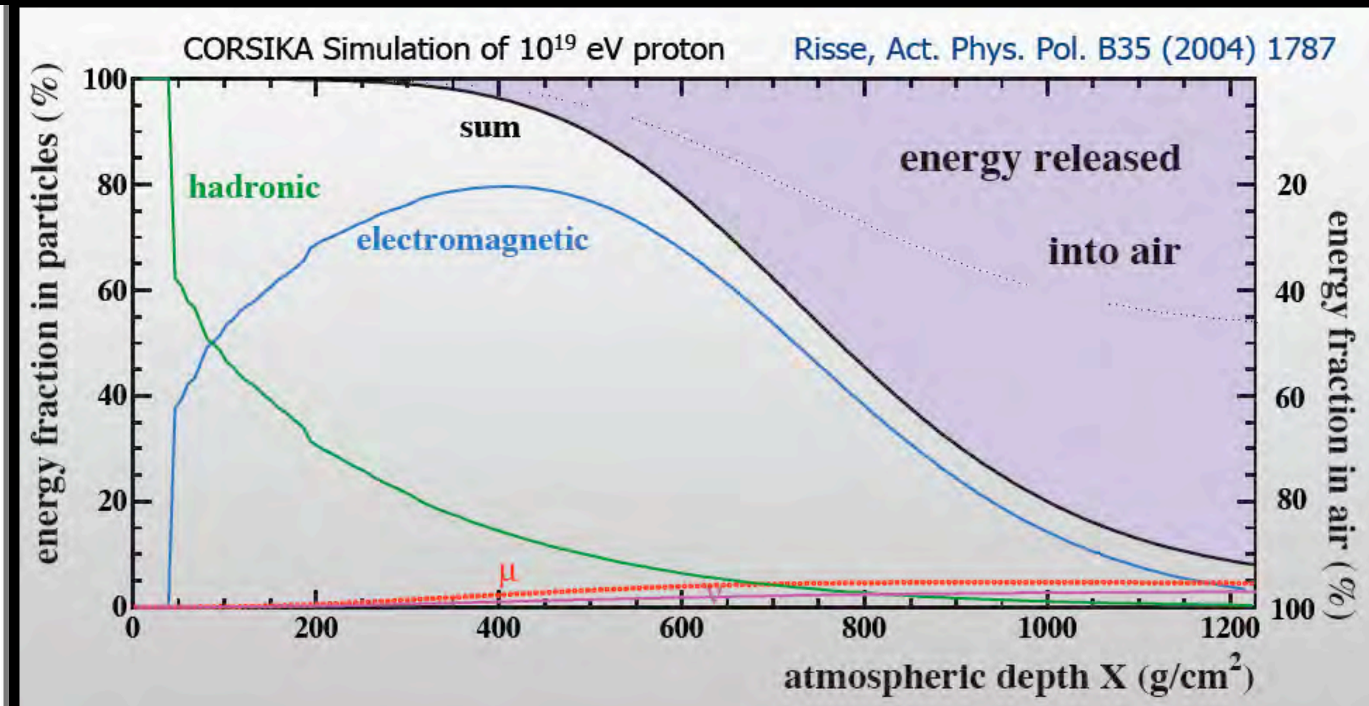

90% of the primary energy of the cosmic ray is dissipated in the atmosphere during shower development

The number of particles increases with atmospheric depth, reaches a maximum and then decreases (electrons attenuates more rapidly than muons)

RADIATION FROM SHOWER DEVELOPMENT

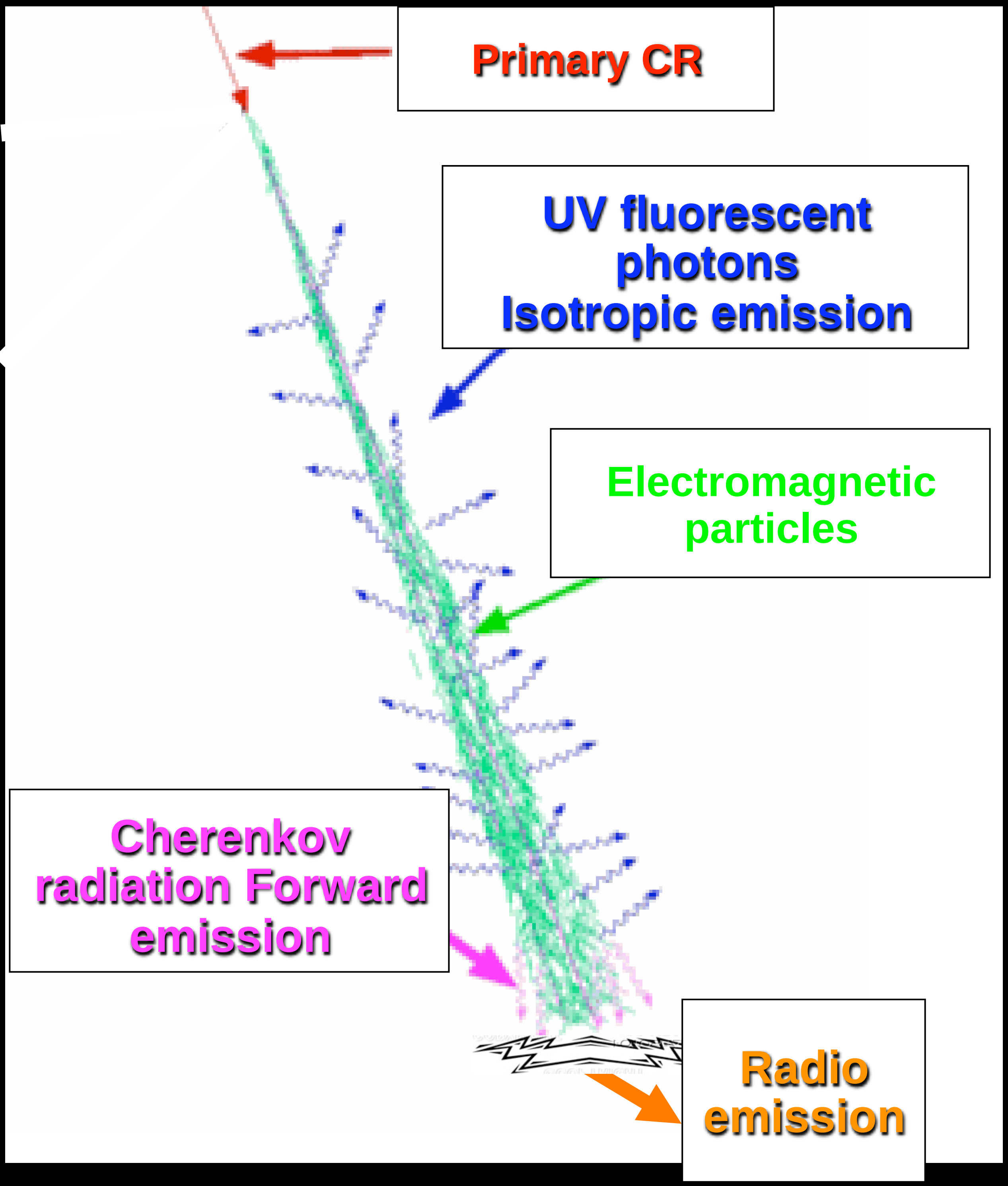

Cherenkov radiation: Electrons and positrons in the shower travel faster than the speed of light in air and emit Cherenkov radiation, mostly in the forward direction

Fluorescence radiation: The passage of air shower e.m. particles in atmosphere results in the excitation of the gas molecules (mostly nitrogen). Some of this excitation energy is emitted in the form of isotropic visible and UV radiation.

Radio emission: Air shower electrons and positrons are deflected in the Earth's magnetic field. Because of their relativistic velocities, they emit synchrotron radiation, beamed very sharply downwards, at radio frequencies below 100 MHz. Many sparkles together produce a bright radio flash

FLUORESCENCE RADIATION

Charged particles from EAS interact with Nitrogen molecules in air . The Nitrogen molecules get excited and they emit (when returning to their ground state) a typical radiation in the wavelength range between 300 nm to 400 nm.

The fluorescence yield between 300 and 400 nm is approx. 4 photons per shower particle per metre of track in the atmosphere.

This radiation (commonly called fluorescence light) is emitted isotropically. It can travel several kilometers throught the atmosphere and detected by an optical telescope, i.e., mirrors and PMTs, typically, equipped with fast response electronics (fluorescence detectors).

Only 0.5% of dE/dX goes into fluorescence. This technique can be exploited only at very high energies (above 10^{17} eV). Like the Cherenkov one, it has a low duty cycle (cloudless, moonless nights)

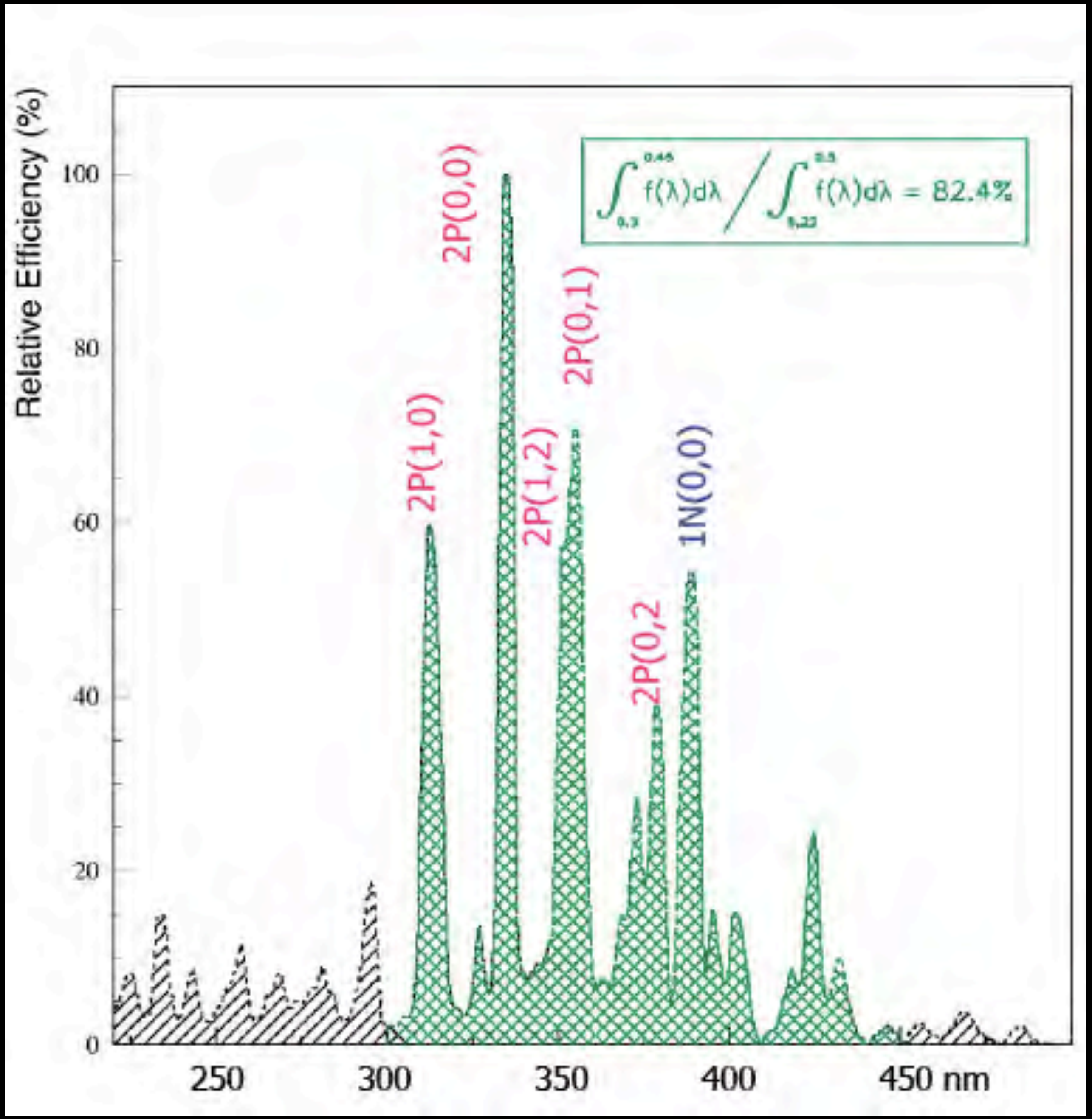

Fluorescence spectrum

RADIO EMISSION FROM EAS

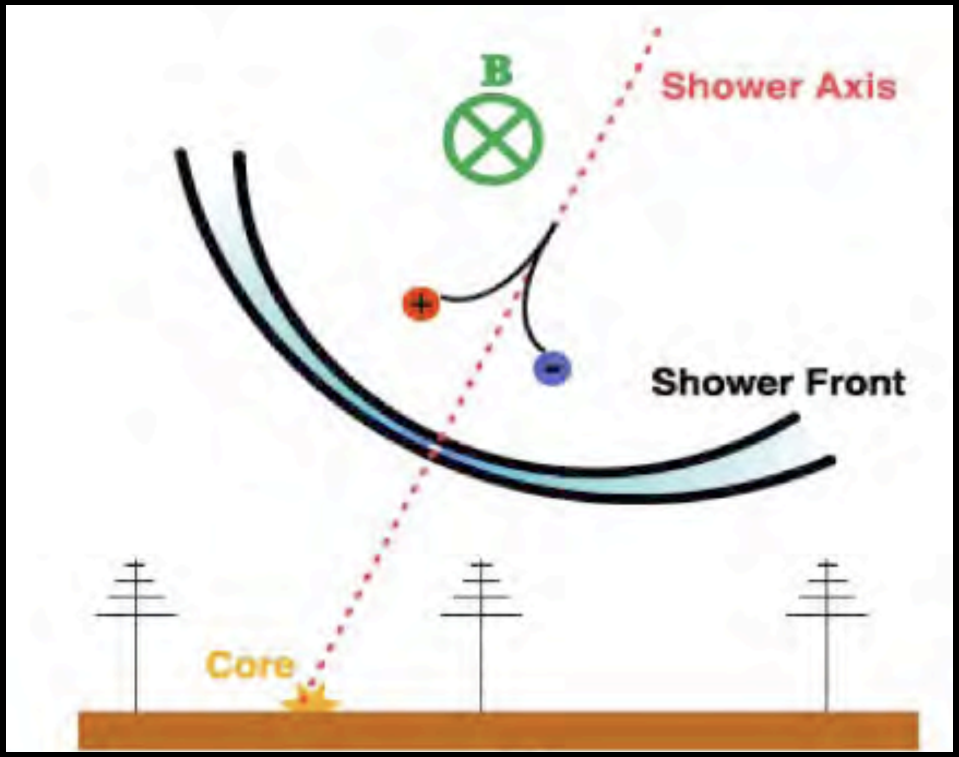

Geomagnetic effect:
deflection of charged particles in Earth's magnetic field (B). Electric current develops when the plasma moves through B. Radiation emitted by time varying electric current

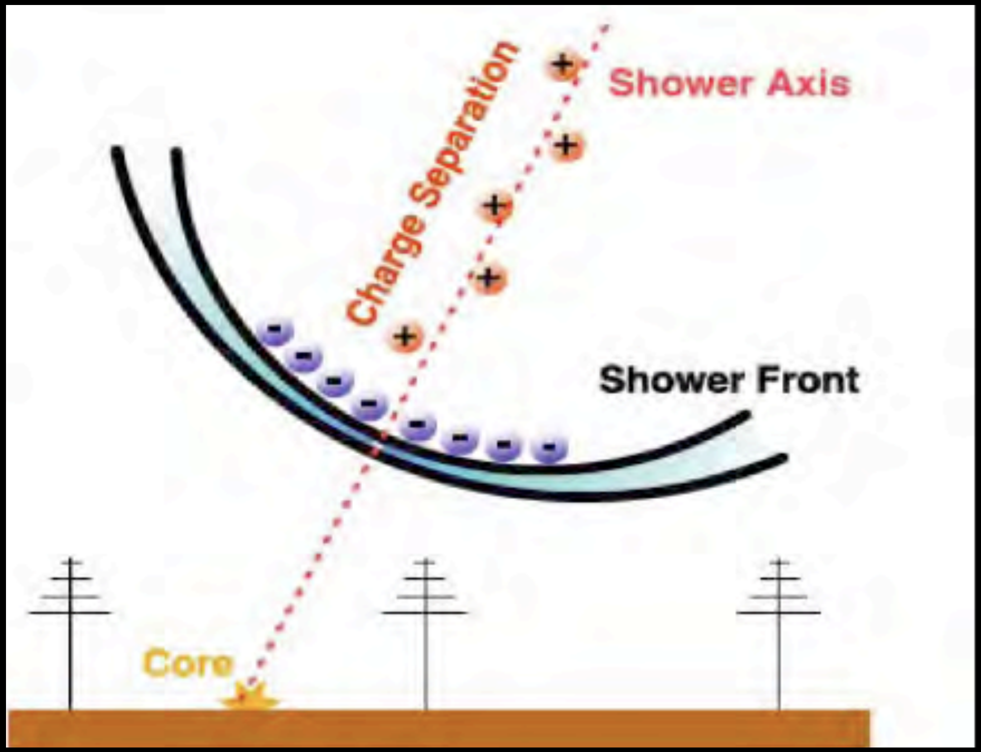

Askarian effect:
radio emission in the form of Cherenkov radiation. Due to the annihilation of positrons an excess of negative charge is created, producing Cherenkov radiation as it moves through the medium (air)

DIFFERENT DETECTORS FOR DIFFERENT EAS OBSERVABLES

Particle detectors (100% duty cycle)

IONIZATION (RPC)
FOR ELECTRONS/PHOTONS AND MUONS

SCINTILLATORS+PMTS
(FOR ELECTRONS/PHOTONS AND MUONS)

CHERENKOV (IN WATER)
FOR ELECTRONS/PHOTONS AND MUONS

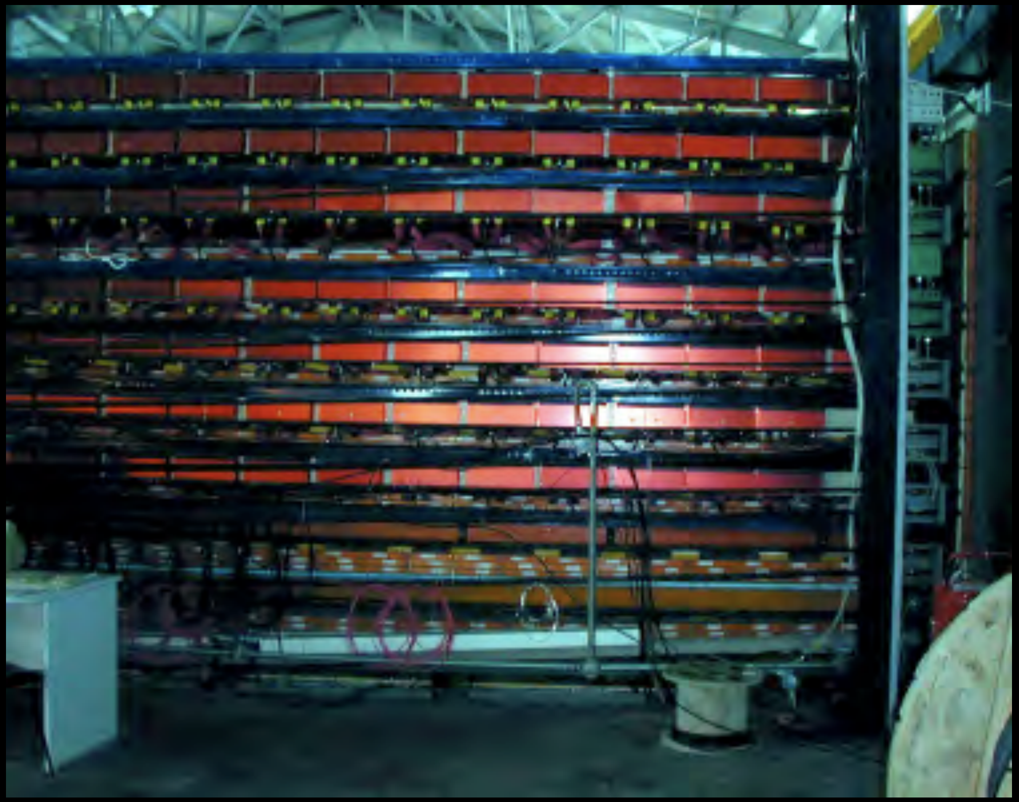

CALORIMETERS (FOR MUONS & HADRONS)

DIFFERENT DETECTORS FOR DIFFERENT EAS OBSERVABLES

Optical detectors (10% duty cycle)

The light from Cherenkov or fluorescence emission is collected by a mirror or a lens and imaged on to a camera made by photosensors (PMTs). Each PMT receives light coming from a specific region of the sky.

When an EAS crosses the field of view of the telescope, It triggers some of the PMTs. Each triggered PMT records the trigger time and the intensity of the signal.

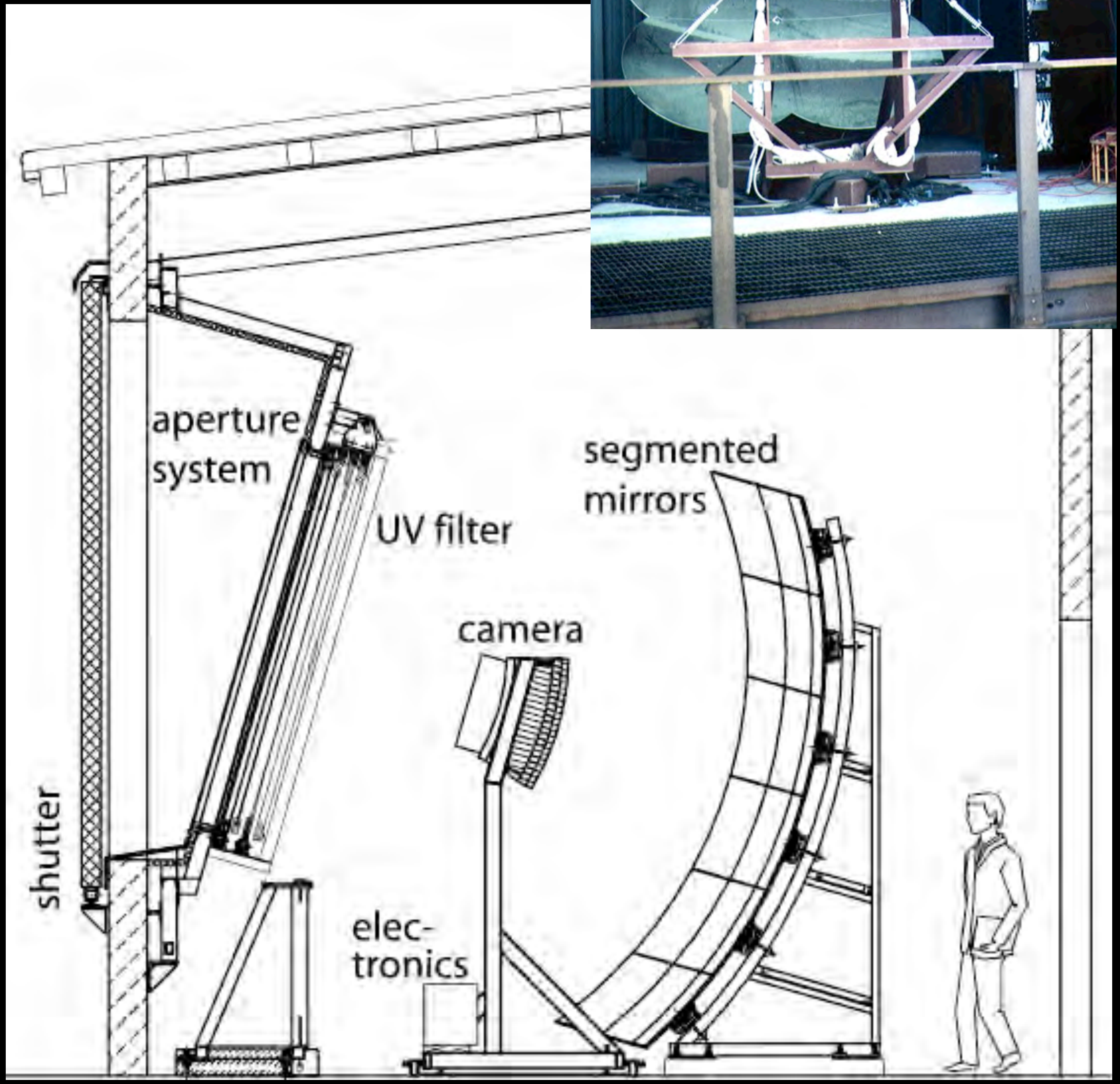

DIFFERENT DETECTORS FOR DIFFERENT EAS OBSERVABLES

Radio detectors (100% duty cycle)

The measurement of the radio signal requires a detection device, i.e, a radio antenna. Typically, one detector station consists of two antennas that are aligned perpendicular to each other, to allow for a measurement of the signal in two polarisations (EW-NS). Antennas can be triggered by traditional EAS arrays, or self-trigger

Antenna triggered by particle detectors

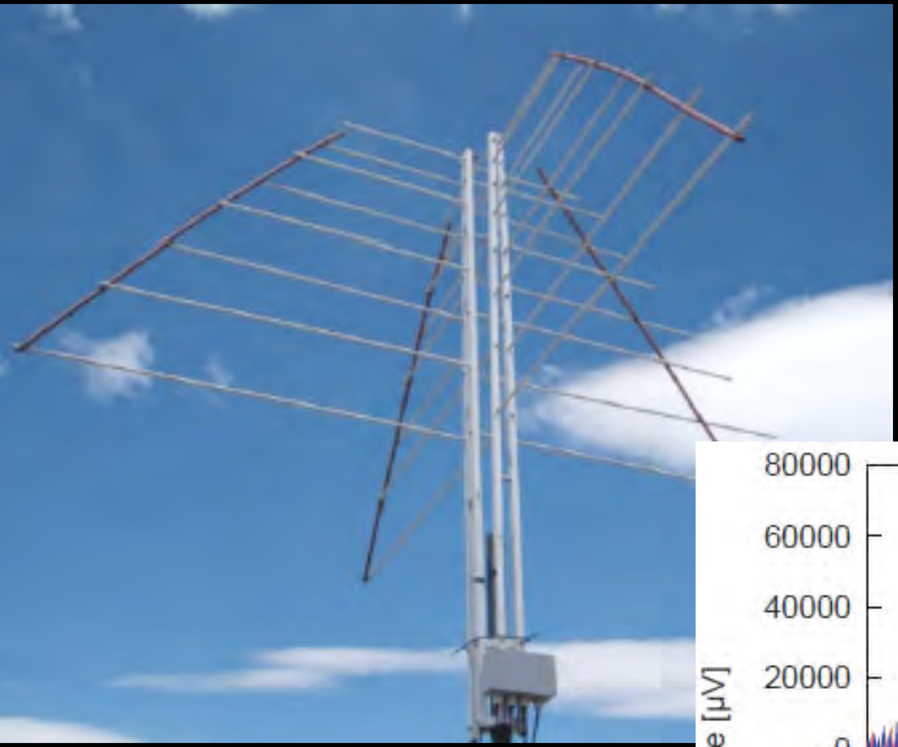

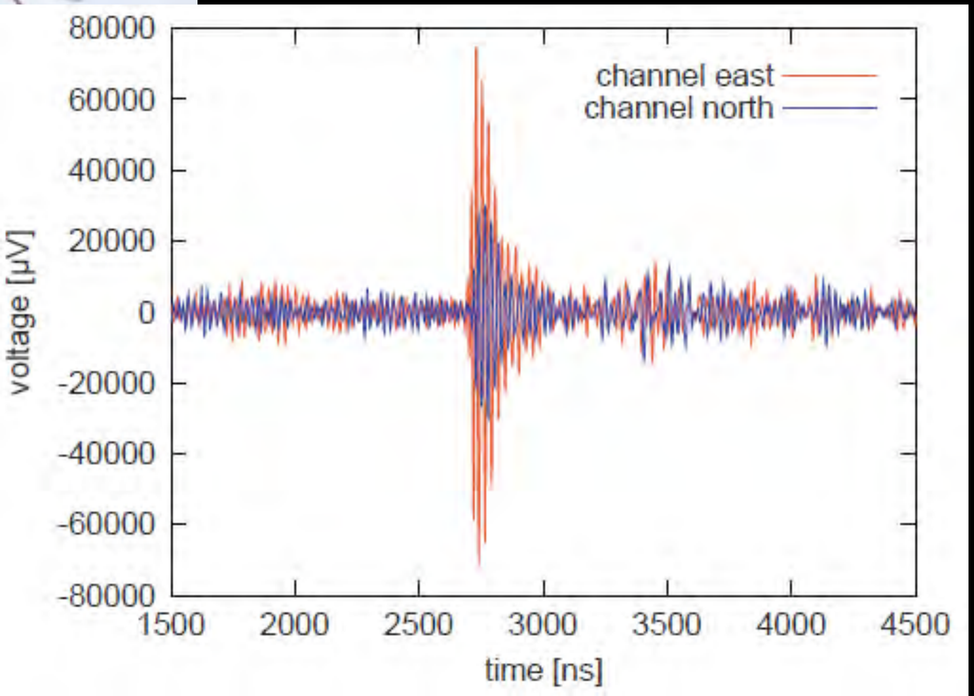

Self-triggered antennas

DIFFERENT DETECTORS FOR DIFFERENT EAS OBSERVABLES

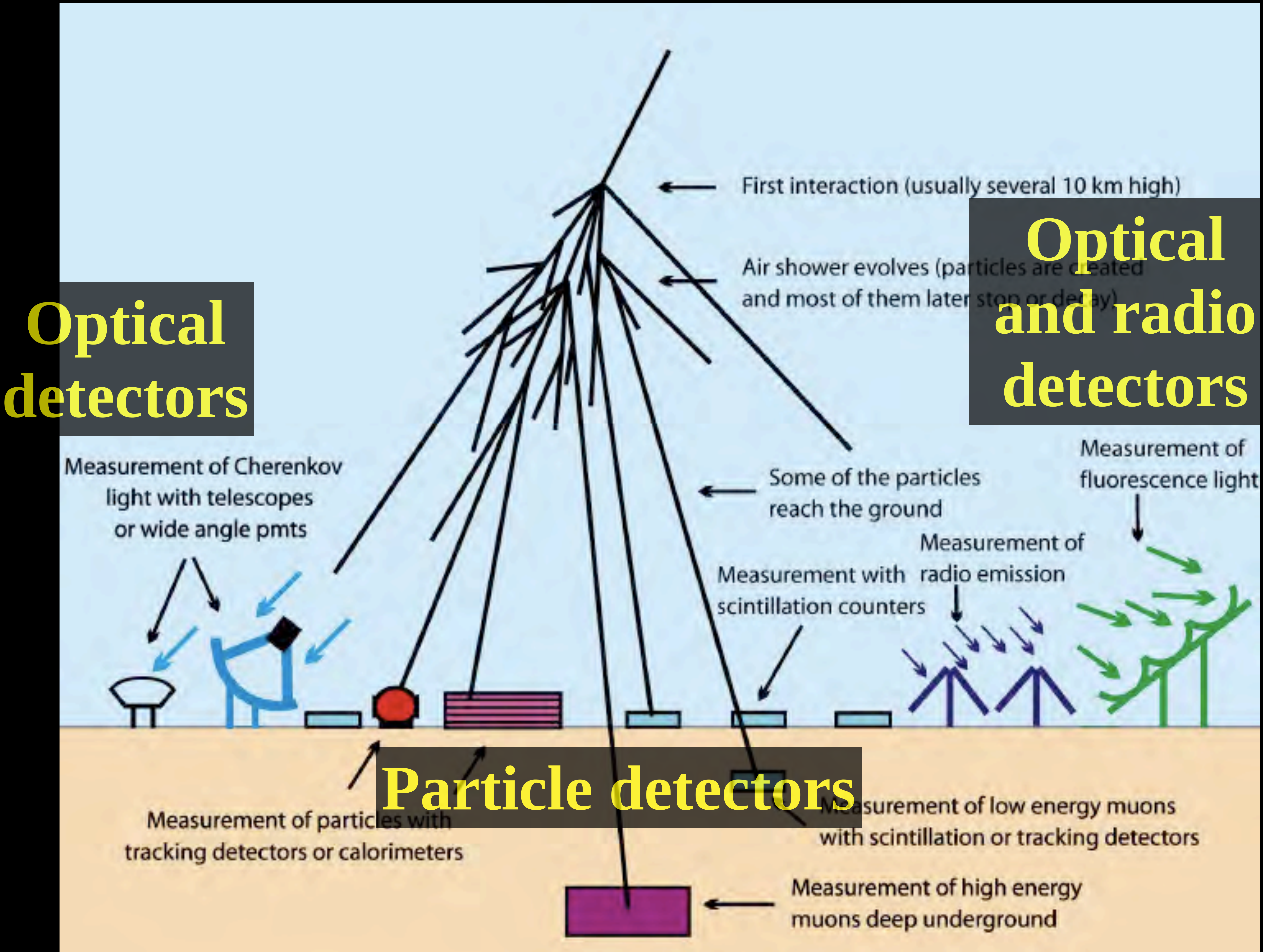

RECENT AND CURRENT EAS PARTICLE DETECTORS

AGASA [Akeno Giant Air Shower Array]

ARGO-YBJ: in Tibet

BAKSAN (Mt. Caucasus, Russia)

Buckland Park Extensive Air Shower Array (Australia) (operational 1971-1998)

CASA [Chicago Air Shower Array] (operational 1990-1998)

EAS-TOP (Italy, above the Gran Sasso laboratory, 1990-2000)

Haverah Park (Leeds University, operational until 1993)

GRAND [Gamma Ray Astrophysics at Notre Dame] (an array of tracking detectors)

GRAPES, India

HEGRA (operational 1988-2002)

ICETOP (South Pole, over ICECUBE)

KASCADE [KArlsruhe Shower Core and Array DEtector].

KASCADE-GRANDE.

MILAGRO (Water Cherenkov experiment near Los Alamos).

Mt. Norikura Observatory in Japan

Pierre Auger Observatory.

SPASE 2 [South Pole Air Shower Array]

SUGAR [Sydney University Giant Air shower Recorder] (operational from 1968 to 1979)

Telescope Array

Tian-Shan Mountain Cosmic Ray Station

Tibet AS-gamma experiment: scintillation counter array

Yakutsk (Russia)

RECENT AND CURRENT "LIGHT" EAS DETECTORS

AIROBICC (non-imaging counters in the HEGRA array)
BLANCA [Broad LAteral Non-imaging C(h)erenkov Array] (at CASA))
TUNKA (array of non-imaging counters near Lake Baikal)

ASHRA [All-sky Survey High Resolution Air-shower detector]
PIERRE AUGER OBSERVATORY
EUSO [Extreme Universe Space Observatory] (proposed for ISS).
HiRes The High Resolution Fly's Eye Cosmic Ray Detector
Telescope Array [TA]

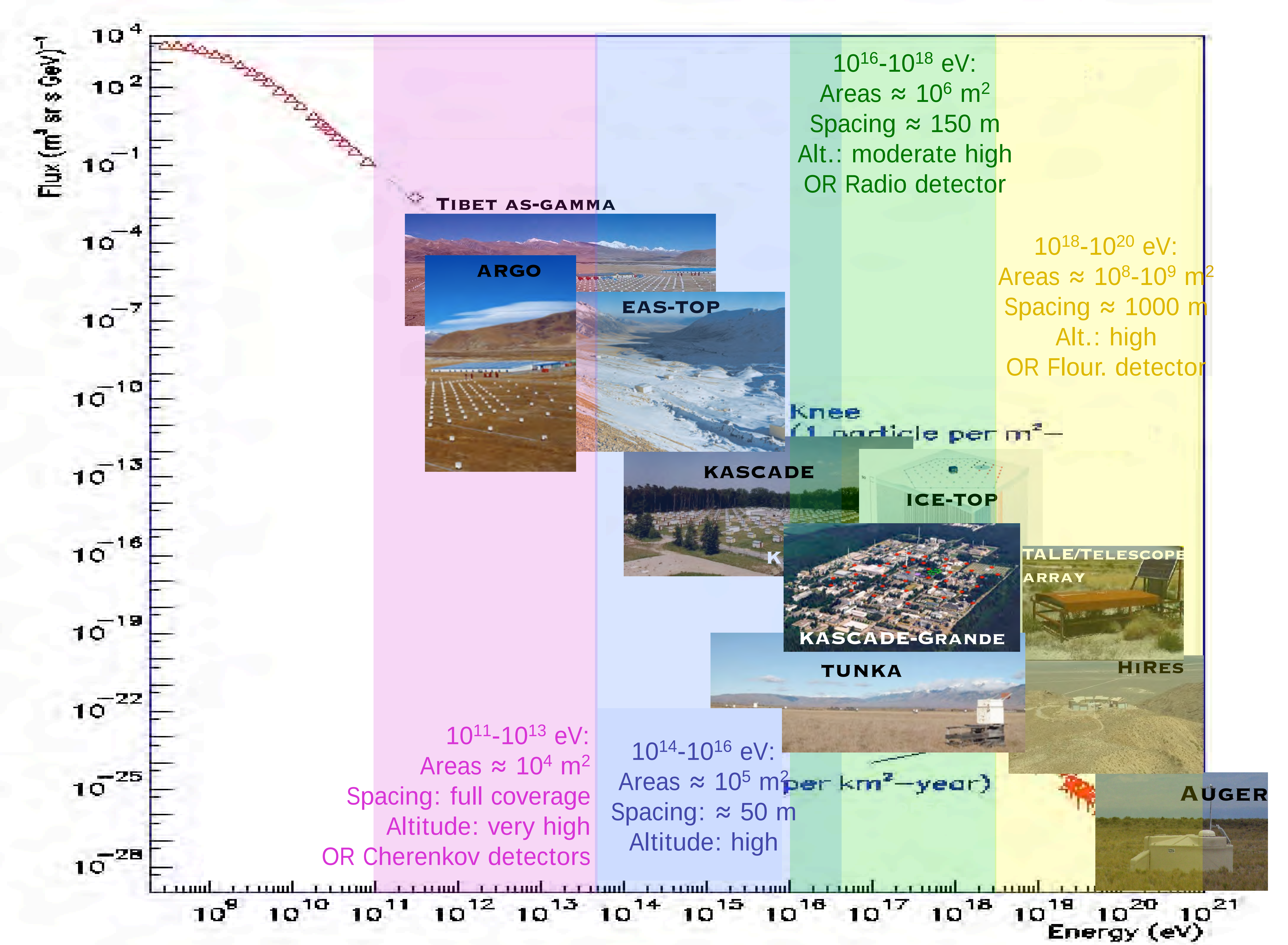

10^{16}-10^{18} eV:
Areas ≈ 10^6 m^2
Spacing ≈ 150 m
Alt.: moderate high
OR Radio detector
10^{18}-10^{20} eV:
Areas ≈ 10^8-10^9 m^2
Spacing ≈ 1000 m
Alt.: high
OR Flour. detector
TIBET AS-GAMMA
ARGO
EAS-TOP
Knee
KASCADE
ICE-TOP
KASCADE-GRANDE
TALE/TELESCOPE ARRAY
TUNKA
HIRES
AUGER
10^{11}-10^{13} eV:
Areas ≈ 10^4 m^2
Spacing: full coverage
Altitude: very high
OR Cherenkov detectors
10^{14}-10^{16} eV:
Areas ≈ 10^5 m^2
Spacing: ≈ 50 m
Altitude: high
per km²—year)
Flux (m² sr s GeV)⁻¹
Energy (eV)

The delicacy of the observations

The subtlety of the analysis

From EAS observables to cosmic ray parameters: An exemplary case: Auger

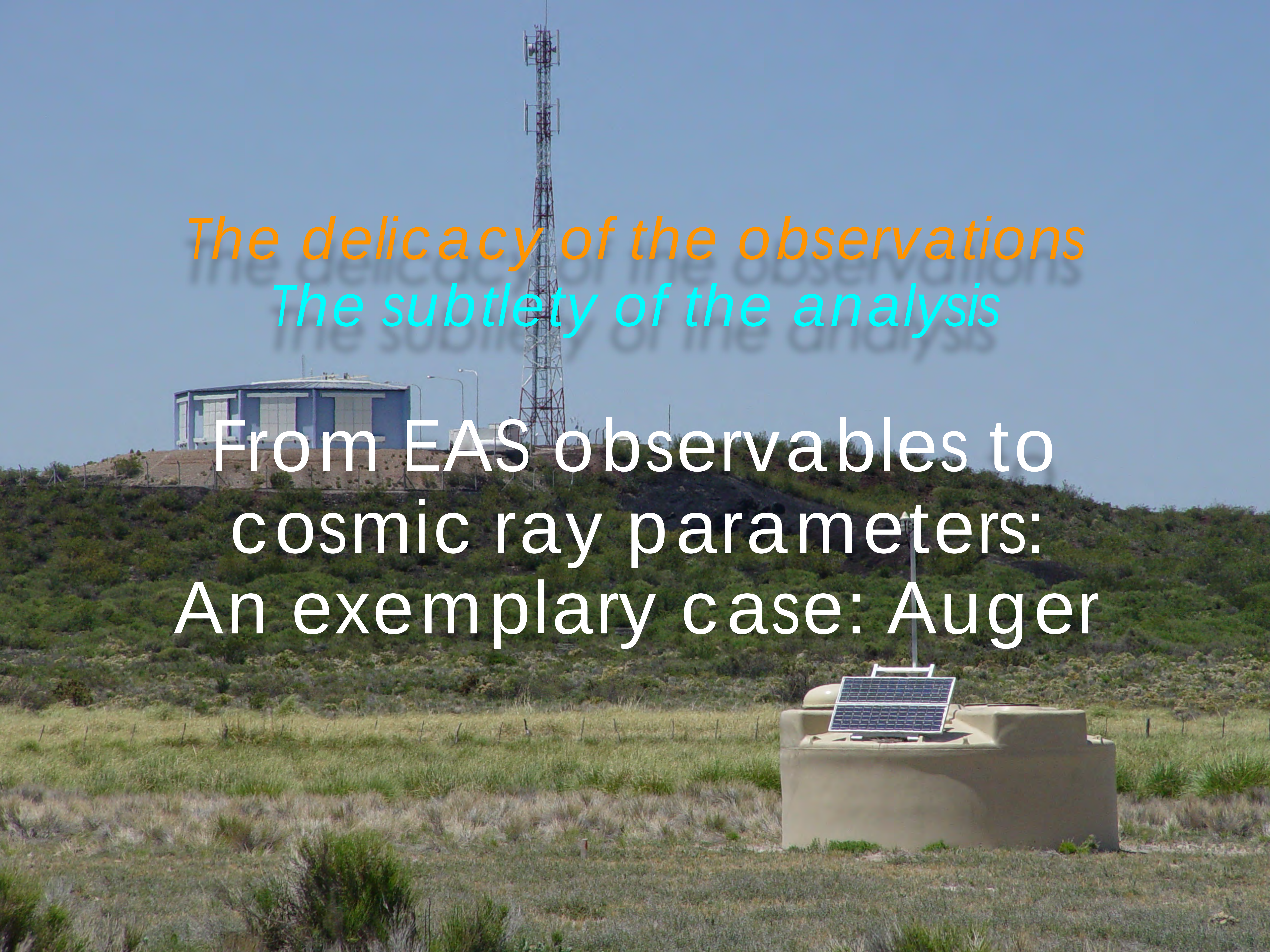

Obserwatorium Pierre Auger

Badanie promieni kosmicznych w zakresie najwyższych obserwowanych energii, E > 10 EeV ($>10^{19}$ eV):

skład
lekkie czy ciężkie jądra, fotony, neutrina, ??
widmo energii
kształt widma w zakresie efektu GZK
rozkład kierunkowy
anizotropia, źródła punktowe

→ wyjaśnienie ich pochodzenia ???

- obserwacja całego nieba – detektory w Argentynie i w USA
- 2 * 3000 km^2 → duża statystyka danych
- hybrydowa detekcja wielkich pęków: dwa układy detektorów

Pierre Auger Cosmic Ray Observatory

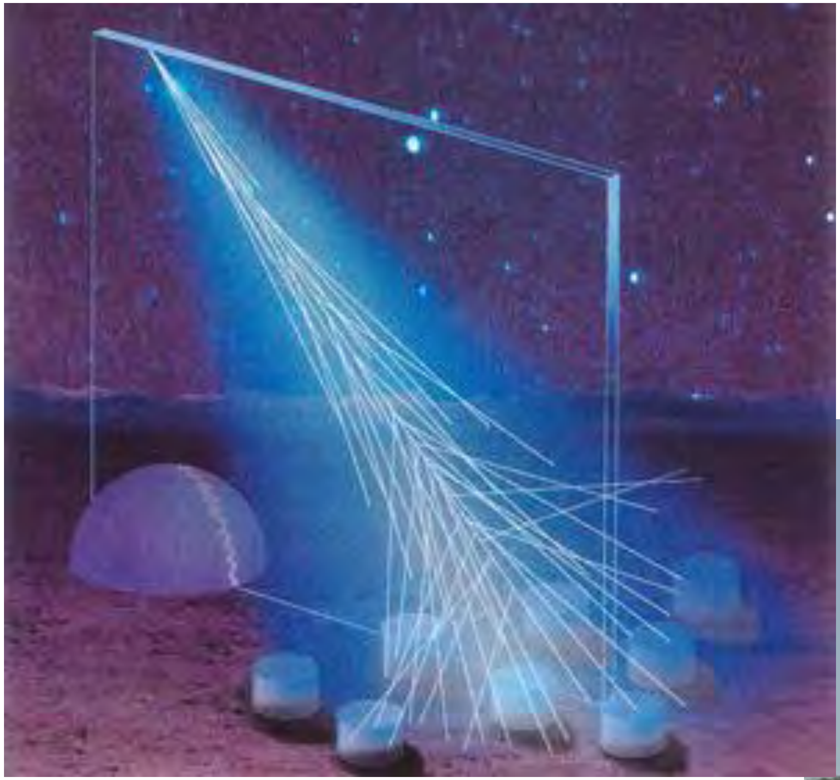

Use earth's atmosphere as a calorimeter. 1600 water Cherenkov detectors with 1.5km distance.

Placed in the Pampa Amarilla in western Argentina.

Detektor naziemny

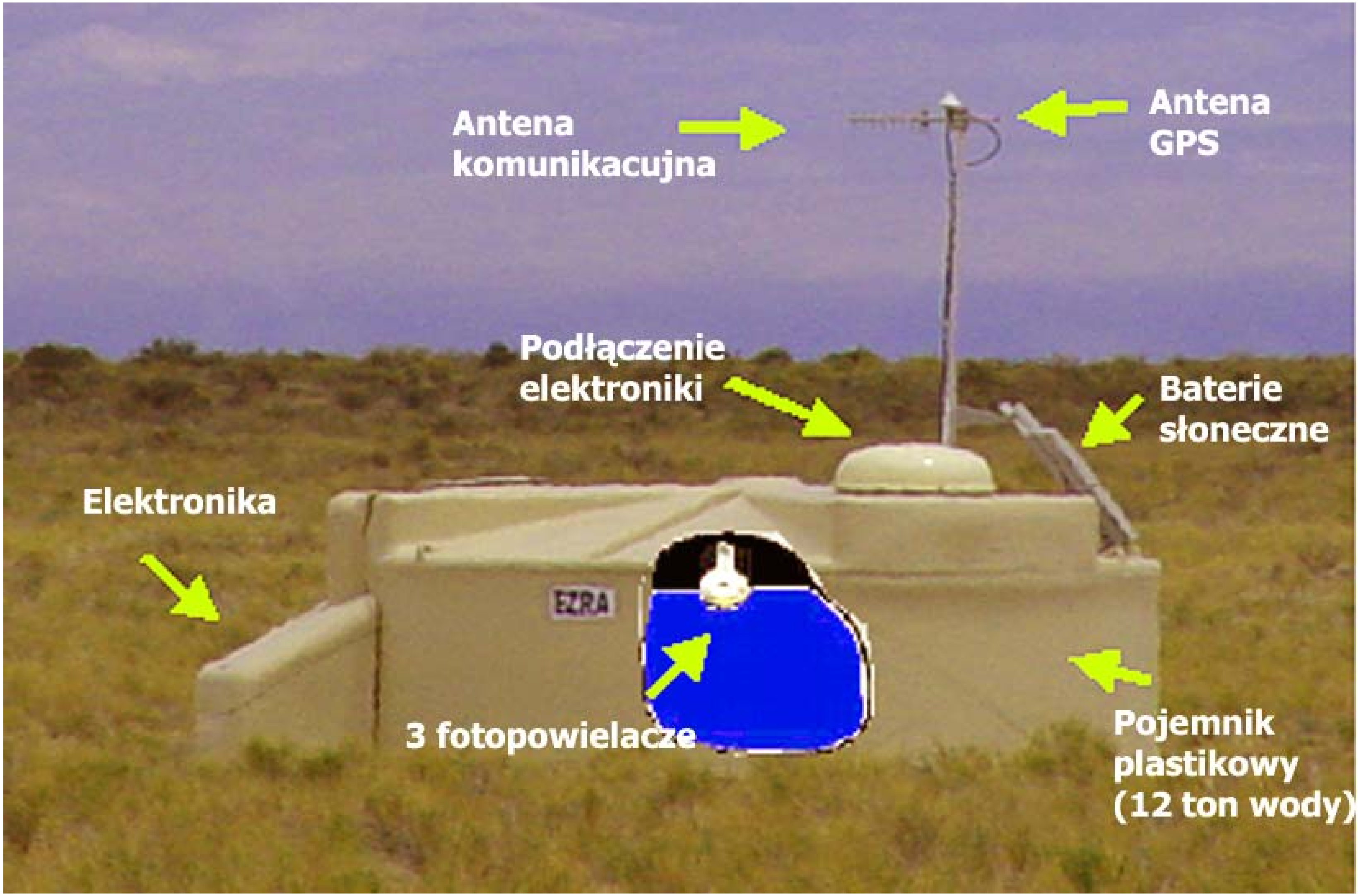

Obserwatorium Pierre Auger

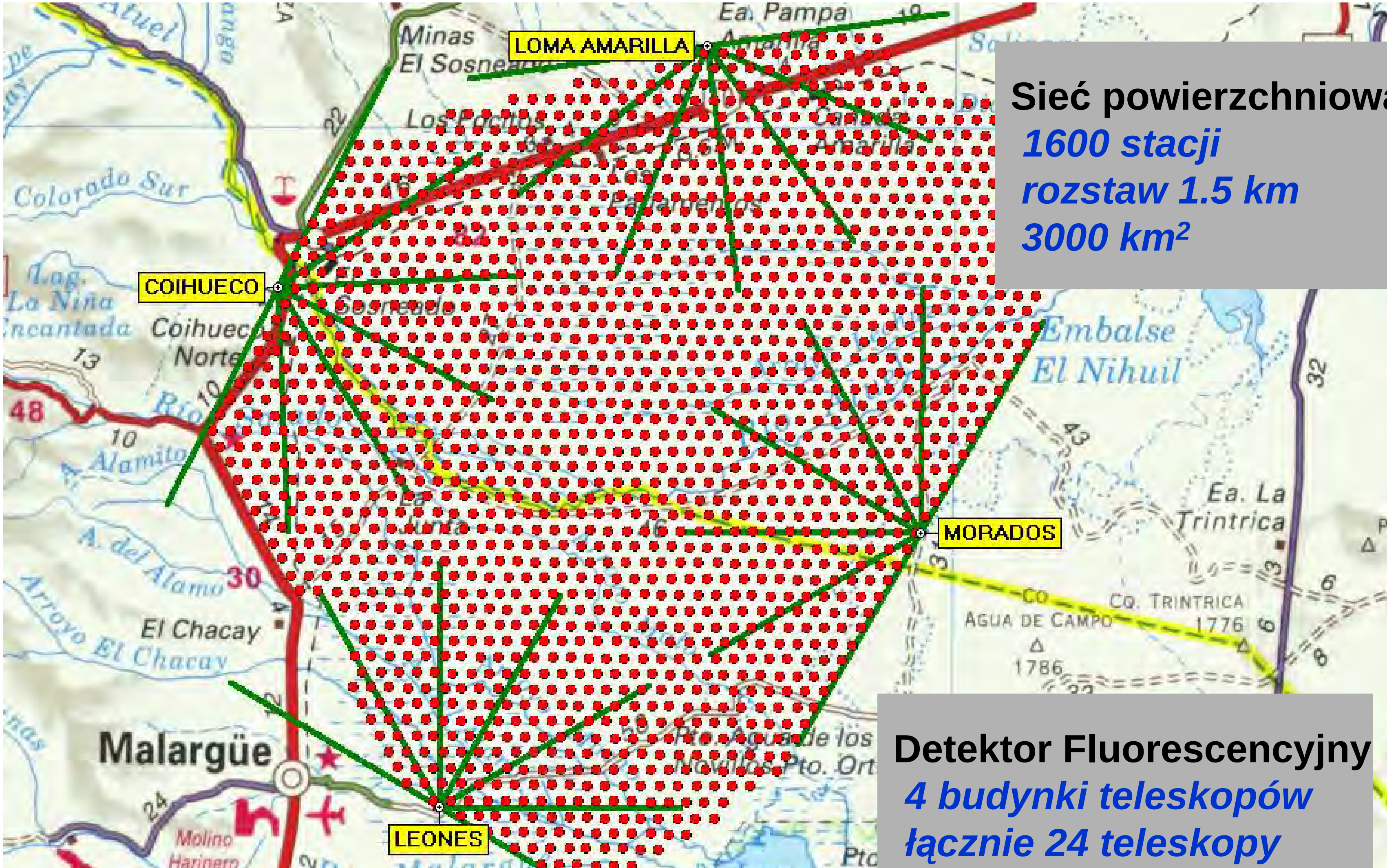

Sieć powierzchniowa

1600 stacji

rozstaw 1.5 km

3000 km^2

Detektor Fluorescencyjny

4 budynki teleskopów

łącznie 24 teleskopy

Detektor Fluorescencyjny

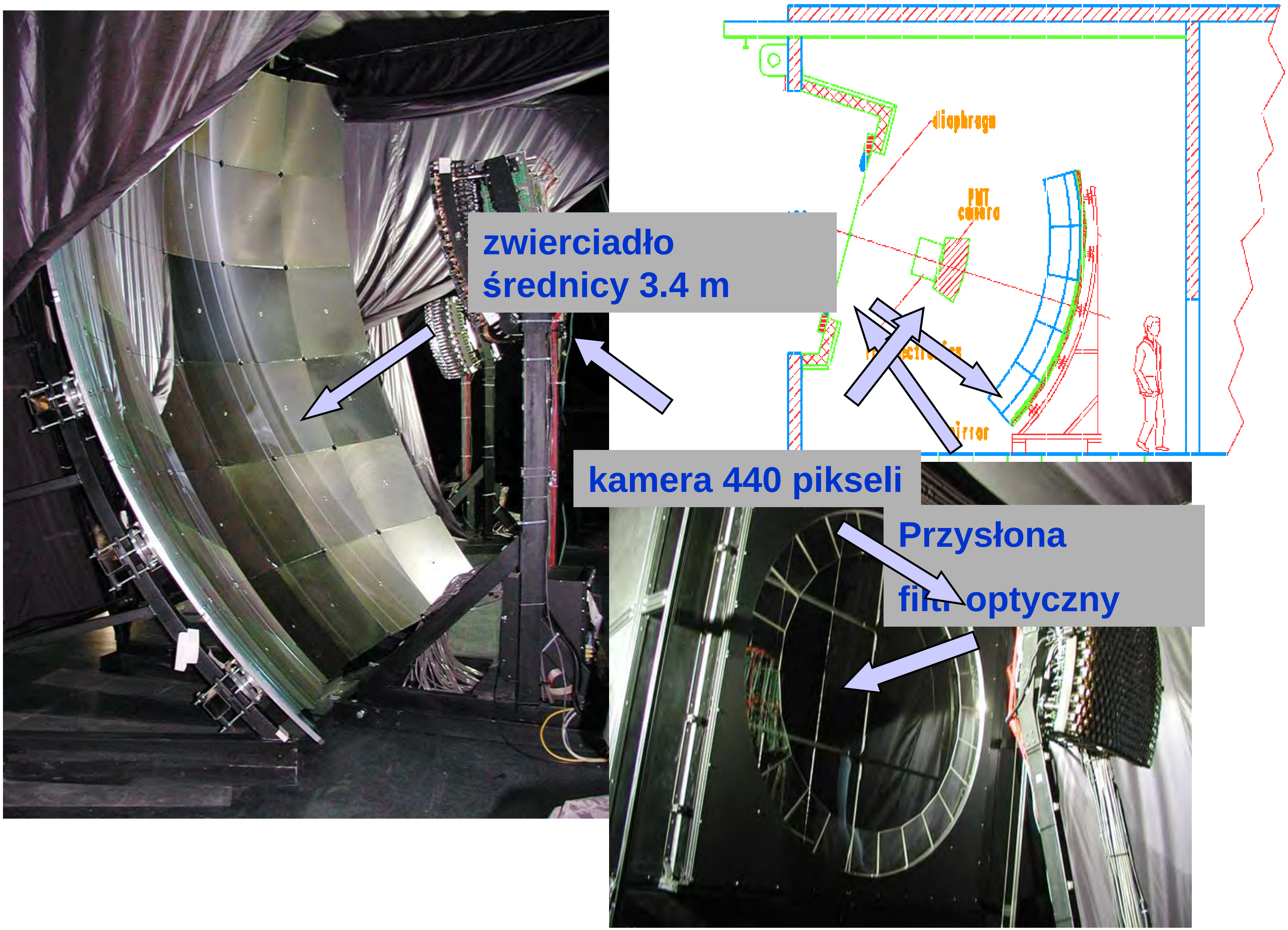

Detektory fluorescencyjne

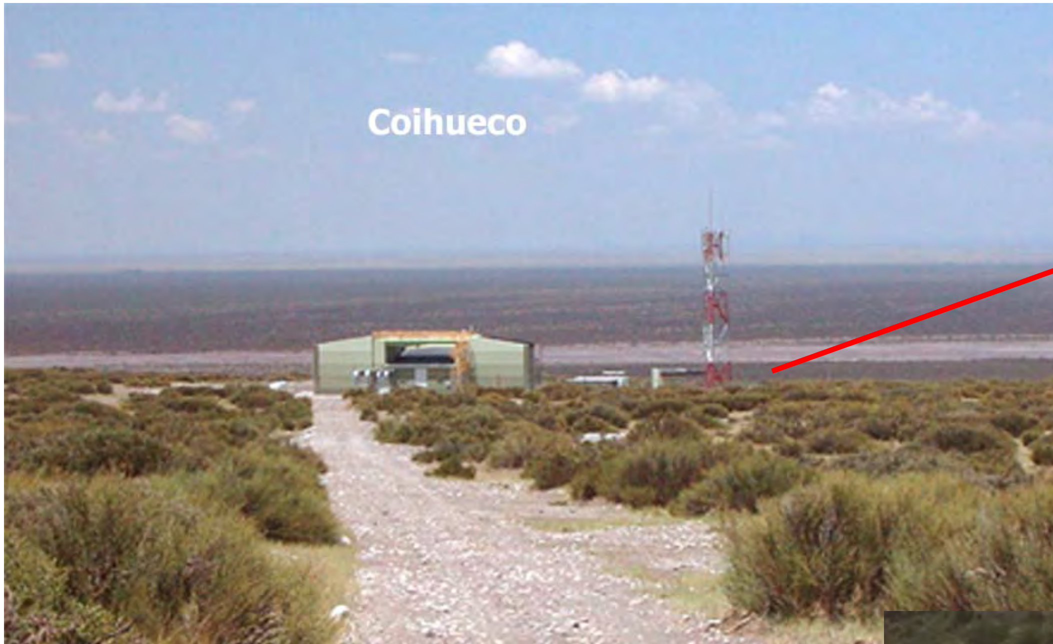

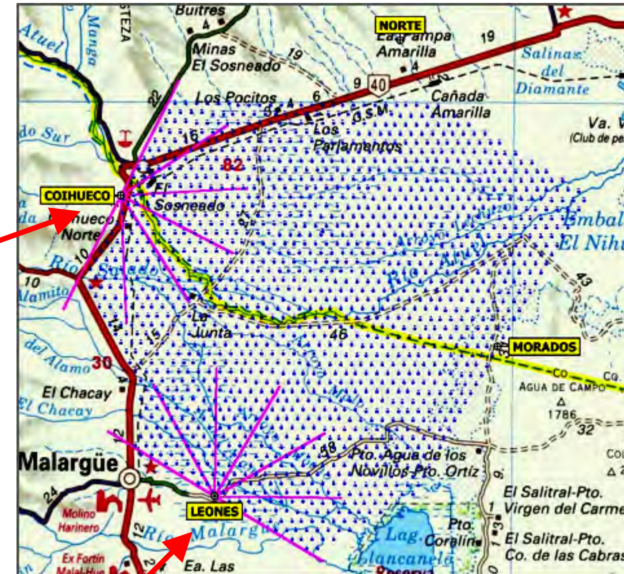

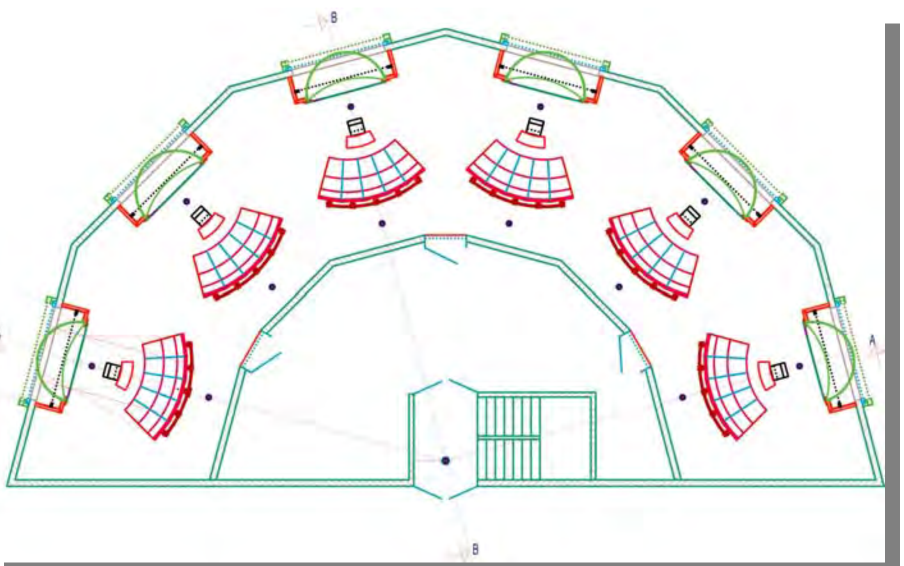

Tanks aligned seen from Los Leones

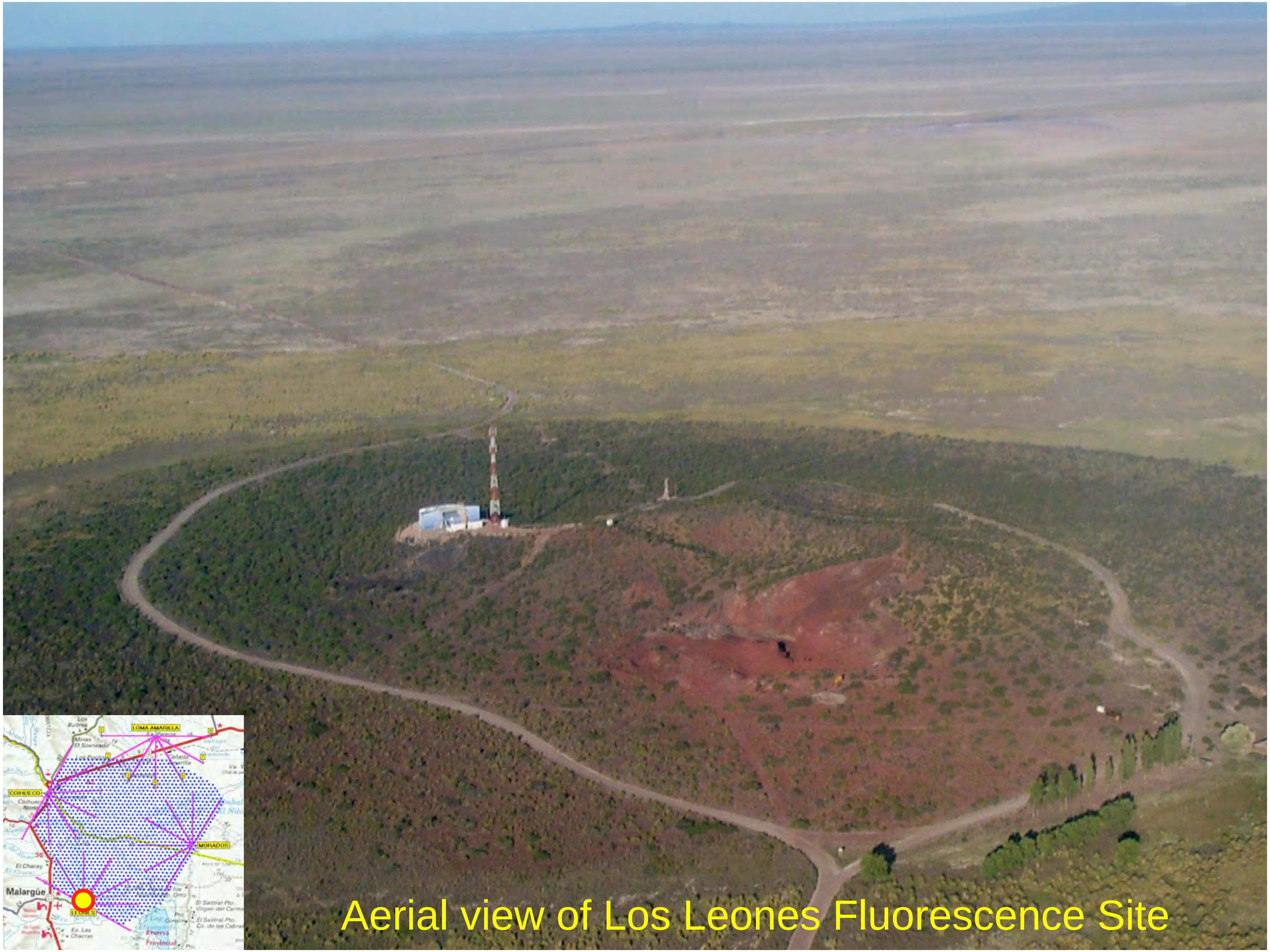

Aerial view of Los Leones Fluorescence Site

Przykład rzeczywistego pęku

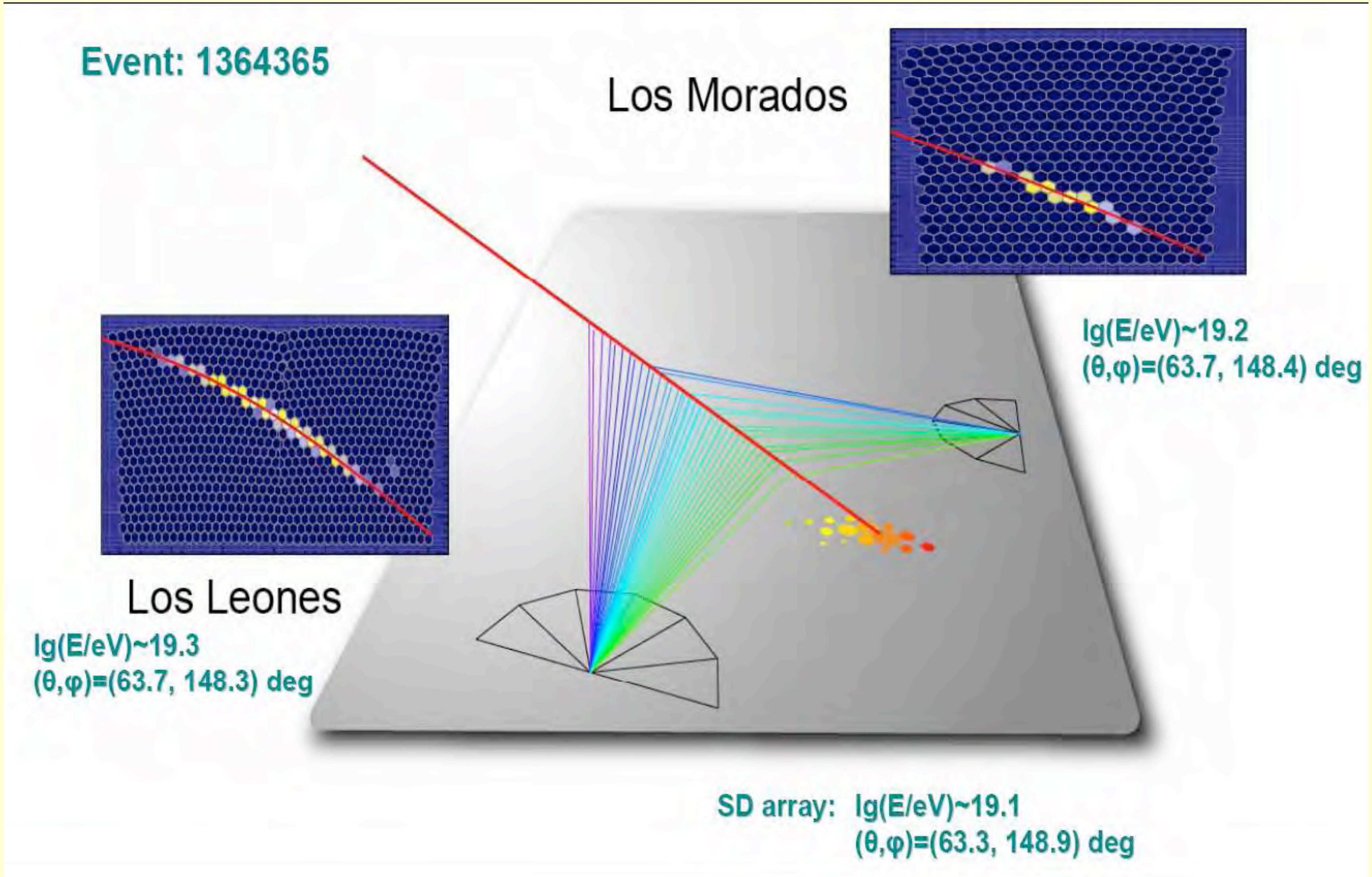

Goals of the Observatory

Detection with high statistics of cosmic rays with energies >10^{19}eV.

- Spectrum
  - ➡ Requiers a good energy determination ≈ 20 - 30 %
- Arrival directions
  - ➡ Angular resolution ≈1°
- Composition
  - ➡ Fast electronics to measure details of the shower front (SD)
  - ➡ Field of view to observe shower development (FD)

➡ Science results

Detector Calibration

Ground-Array

Throughgoing Muons

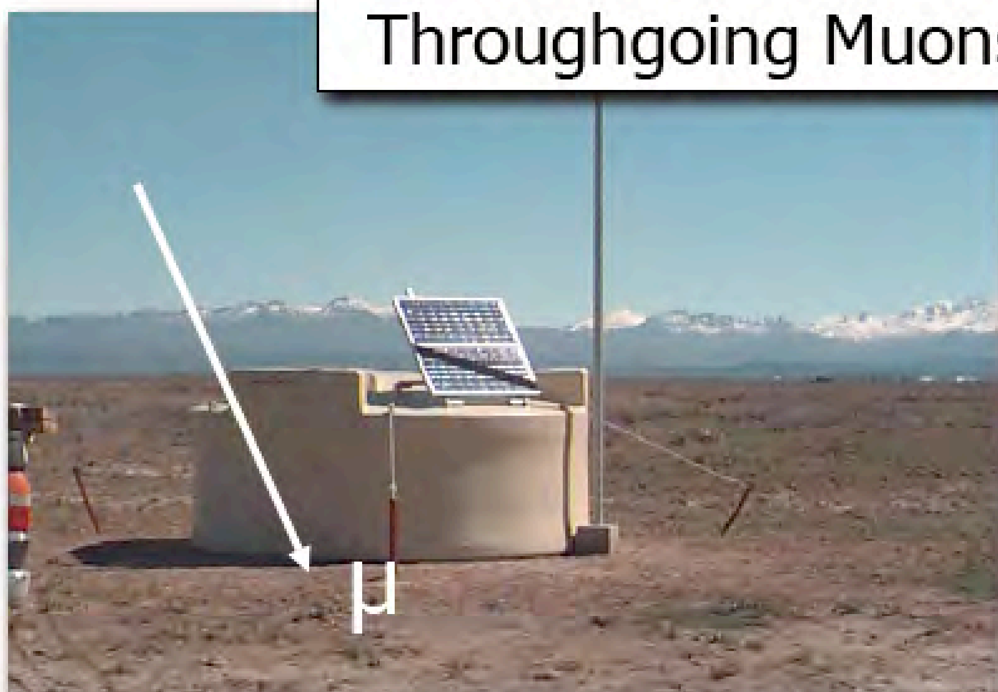

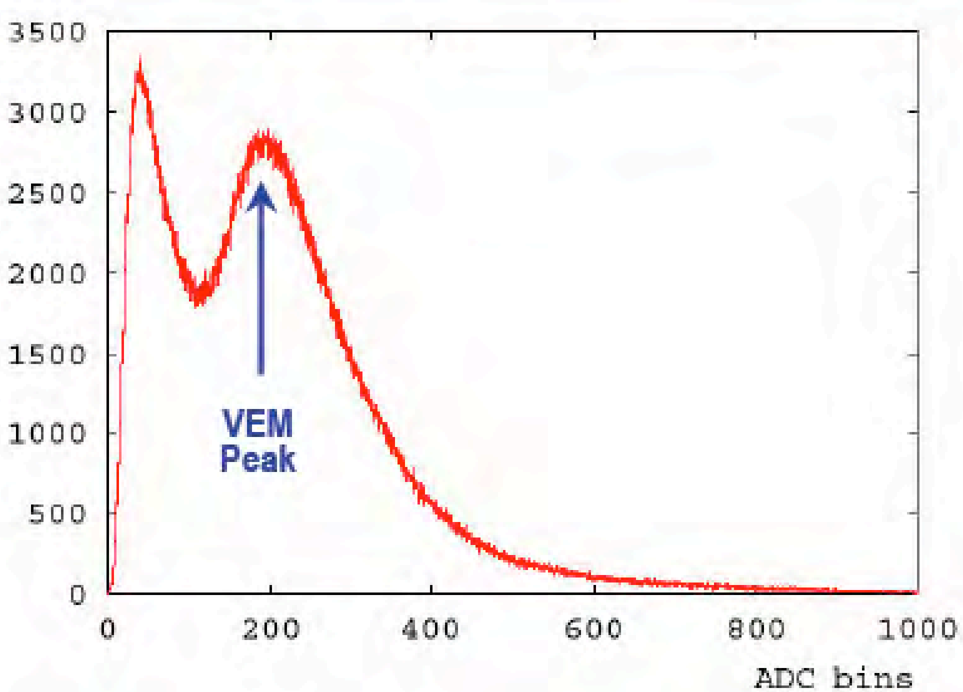

Fluorescence Telescopes

Diffuse Lightsource

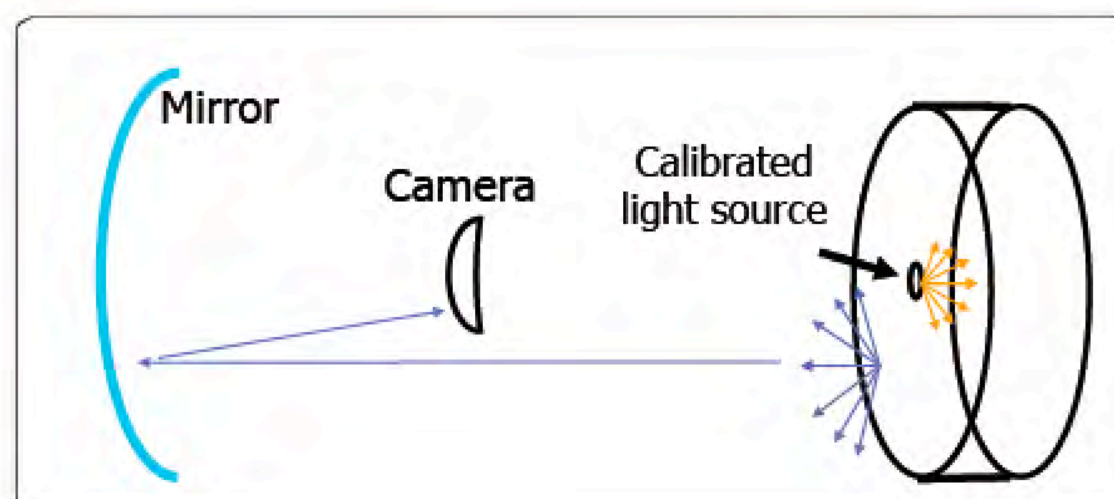

ARRIVAL DIRECTION

Most straightforward measurements by EAS arrays

The shower axis preserves the direction of the incoming particle

Time of flight technique:

Time differences among the arrival times of shower particles in the different detectors give the arrival direction

Angular accuracy

Less than degree for particle arrays

Fraction of degree for “light” arrays

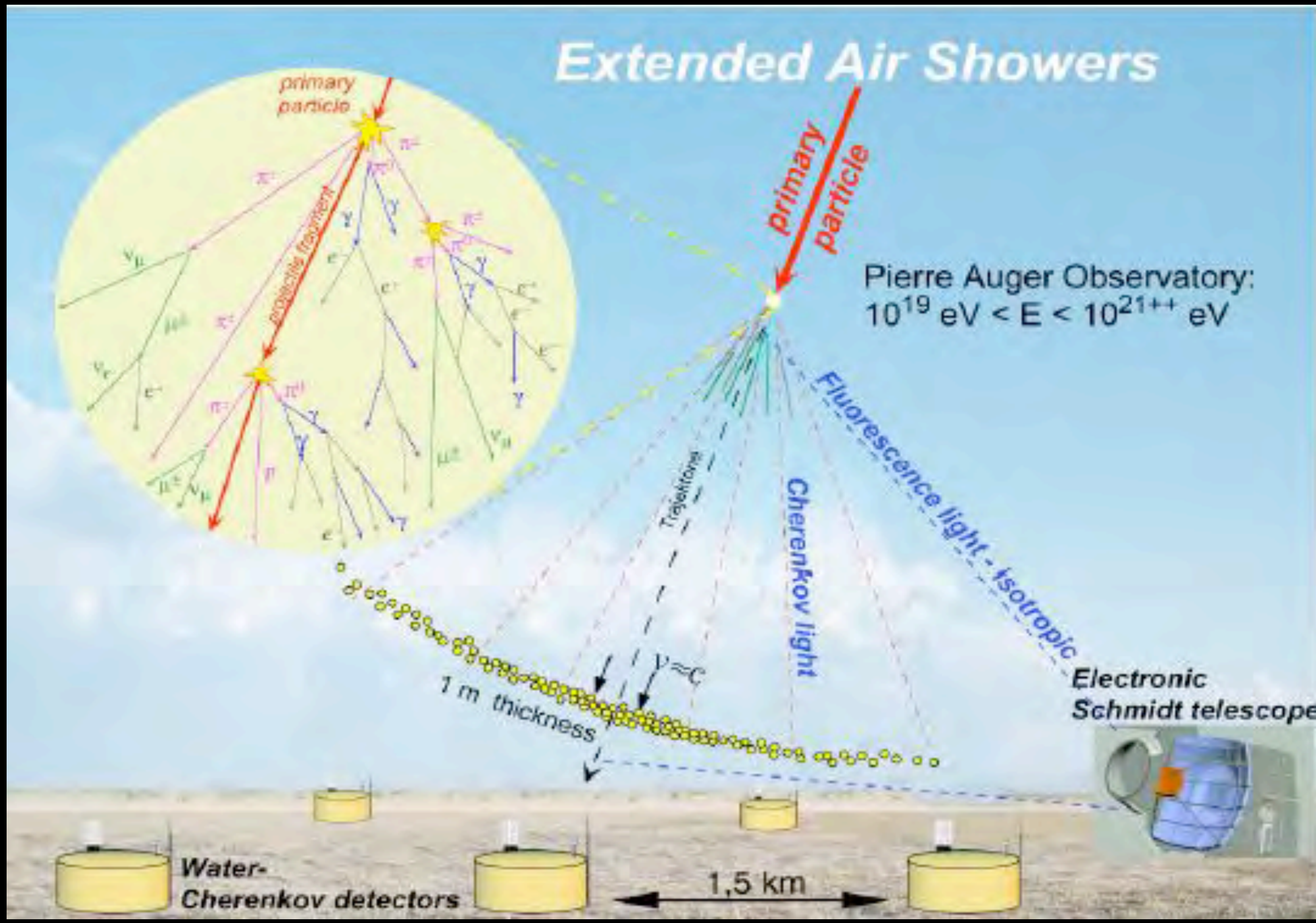

Obserwable
(analiza śladu pęku widzianego przez detektor powierzchniowy)

(P. Billoir, O. Blanch Bigas, Nucl. Phys. Proc. Suppl. 168 (2007) 225-231)

- **długość L i szerokość W: główna i boczna oś elipsoidy inercji ważonej przez sygnał stacji.**
- **prędkość efektywna <V>: dla każdej pary stacji (odległość zrzutowana na główną oś elipsoidy/ różnica pomiędzy czasem triggera)**
- **odchylenie standartowe prędkości efektywnej $\sigma_{<v>}$**

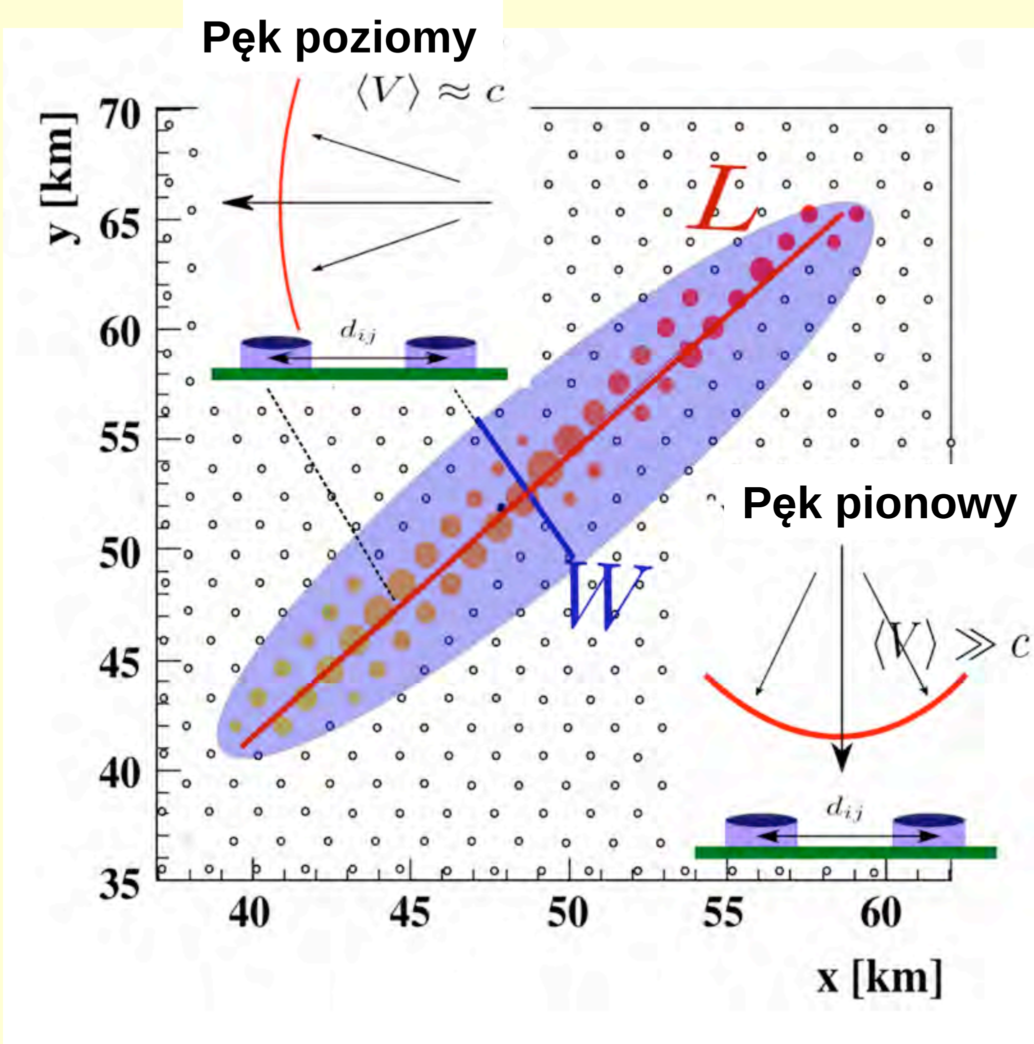

ARRIVAL DIRECTION FROM THE FLUORESCENCE DETECTOR

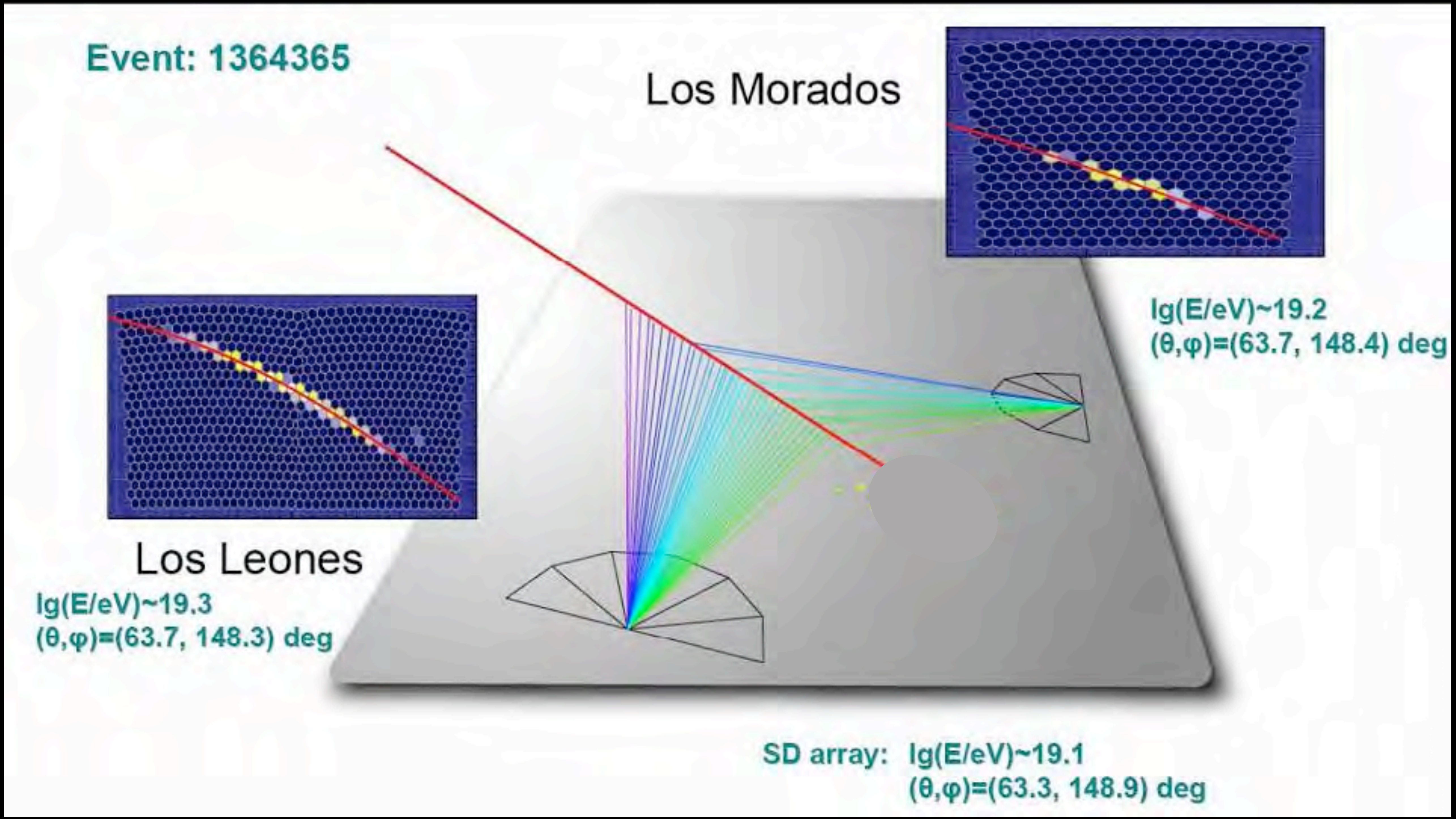

When an EAS is observed by two or more FDs, the arrival direction is defined by the intersection of the SDPs. Higher precision, check of the geometry

ARRIVAL DIRECTION FROM THE HYBRID DETECTOR

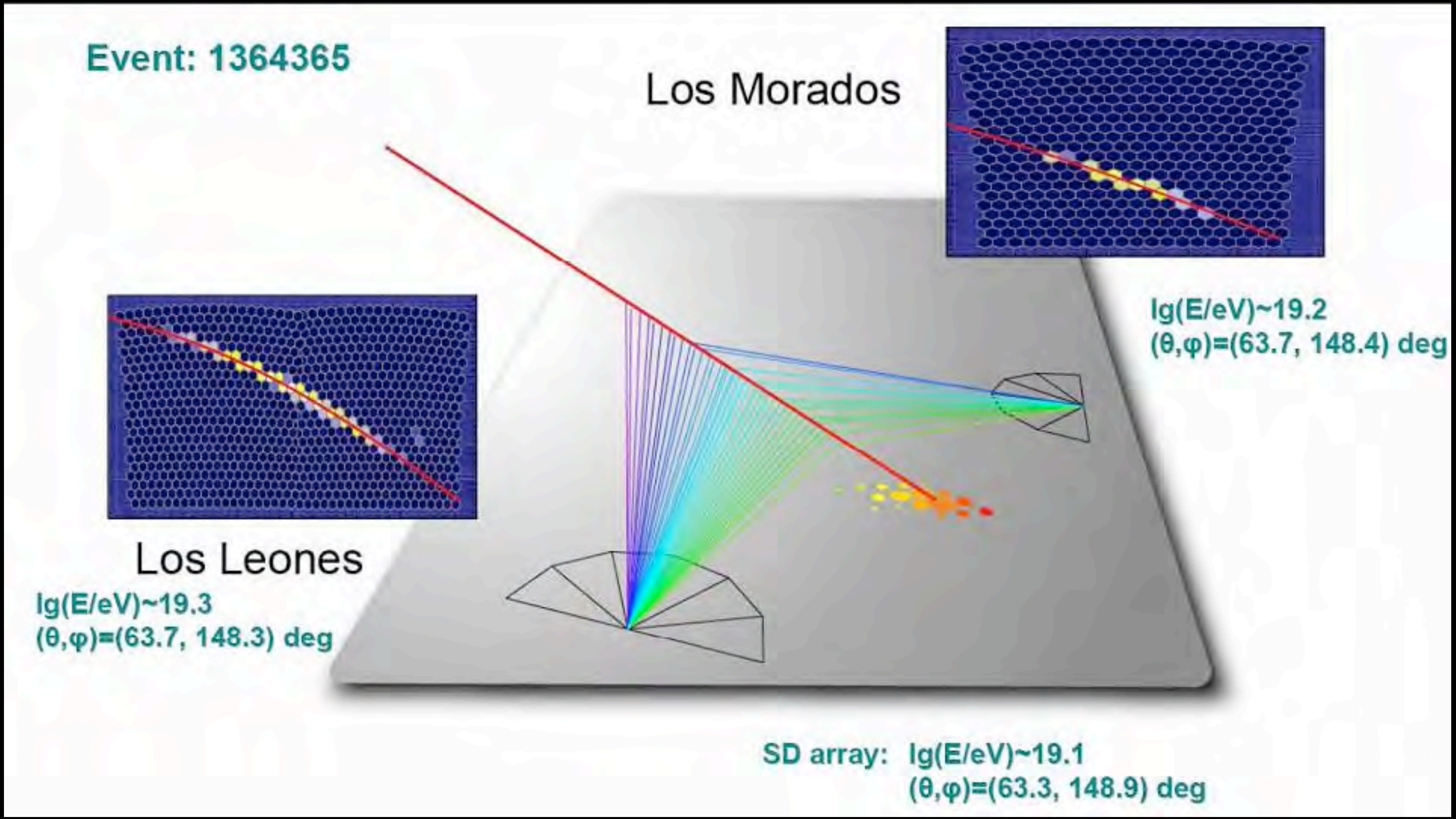

When an EAS is observed by SD and FD simultaneously (hybrid event), the geometry of the shower is fixed by SD (core position).

The angular resolution becomes ≈ 0.5 deg

Primary energy determination: SD

SD measures the lateral structure of the shower at ground

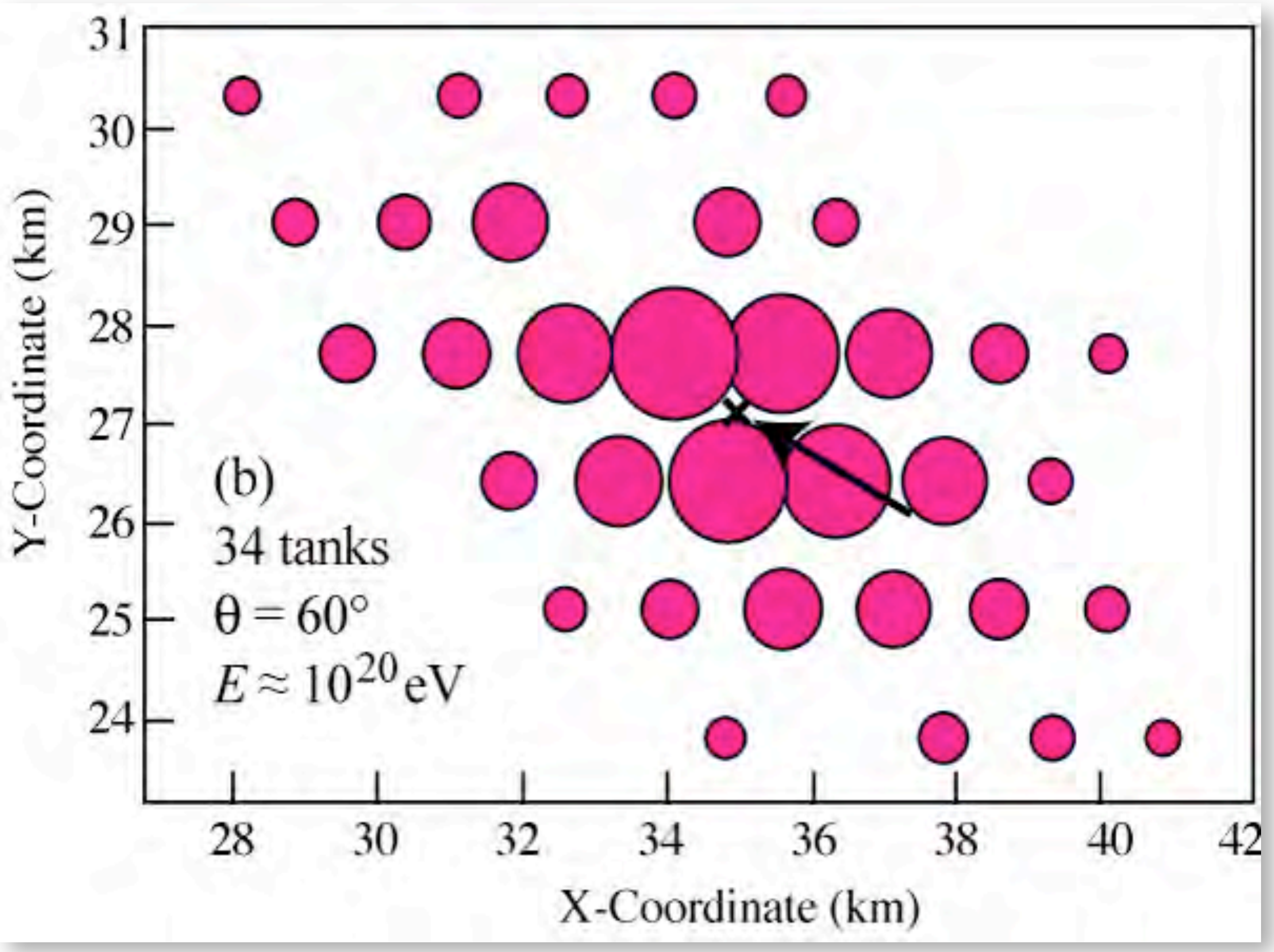

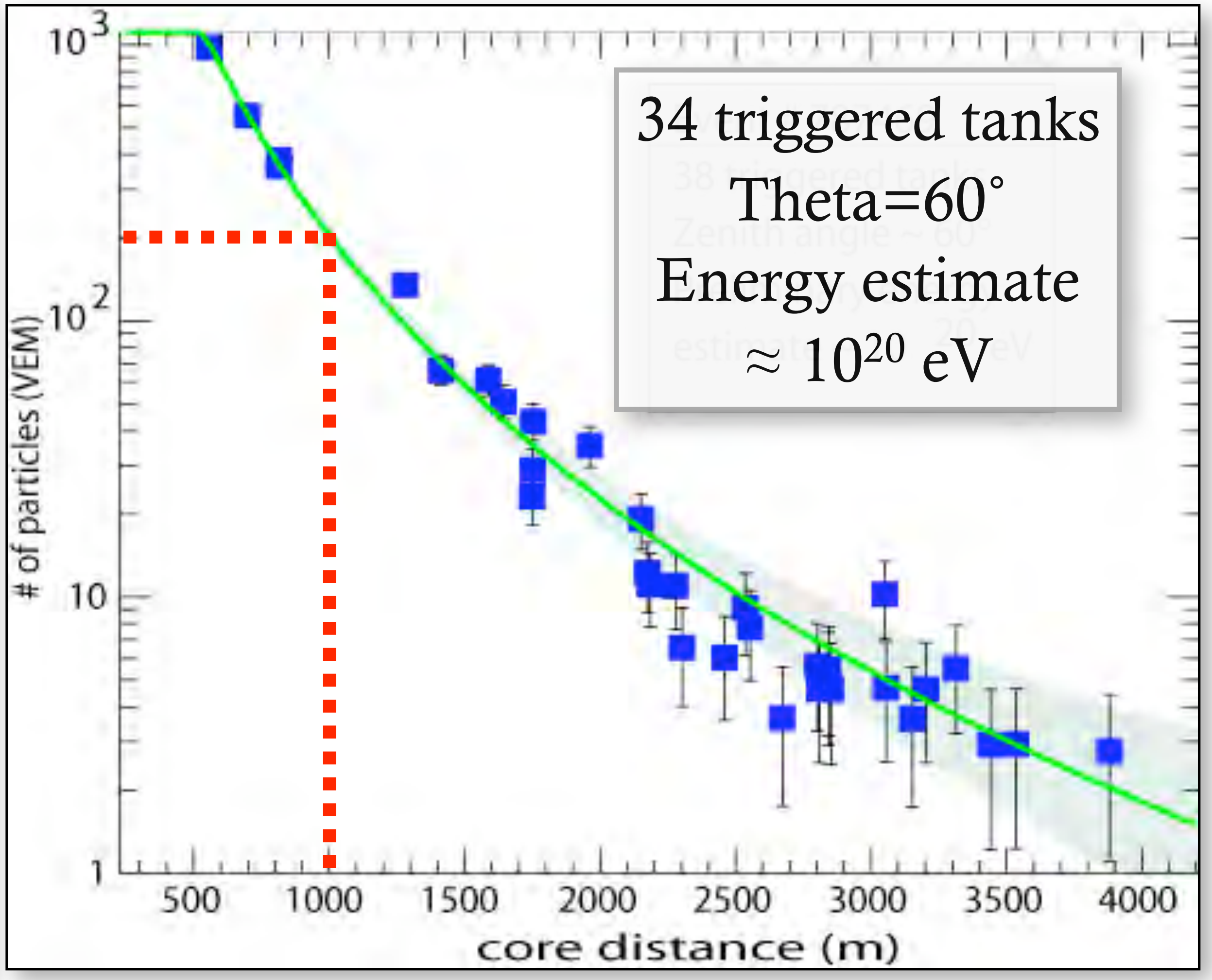

One event seen by SD **Particle lateral distribution**

- Reconstruct geometry (arrival direction & impact point)
- Fit particle lateral distribution (LDF)
- **S(1000) [signal at 1000 m] is the Auger energy estimator**

  ("ideal" distance depends on detectors spacing)

Primary energy determination: FD

FD records the longitudinal profile of the shower during its development in atmosphere

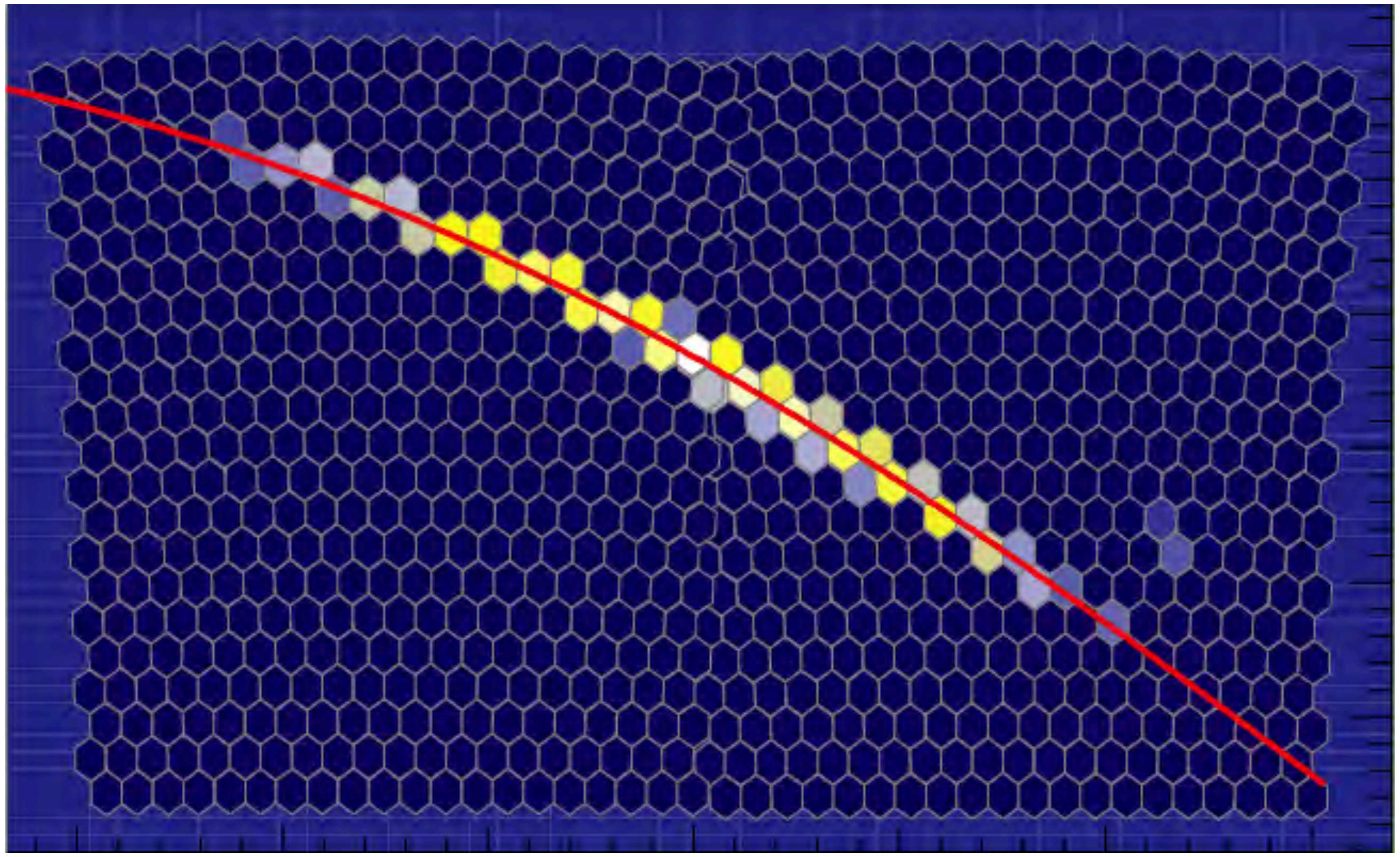

One event seen by FD

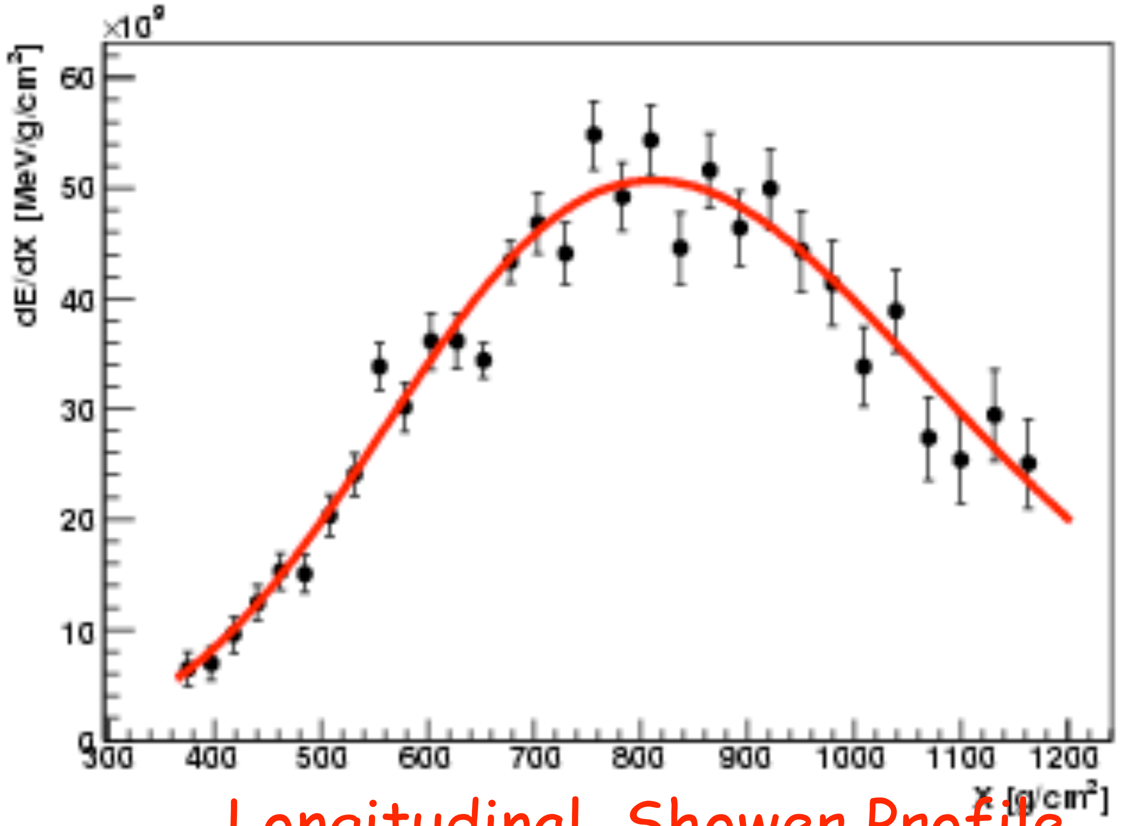

Longitudinal Shower Profile

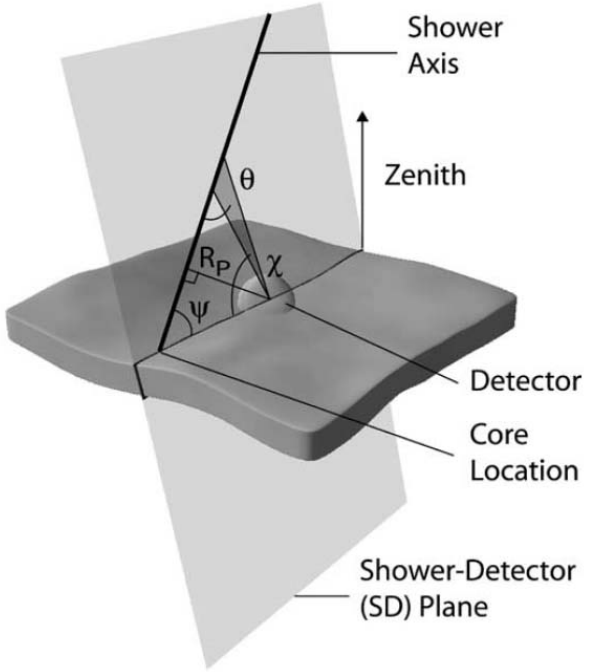

- Reconstruct geometry (shower detector plane, SDP, and shower axis in SDP)
- Fit longitudinal shower profile
- E ∝ area under the curve
- Calorimetric measurement

$$\int \frac{dE}{dX} dX \sim E$$

Primary energy determination: SD+FD

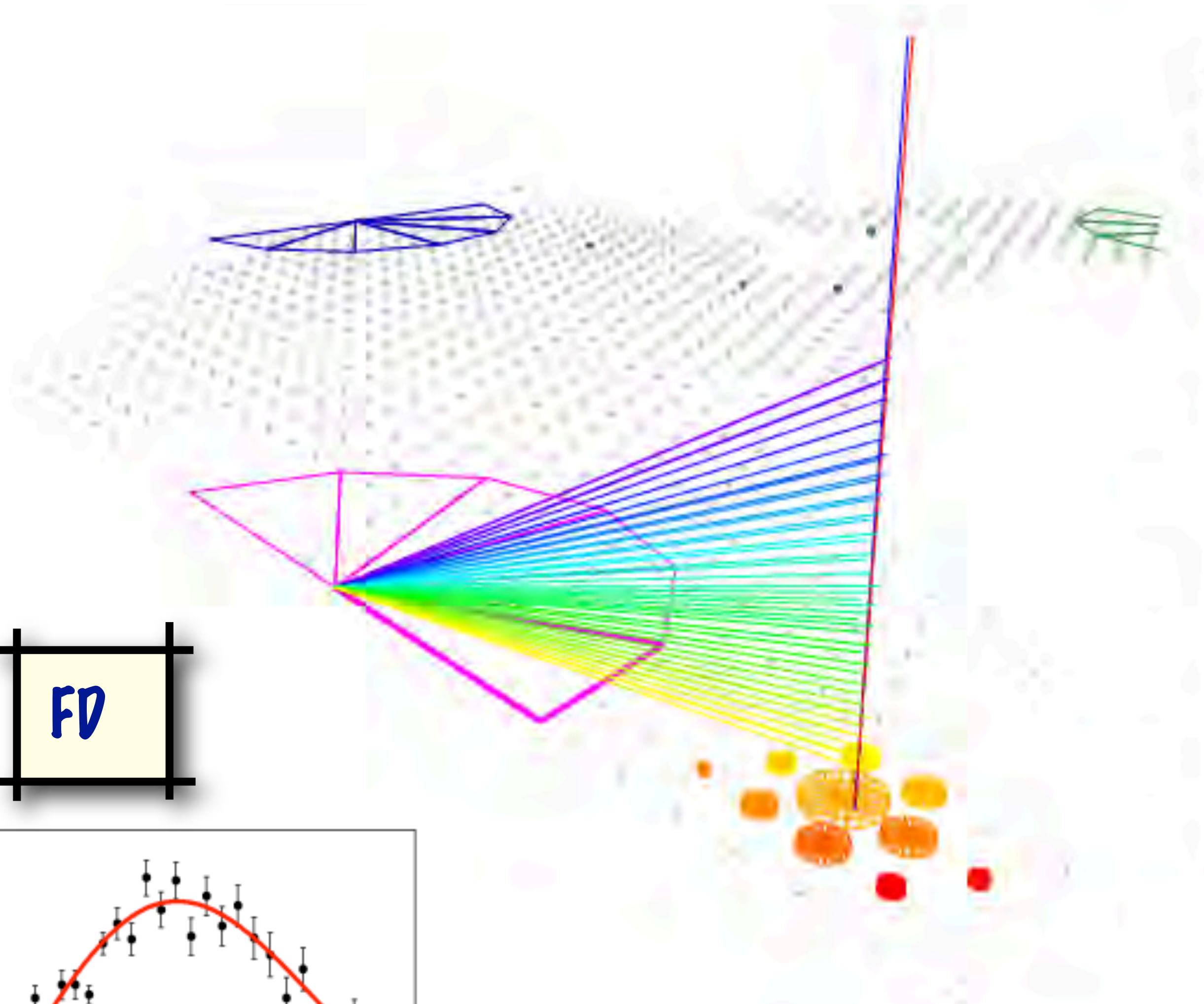

Hybrid Events are used to calibrate the SD energy estimator, S(1000) (converted to the median zenith angle, S38) from the FD calorimetric energy

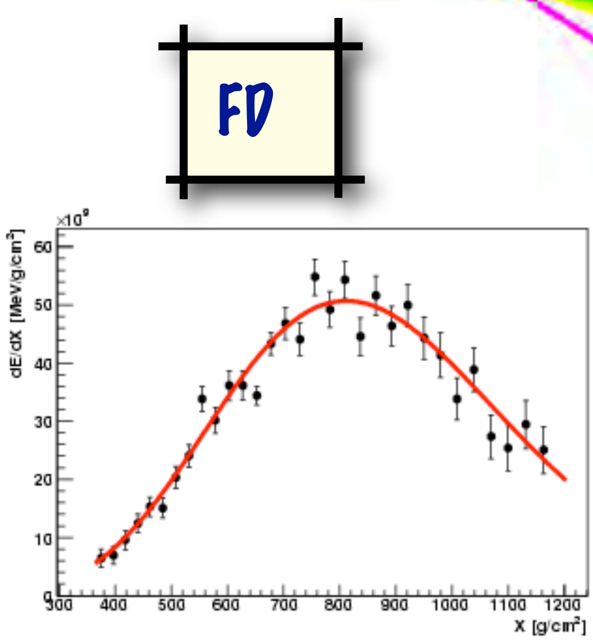

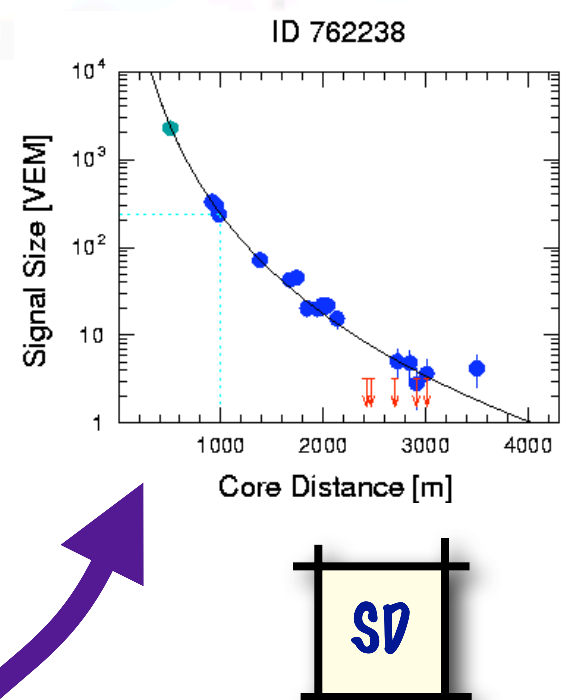

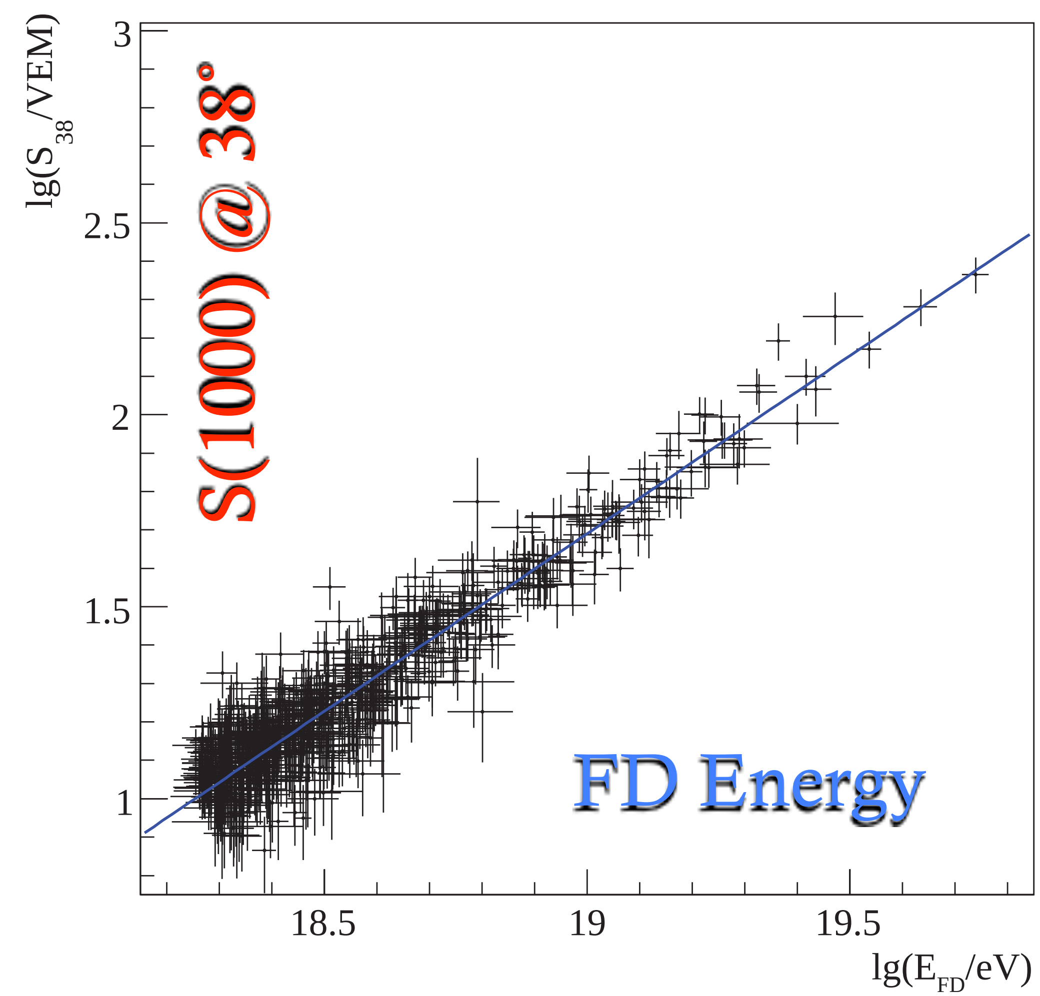

Primary energy determination: SD+FD

Hybrid Events are used to calibrate the SD energy estimator, S(1000) (converted to the mediam zenith angle, S38) from the FD calorimetric energy

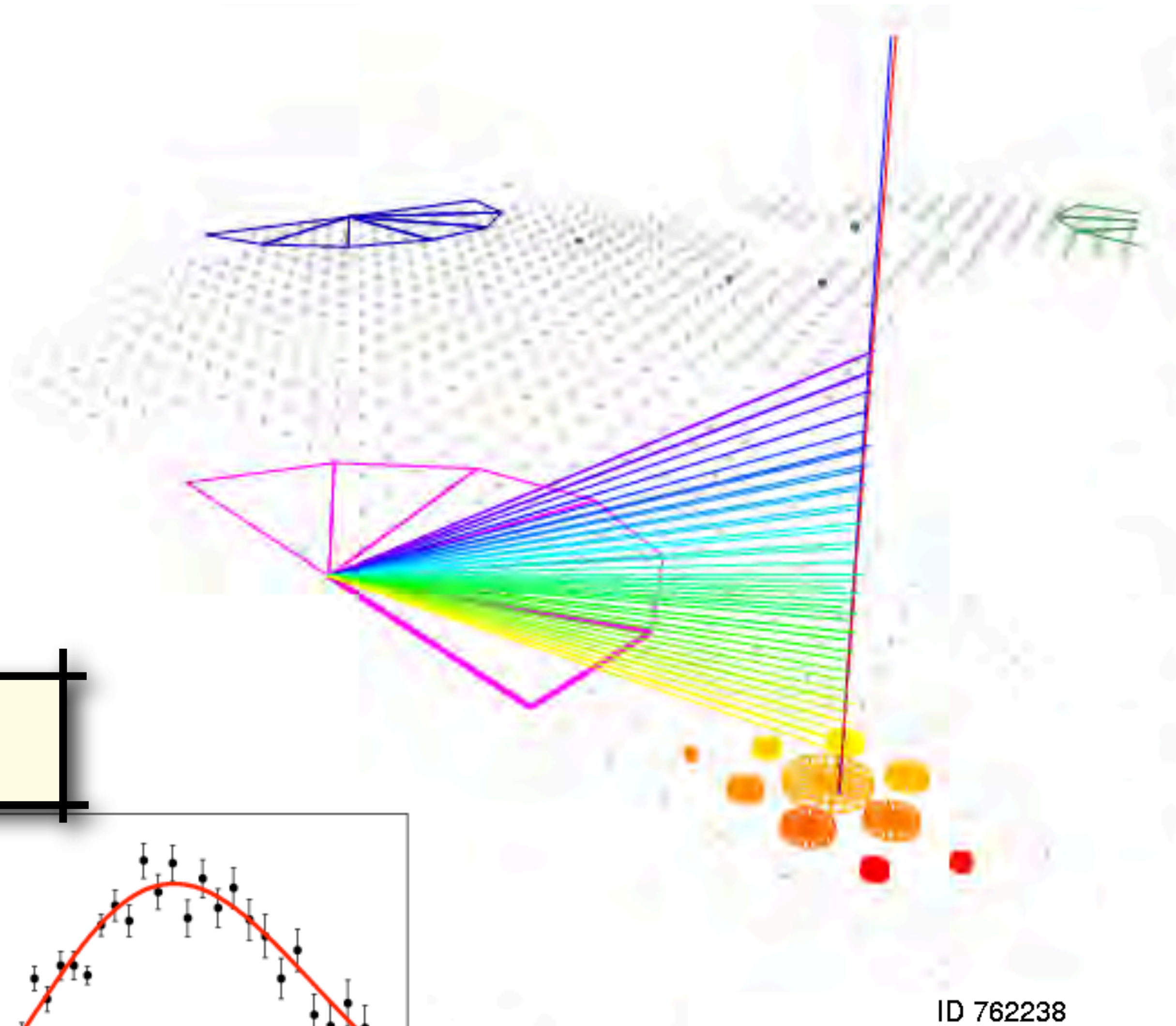

FD

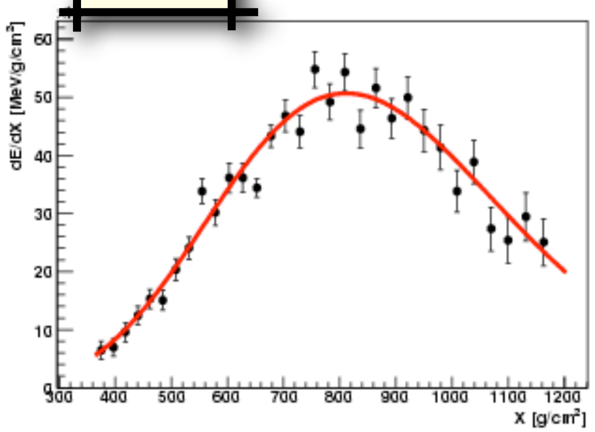

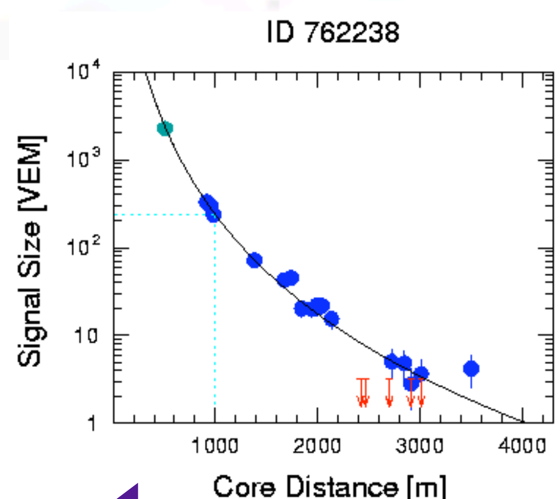

SD

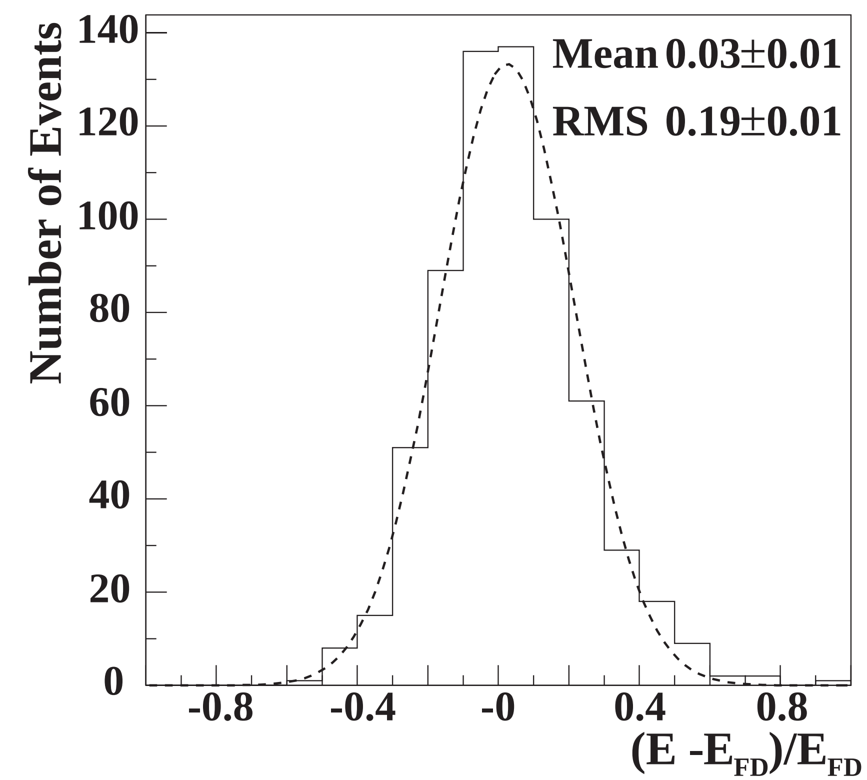

Energy resolution: statistical ≈ 19%

FD Energy systematic uncertainty

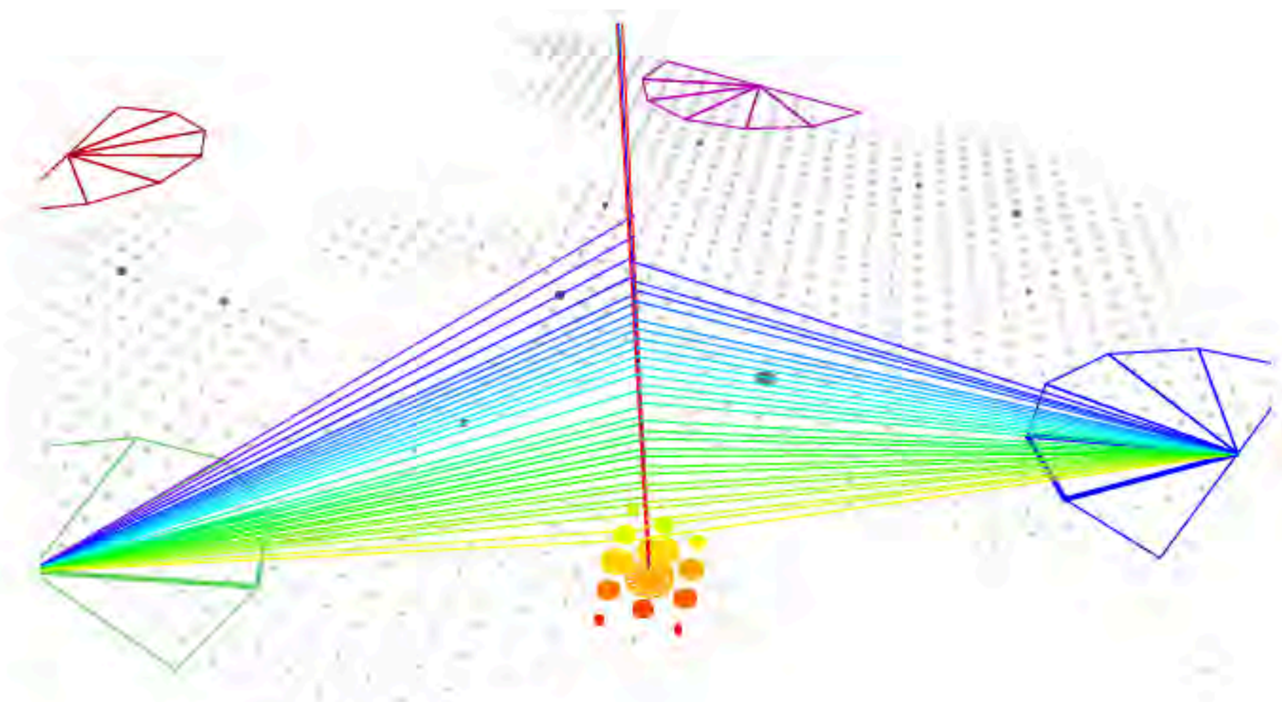

Stereo events

⇒ reconstruction uncertainty

- 10%, consistent with MC

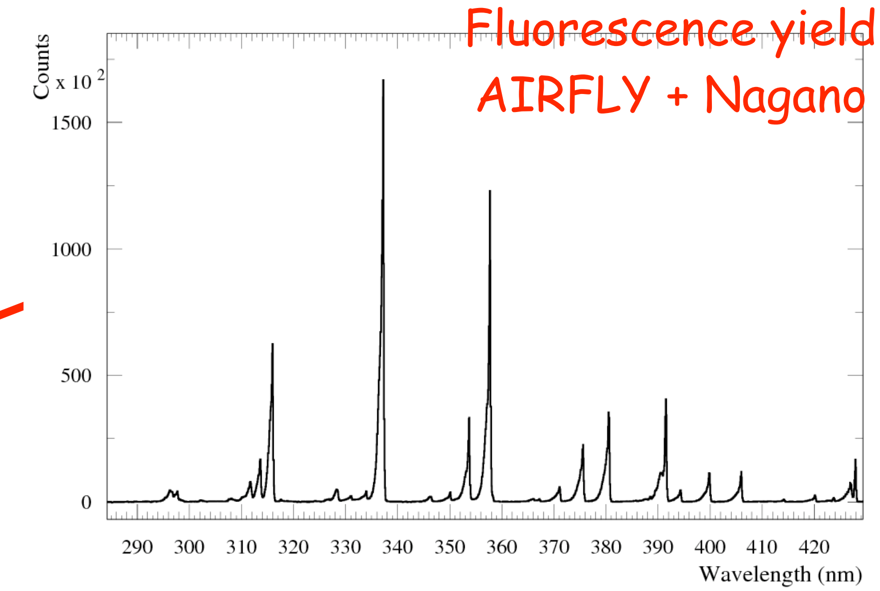

Source	Systematic uncertainty
Fluorescence yield	14%
P,T and humidity effects on yield	7%
Calibration	9.5%
Atmosphere	4%
Reconstruction	10%
Invisible energy	4%
TOTAL	22%

Total FD E uncertainty: 22%

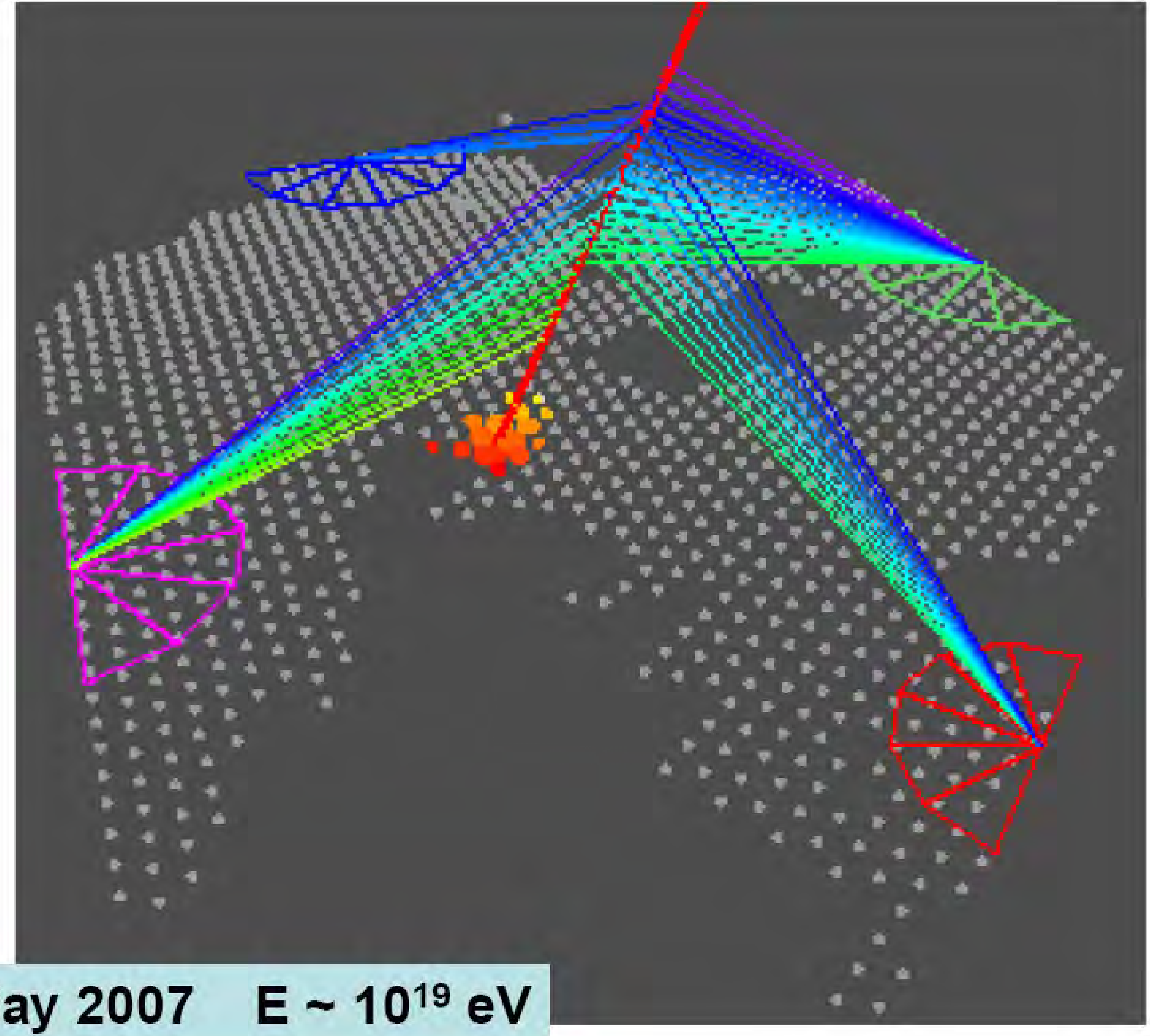

20 May 2007 E ~ 10^{19} eV

Extending the energy range with hybrid events

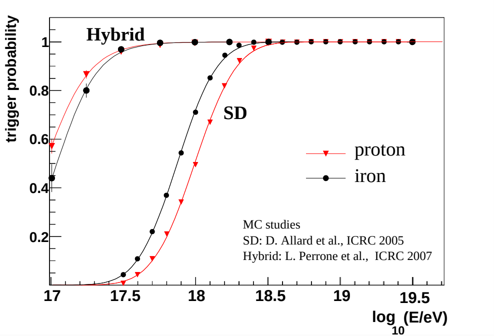

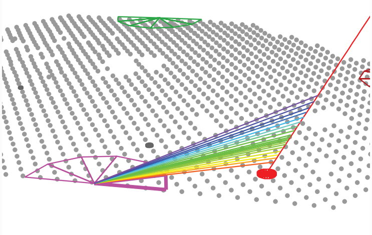

- energy threshold $10^{18}\,\mathrm{eV}$ covering the ankle region
- good energy resolution $\sigma(E)/E < 10\%$
- calorimetric energy measurement

Veberič (633),
Valore (920),
Chirinos (994),
Bonifazi (1079),
Micheletti (1081)

STATUS & PERFORMANCE

Extensive monitoring of atmosphere and of performances

PIERRE AUGER OBSERVATORY

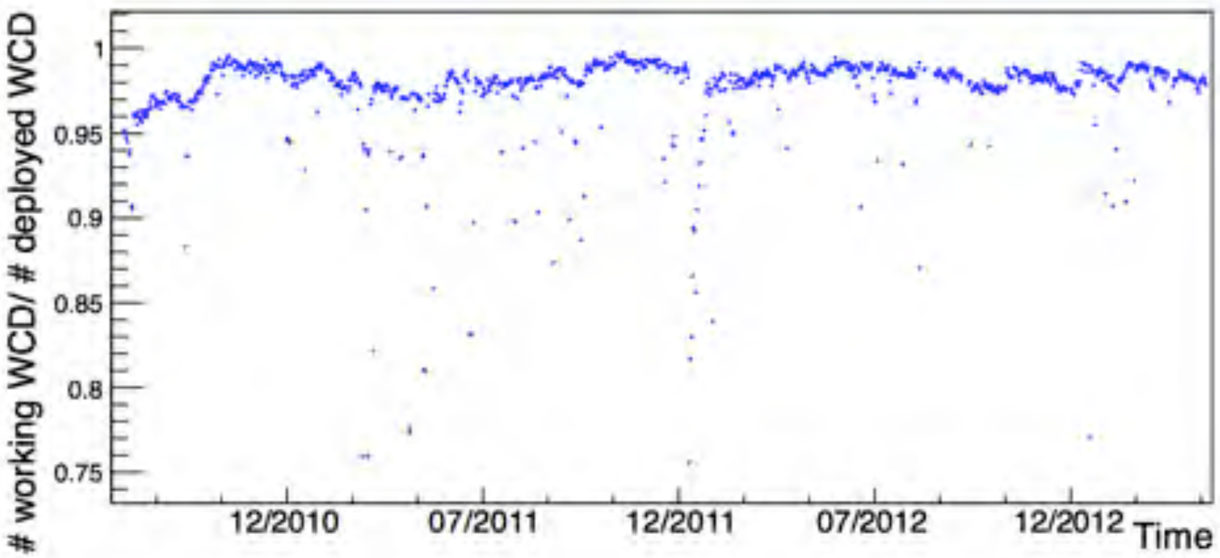

Array activity

Cloud monitoring

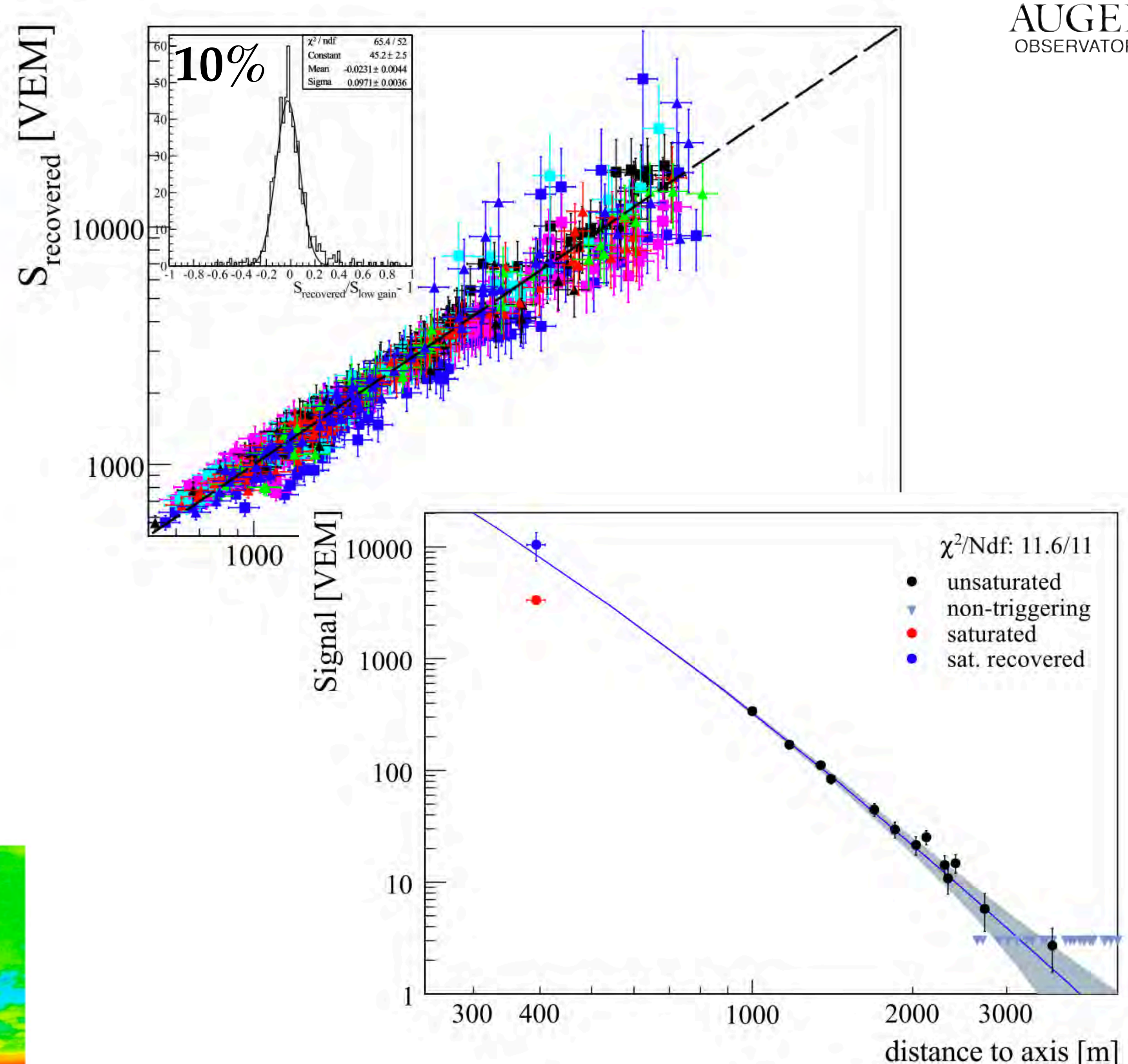

Treatment of saturated SD signals

ENERGY SCALE I

Telescope optical properties

PIERRE AUGER OBSERVATORY

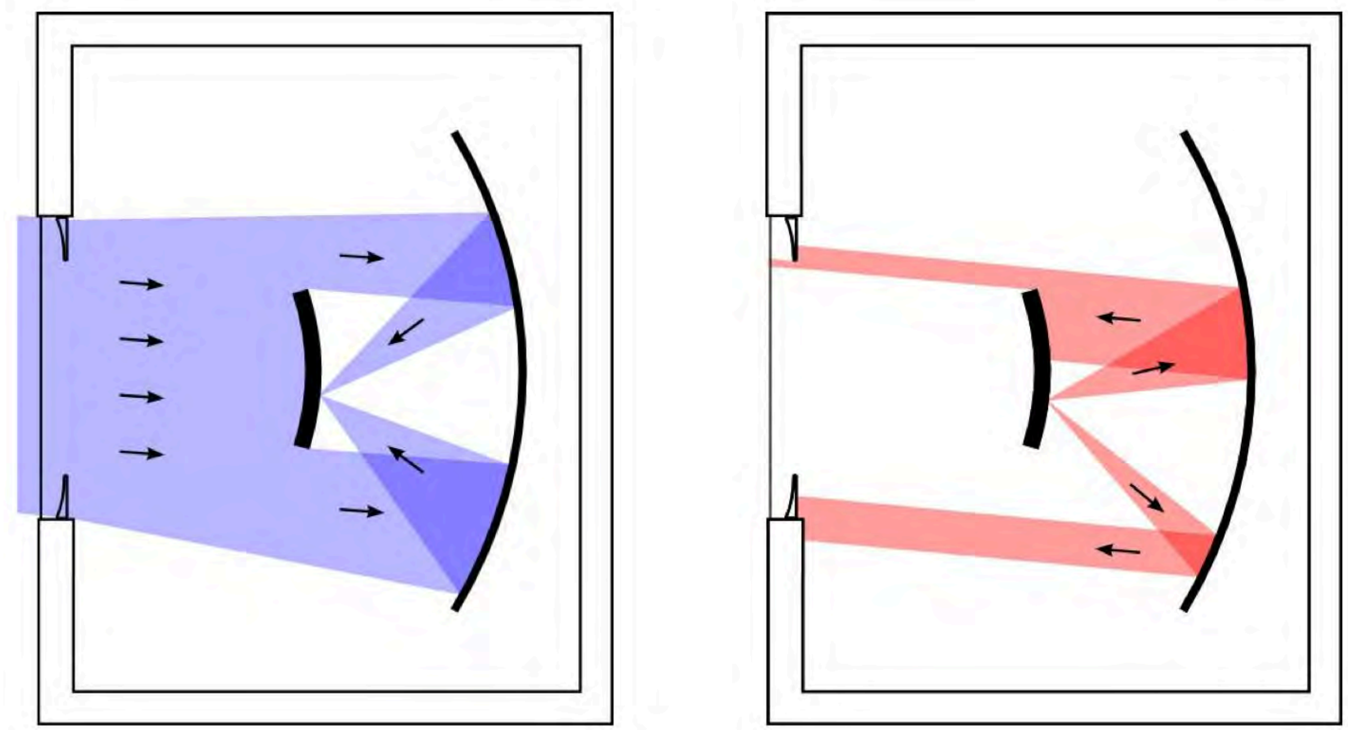

Joint Auger/TA effort to conduct a common calibration campaign

"To study the optics of the telescope in more detail, telescope components like the mirror, the camera, the corrector lens or the filter have been manipulated (e.g. cleaned), covered or removed."

Ravignani (693), Tueros (705),
Schulz (769), Bäuml (806),
Verzi (928), Matthews (1218)

ENERGY SCALE III

PIERRE AUGER OBSERVATORY

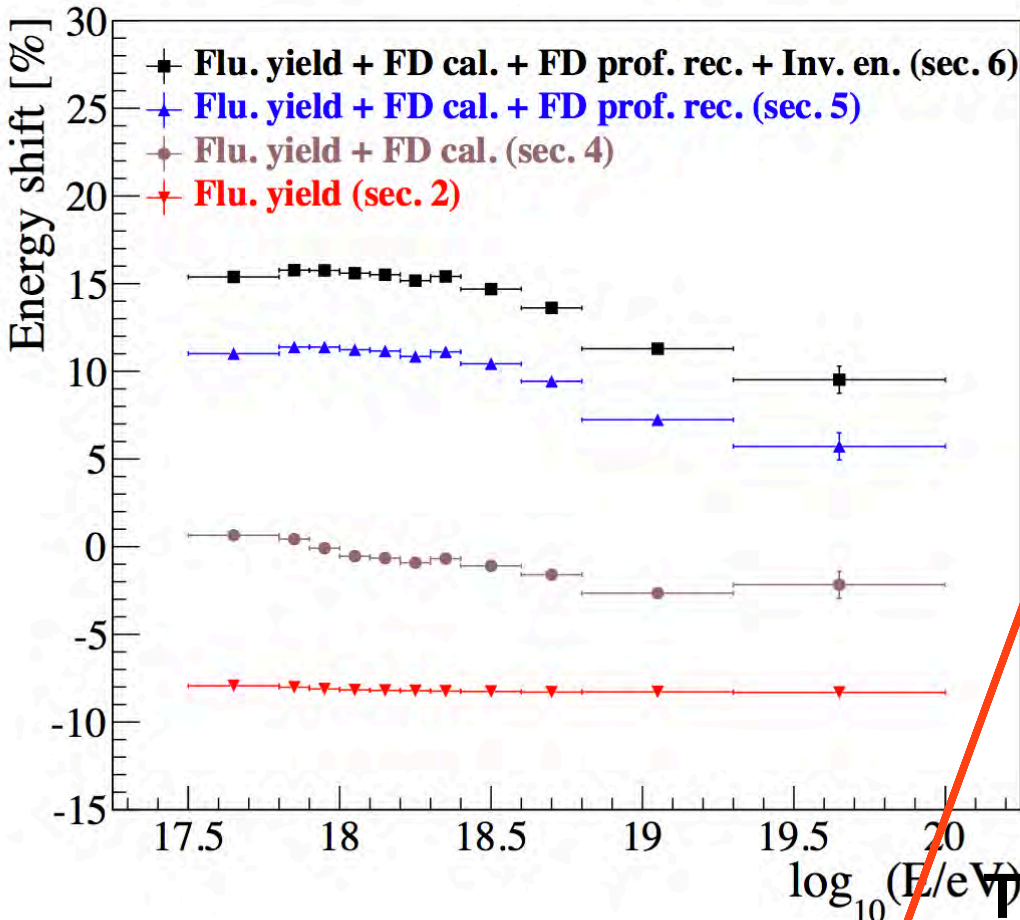

Uncertainties entering into the SD calibration fit	
Sub total FD energy resolution	7% ÷ 8%
Sub total SD energy resolution	17% ÷ 12%

1 EeV 10 EeV

The fluorescence yield

The atmosphere

The absolute calibration of the telescopes

Reconstruction of the longitudinal profile of the showers

The invisible energy

Changes in FD energies at 10^{18} eV	
Airfly fluorescence yield (sec. 2)	-8.2%
New optical efficiency	4.3%
Calibr. database update	3.5%
Sub total (FD calibration - sec. 4)	7.8%
Likelihood fit of the profile	2.2%
Folding with the point spread function	9.4%
Sub total (FD profile reconstruc. - sec. 5)	11.6%
New invisible energy (sec. 6)	4.4%
Total	15.6%

Systematic uncertainties on the energy scale	
Absolute fluorescence yield	3.4%
Fluor. spectrum and quenching param.	1.1%
Sub total (Fluorescence yield - sec. 2)	3.6%
Aerosol optical depth	3%÷6%
Aerosol phase function	1%
Wavelength depend. of aerosol scatt.	0.5%
Atmospheric density profile	1%
Sub total (Atmosphere - sec. 3)	3.4%÷6.2%
Absolute FD calibration	9%
Nightly relative calibration	2%
Optical efficiency	3.5%
Sub total (FD calibration - sec. 4)	9.9%
Folding with point spread function	5%
Multiple scattering model	1%
Simulation bias	2%
Constraints in the Gaisser-Hillas fit	3.5% ÷ 1%
Sub total (FD profile rec. - sec. 5)	6.5% ÷5.6%
Invisible energy (sec. 6)	3%÷1.5%
Stat. error of the SD calib. fit (sec. 7)	0.7%÷1.8%
Stability of the energy scale (sec. 7)	5%
Total	14%

AUGER ENERGY SPECTRA

Ravignani (693),
Tueros (705),
Schulz (769),
Bäuml (806),
Verzi (928),
Matthews (1218)

PIERRE AUGER OBSERVATORY

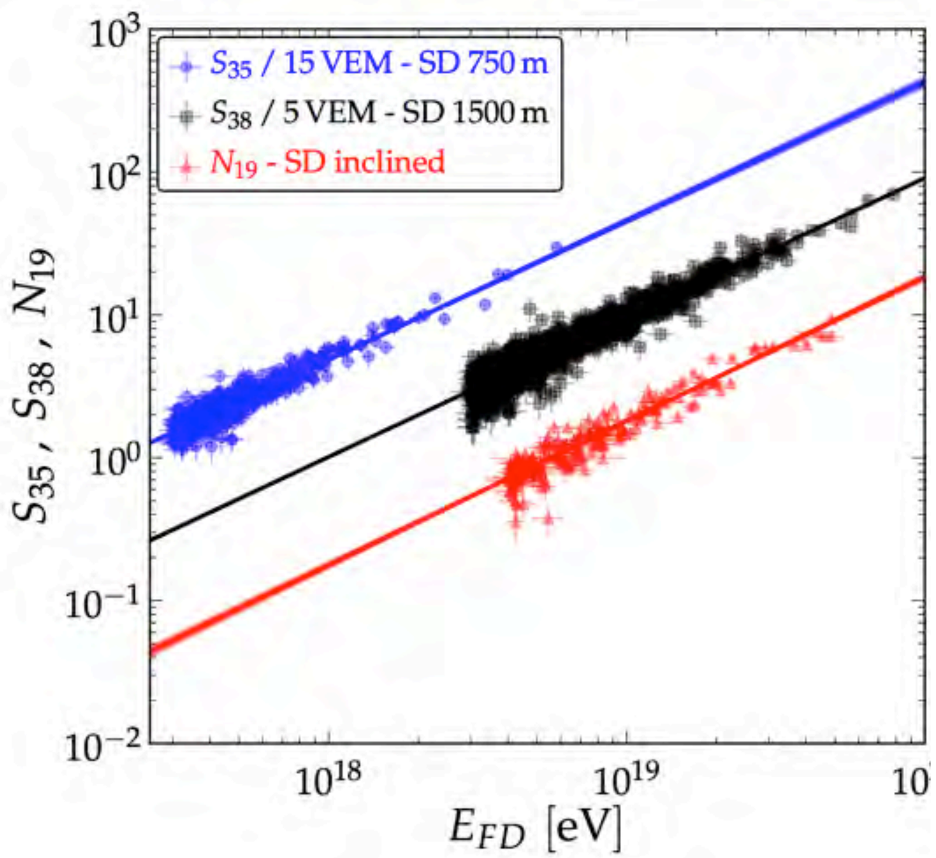

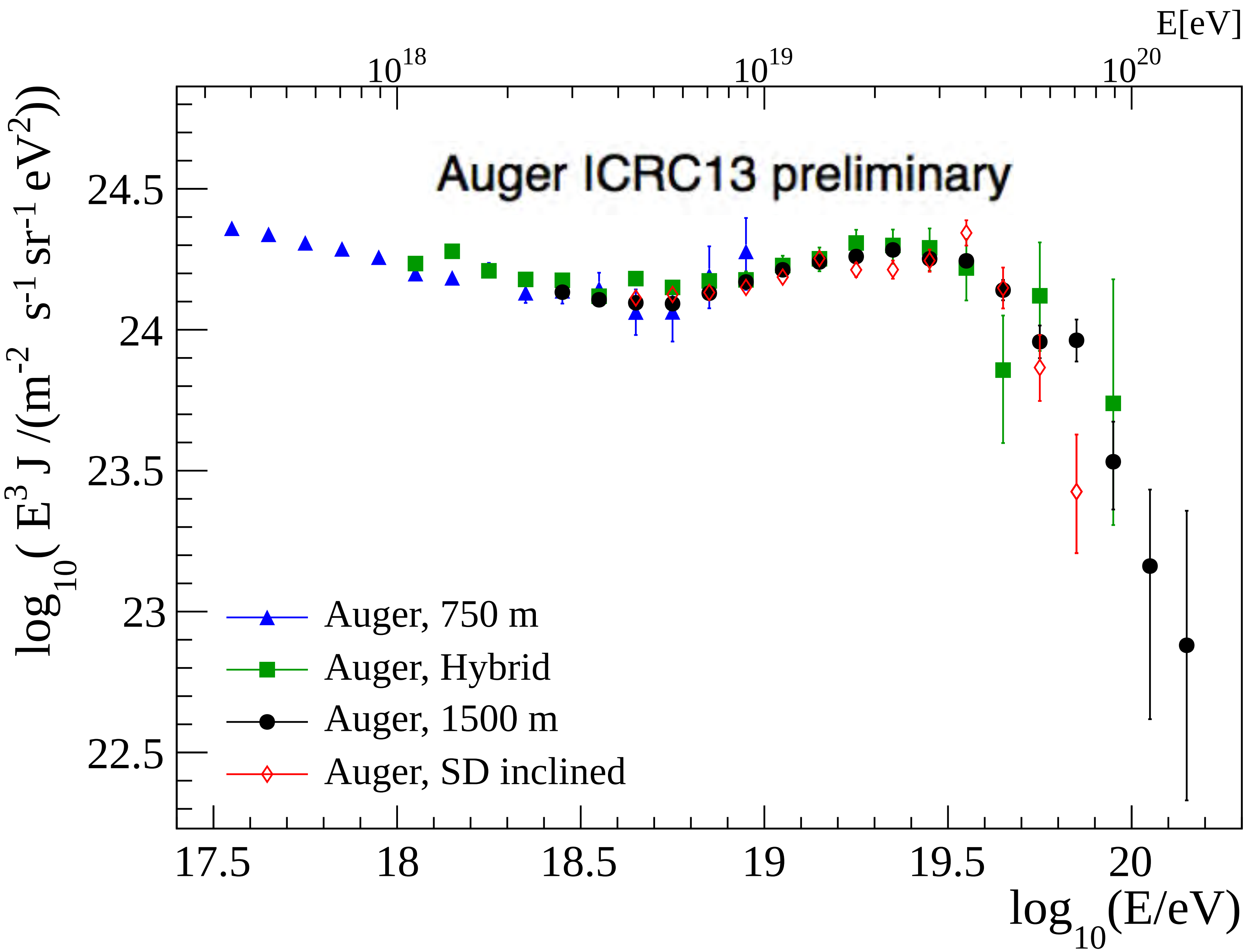

Ravignani (693), Tueros (705), Schulz (769), Bäuml (806),Verzi (928), Matthews (1218)

THE AUGER ENERGY SPECTRUM

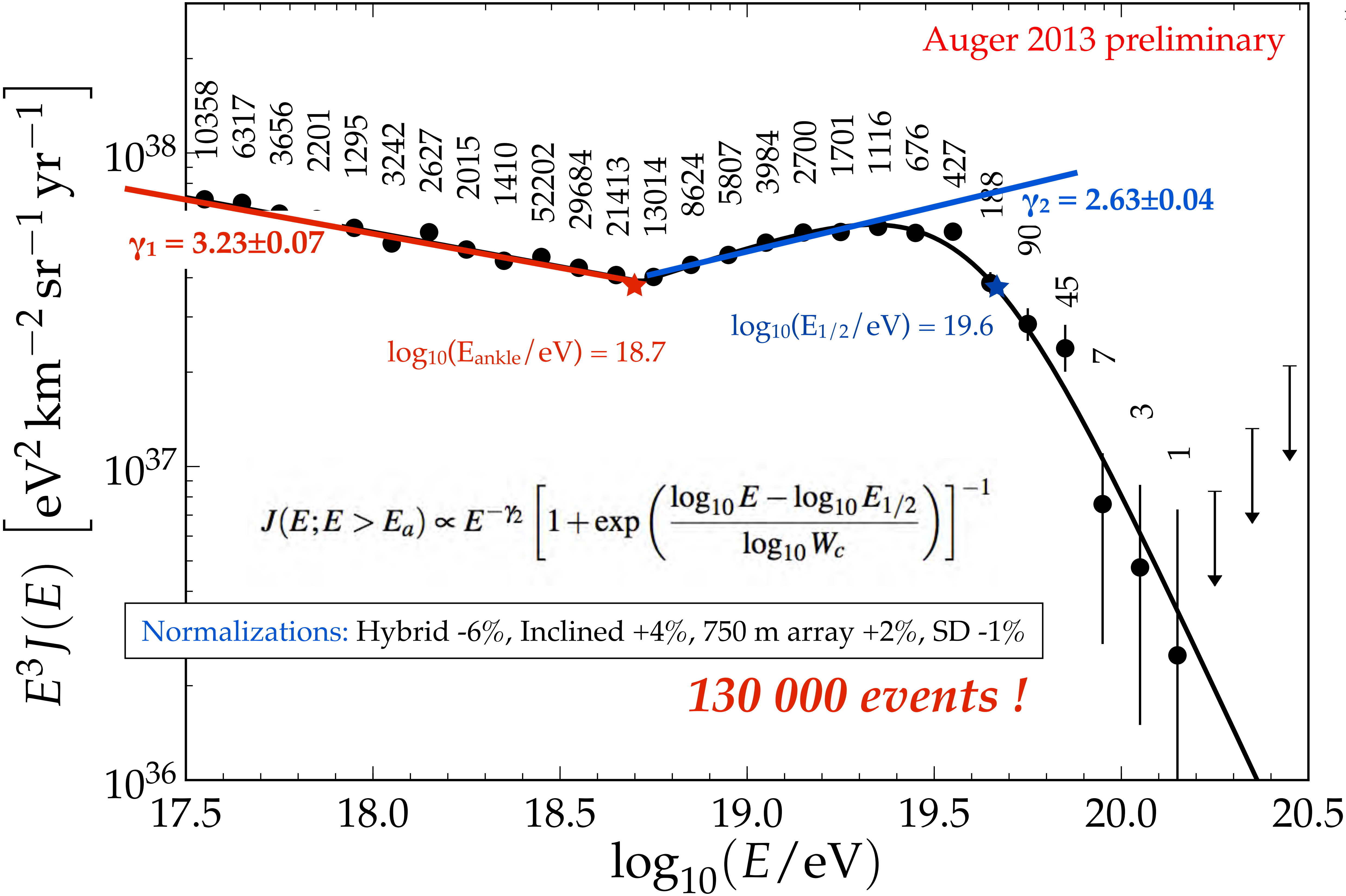

MASS COMPOSITION

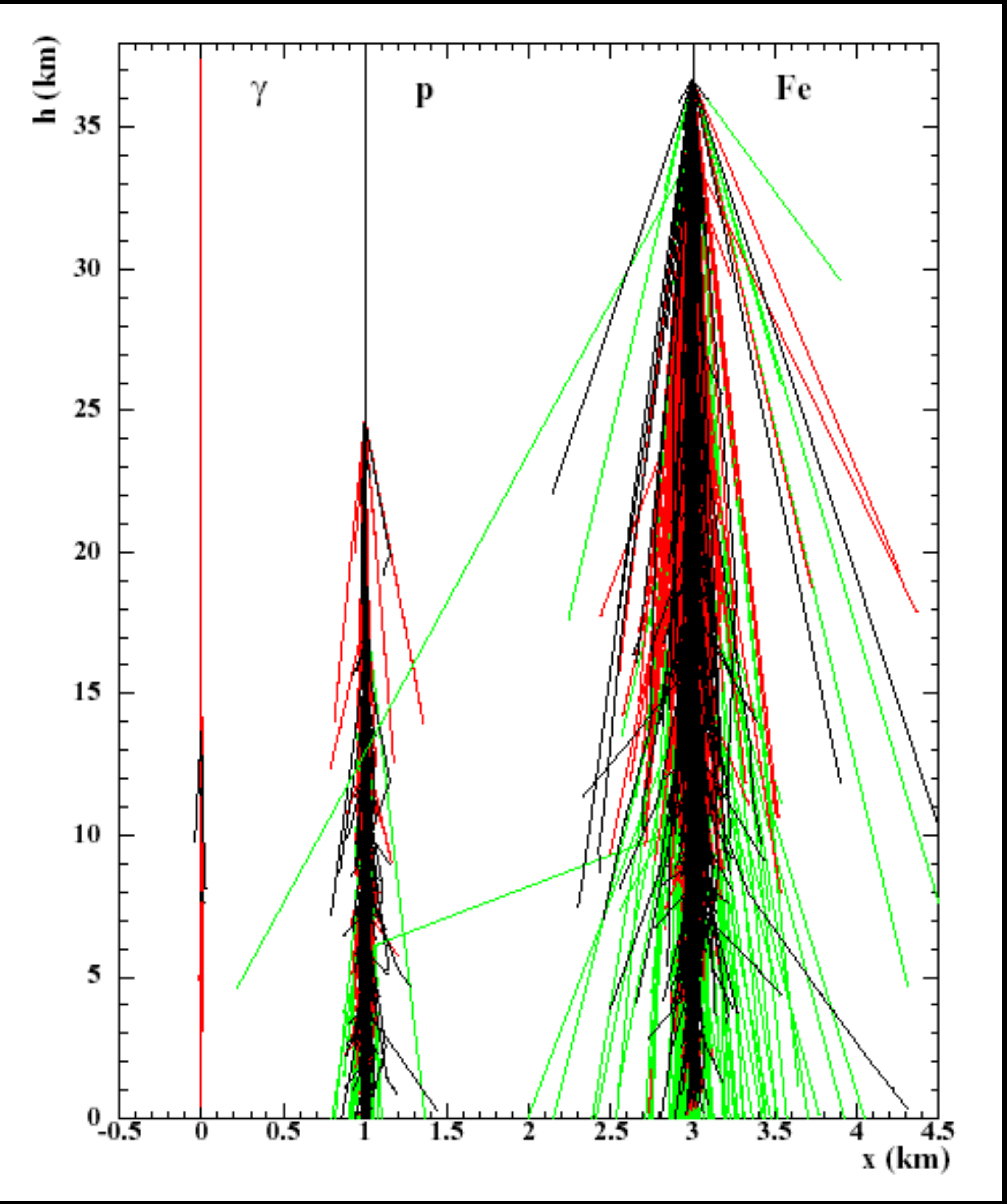

- Observables sensitive to composition:
  - Relative number of electrons and muons (primary nucleus produces more muons than a primary proton)
  - Depth of shower maximum (at fixed energy, a nucleus-shower develops faster than a proton-shower)
  - Shower front curvature (the higher the first interaction, the flatter the front)
- Subtlety of the analysis:
  - Great complexity: requires the use of shower simulations
  - Uncertainties in the simulations:
    - Sensitivity to nuclear models (interaction CR-air nucleus)
    - Energy domain not always covered by accelerators

MASS COMPOSITION WITH THE FLUORESCENCE DETECTOR

Xmax, depth of EAS maximum, is the main EAS observable sensitive to CR mass

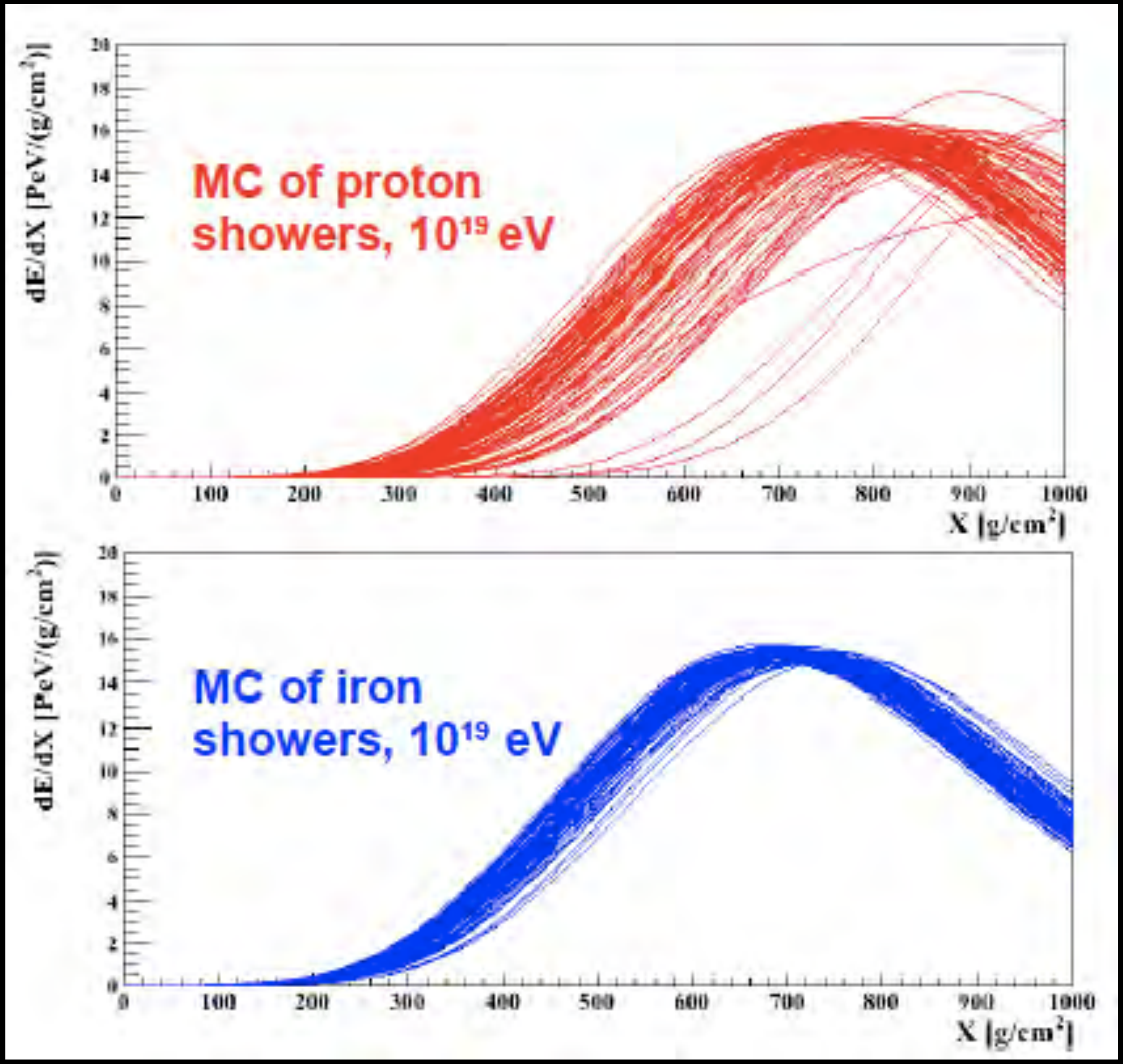

First interaction of heavy primaries is shallower and fluctuates less.
RMS(Xmax) mass sensitive too

EAS development observed by FD:
Xmax accuracy ≈ 20 g/cm2 (by "stereo" events)

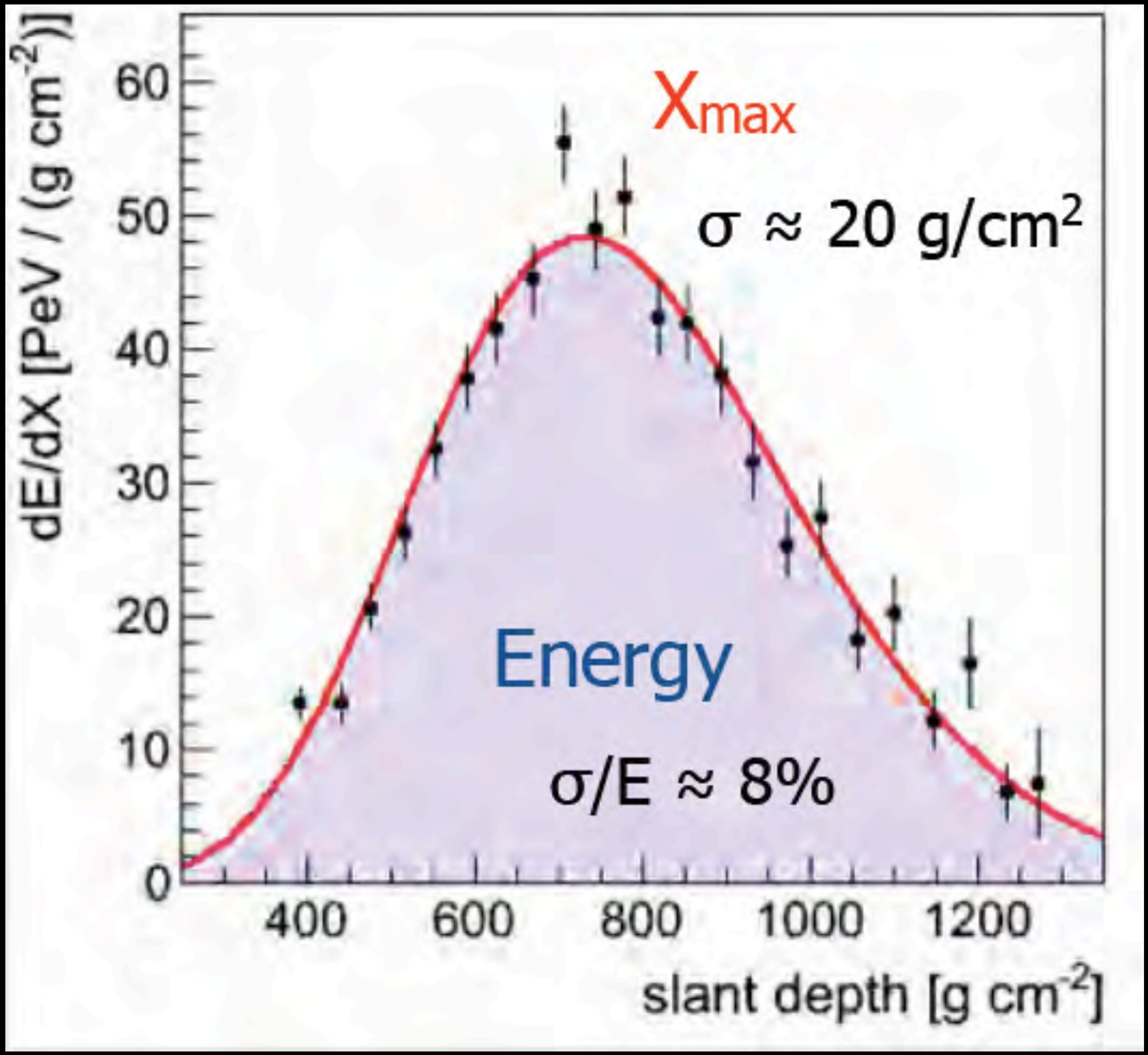

N.B.: the "correspondence" XMAX-mass depends on extrapolations of hadronic models at UHE!

Kuempel (669),
Ahn (690),
Garcia-Gamez (694),
Pieroni (697),
de Souza (751),
Hanlon (964)

MASS COMPOSITION I

<X_{max}> and $\sigma(X_{max})$ data

PIERRE AUGER OBSERVATORY

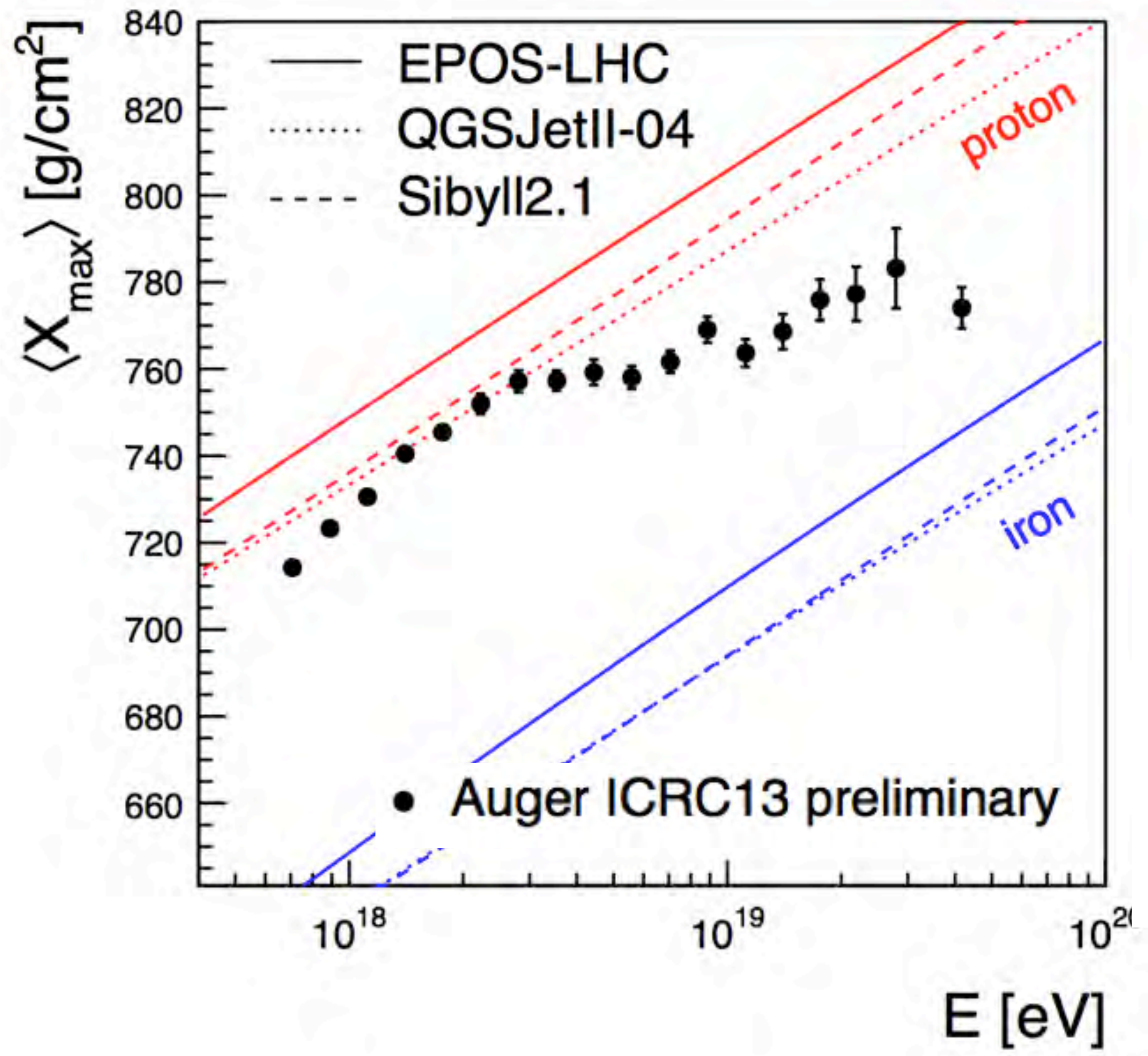

Extensive cross checks and verifications

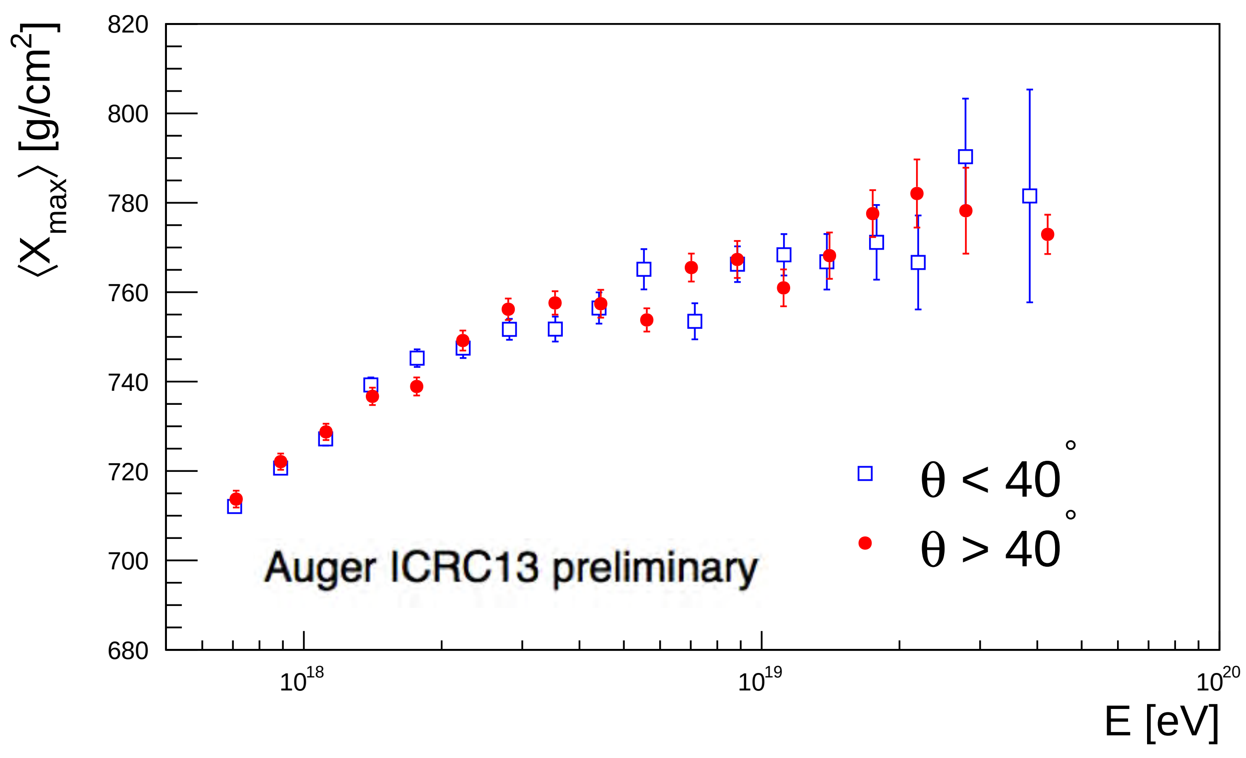

Kuempel (669),
Ahn (690),
Garcia-Gamez (694),
Pieroni (697),
de Souza (751),
Hanlon (964)

MASS COMPOSITION I

$\langle X_{max} \rangle$ and $\sigma(X_{max})$ data

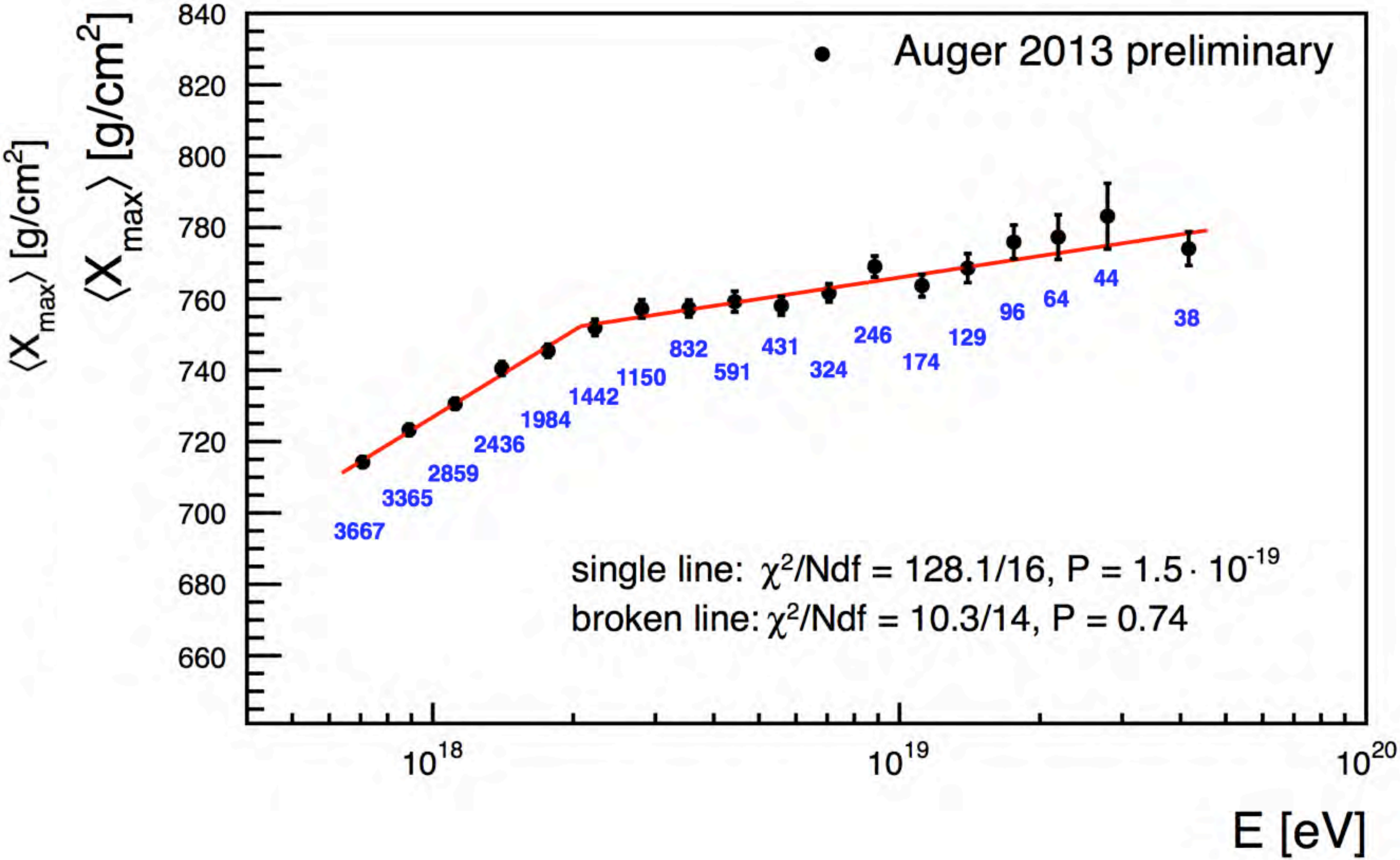

Kuempel (669),
Ahn (690),
Garcia-Gamez (694),
Pieroni (697),
de Souza (751),
Hanlon (964)

MASS COMPOSITION II

$\langle X_{max} \rangle$ and $\sigma(X_{max})$ data

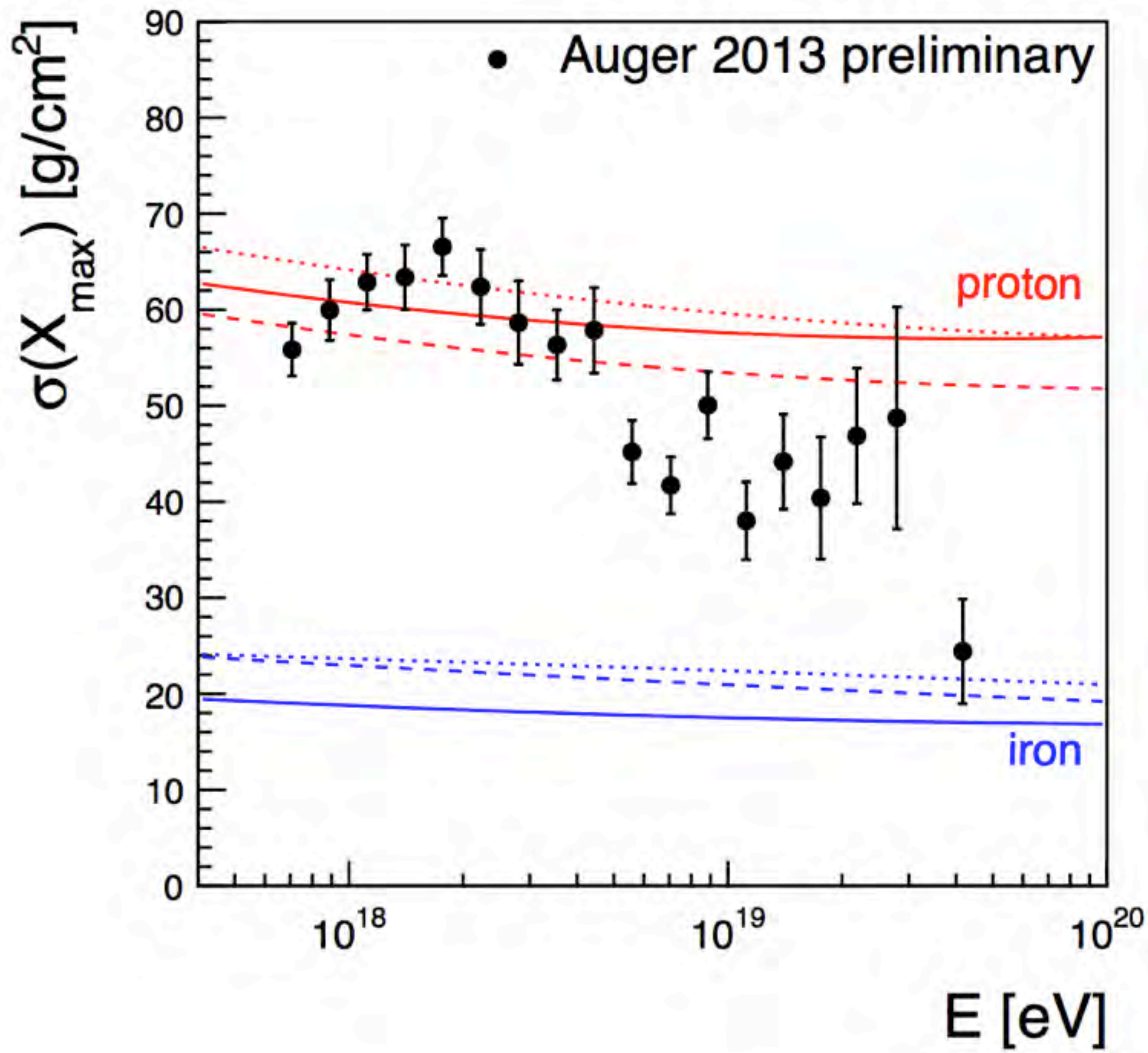

Asymmetry of the Signal Risetime

Vertical
symmetry in the signals

Inclined
asymmetry!!

Very inclined
no asymmetry

$< t_{1/2}/r >= a + b\cos\zeta$
(by grouping events in E and $sec\theta$ bins)

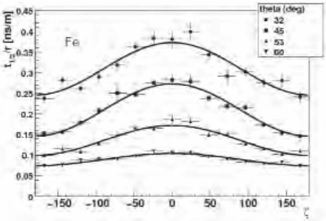

Early-late asymmetry b/a.
Θ is the b/a maximum,
is sensitive to the primary mass

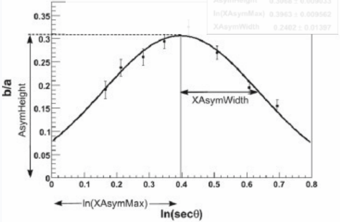

Θ results

D. Garcia-Pinto, ICRC 2011

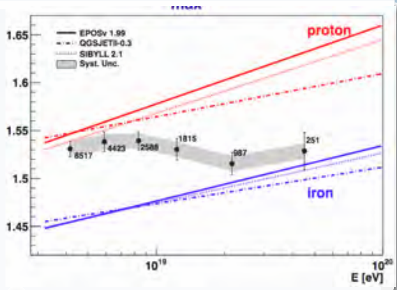

Data from January 2004 to December 2010
18581 events selected

Quality cuts

- Events with $E > 3 \times 10^{18}\mathrm{eV}$
- $30^\circ < \theta < 60^\circ$
- Event must pass the fiducial trigger (T5 trigger)
- SD stations with $S > 10\mathrm{VEM}$ at $500m < r_{core} < 2000m$
- Hottest station cannot be saturated

Systematics: $\Theta \leqslant 10\mathrm{g/cm^2}$

- Core reconstruction
- Event selection
- Value of $t_{1/2}$ vs r

Kuempel (669), Ahn (690), Garcia-Gamez (694), Pieroni (697), de Souza (751), Hanlon (964)

MASS COMPOSITION V

Muon Production Depth distribution (MPD) in a nutshell

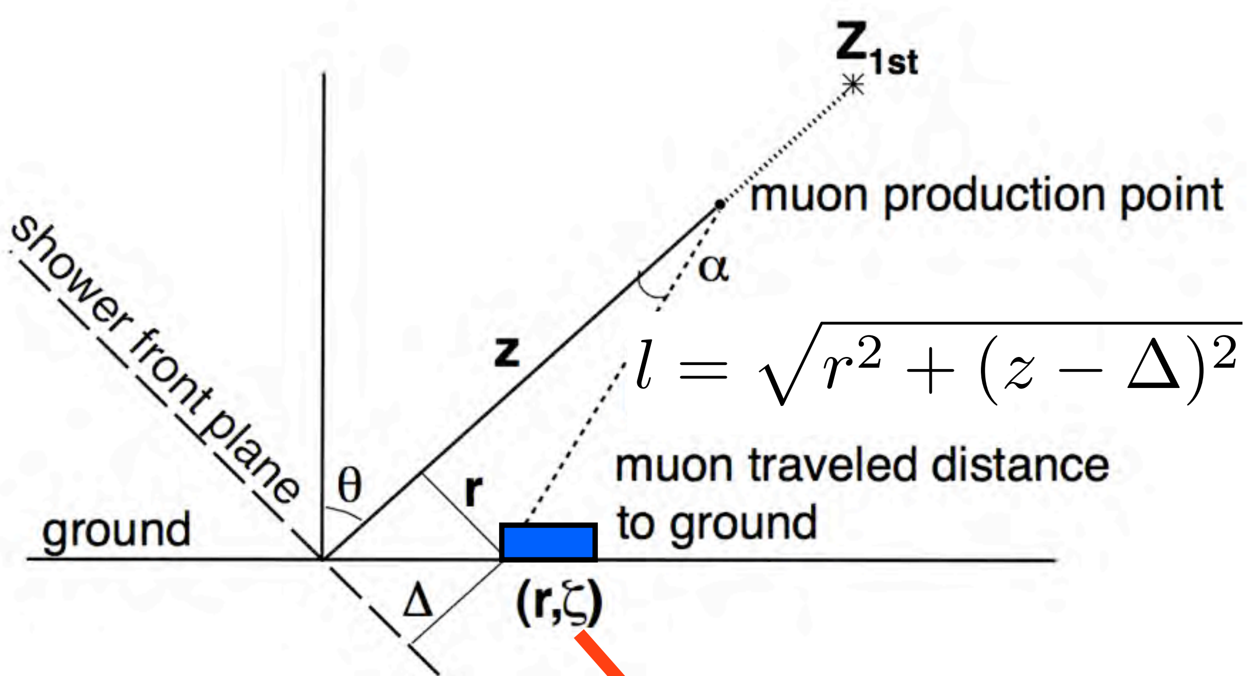

Measured

Obtained

$$z = \frac{1}{2}\left(\frac{r^2}{ct_g} - ct_g\right) + \Delta$$

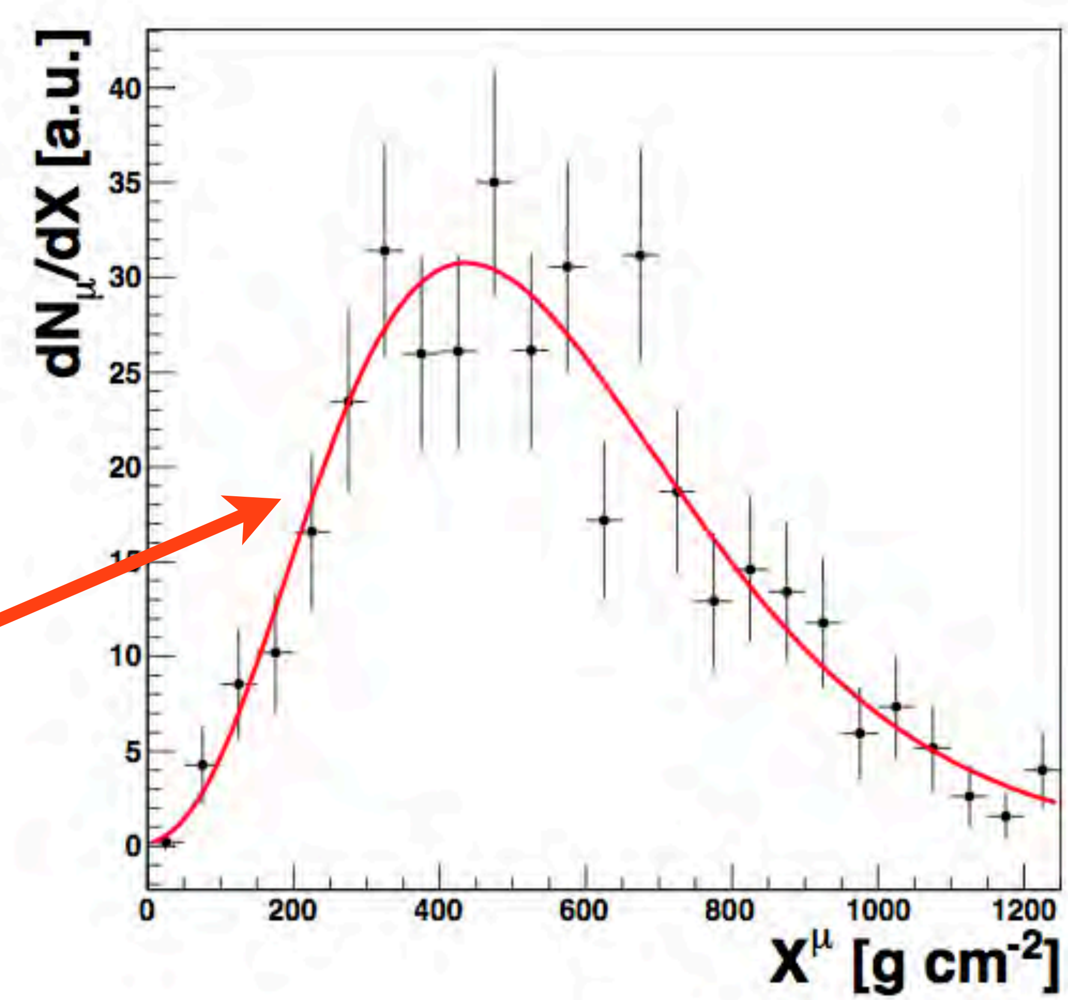

MASS COMPOSITION VI

MPD in a nutshell

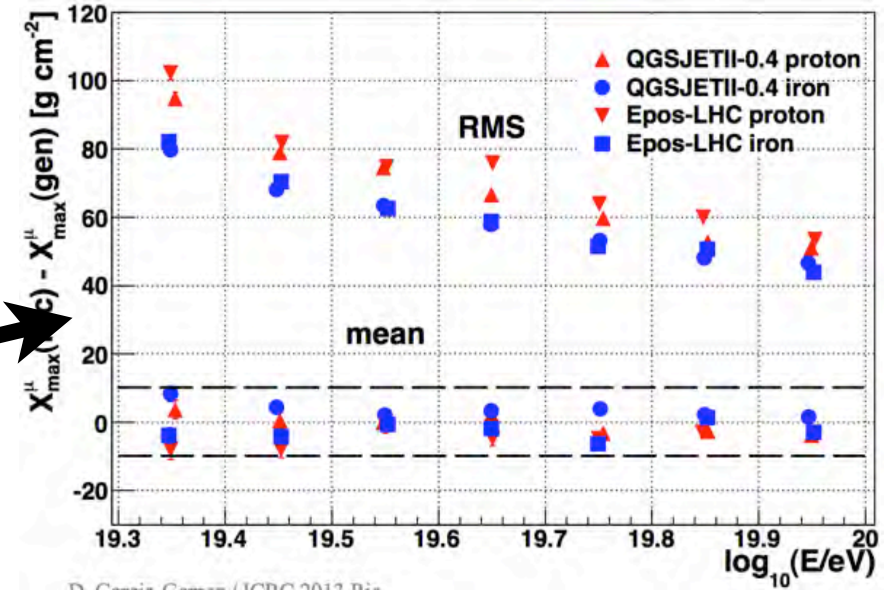

Decent resolution & no bias

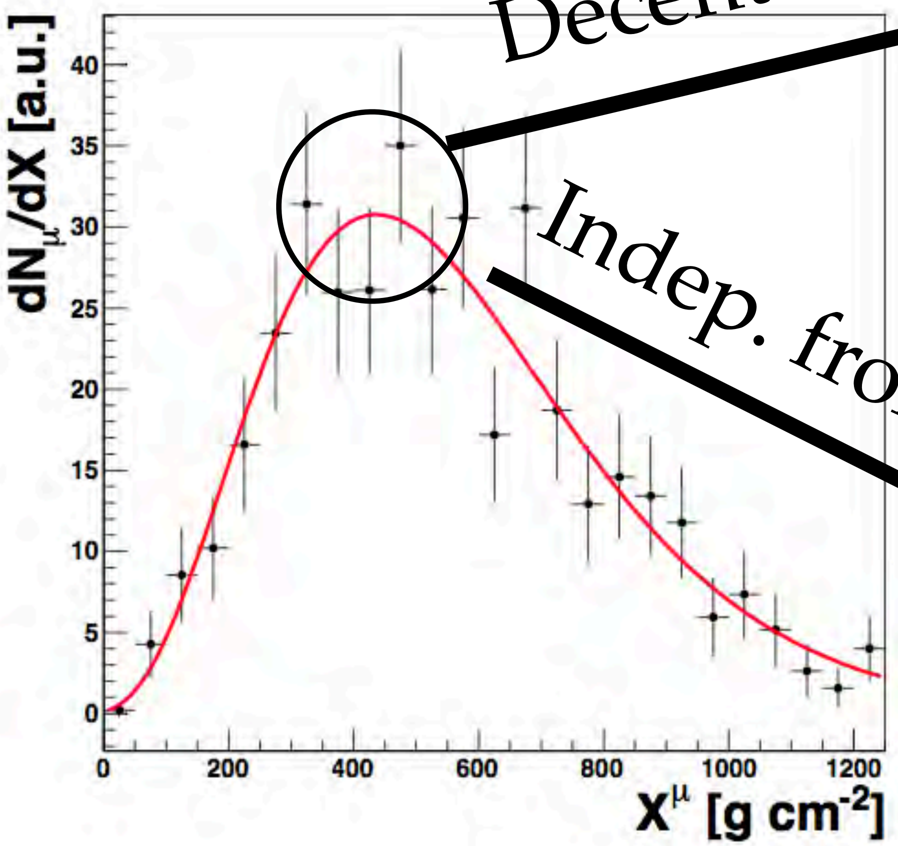

Indep. from X_{max} and higher E

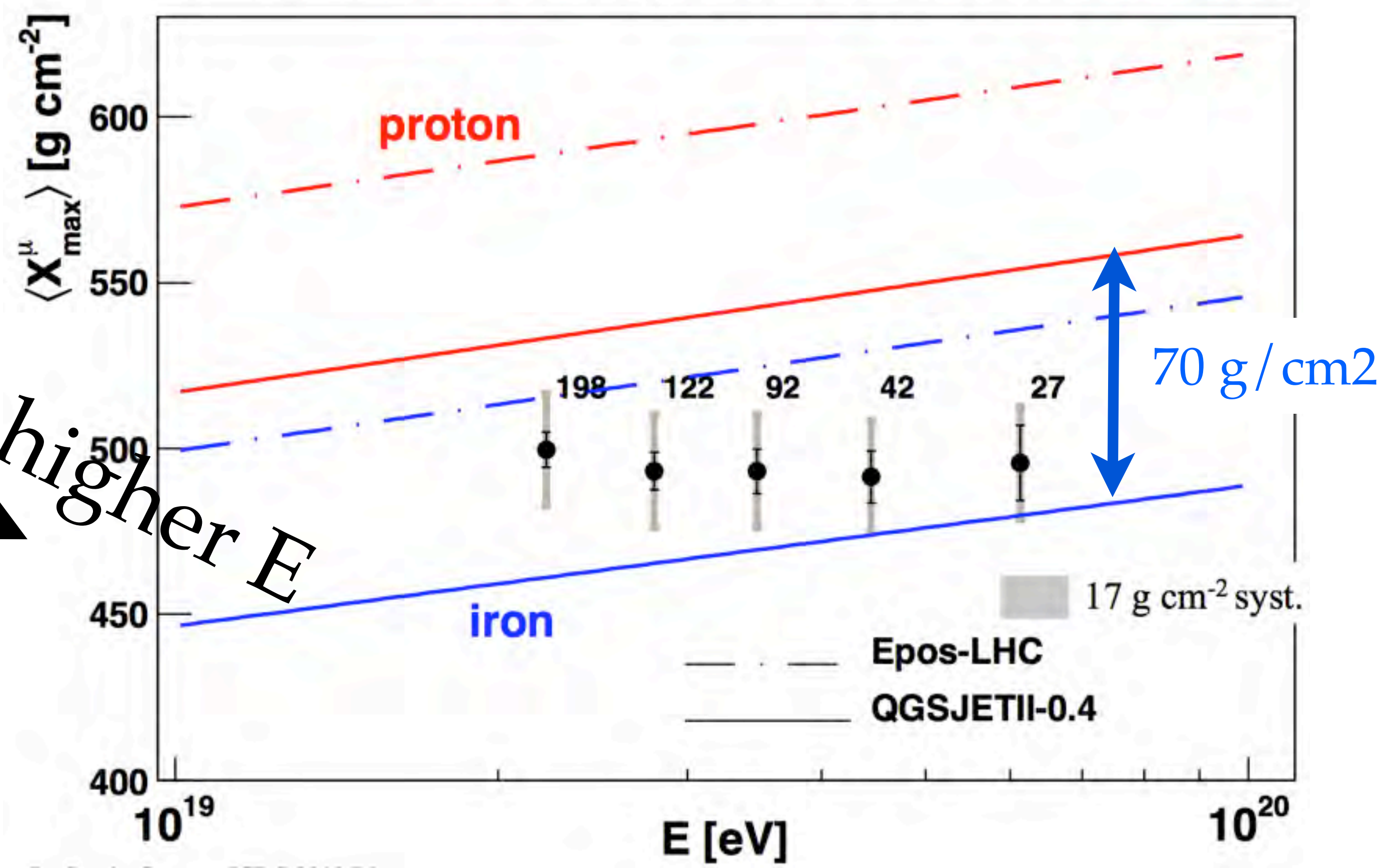

MASS COMPOSITION VII

<lnA> from MPD & <Xmax>

Different rapidity gap distributions

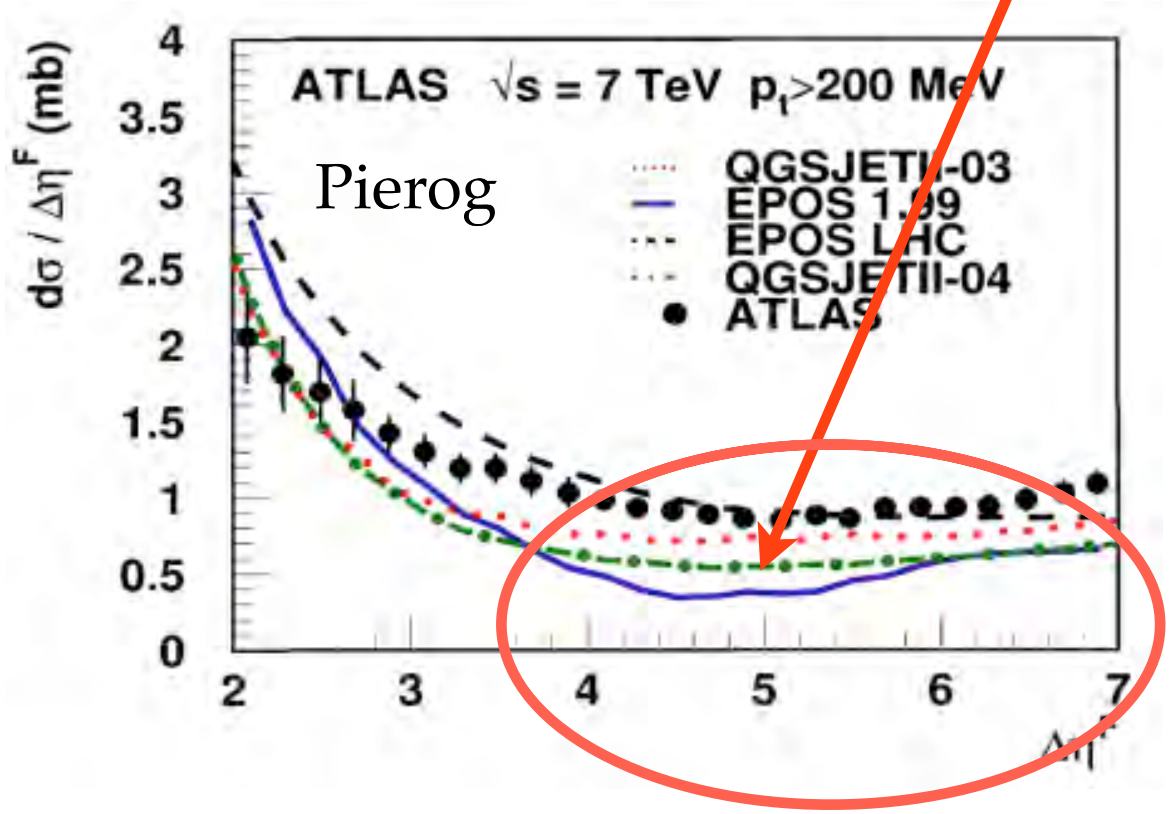

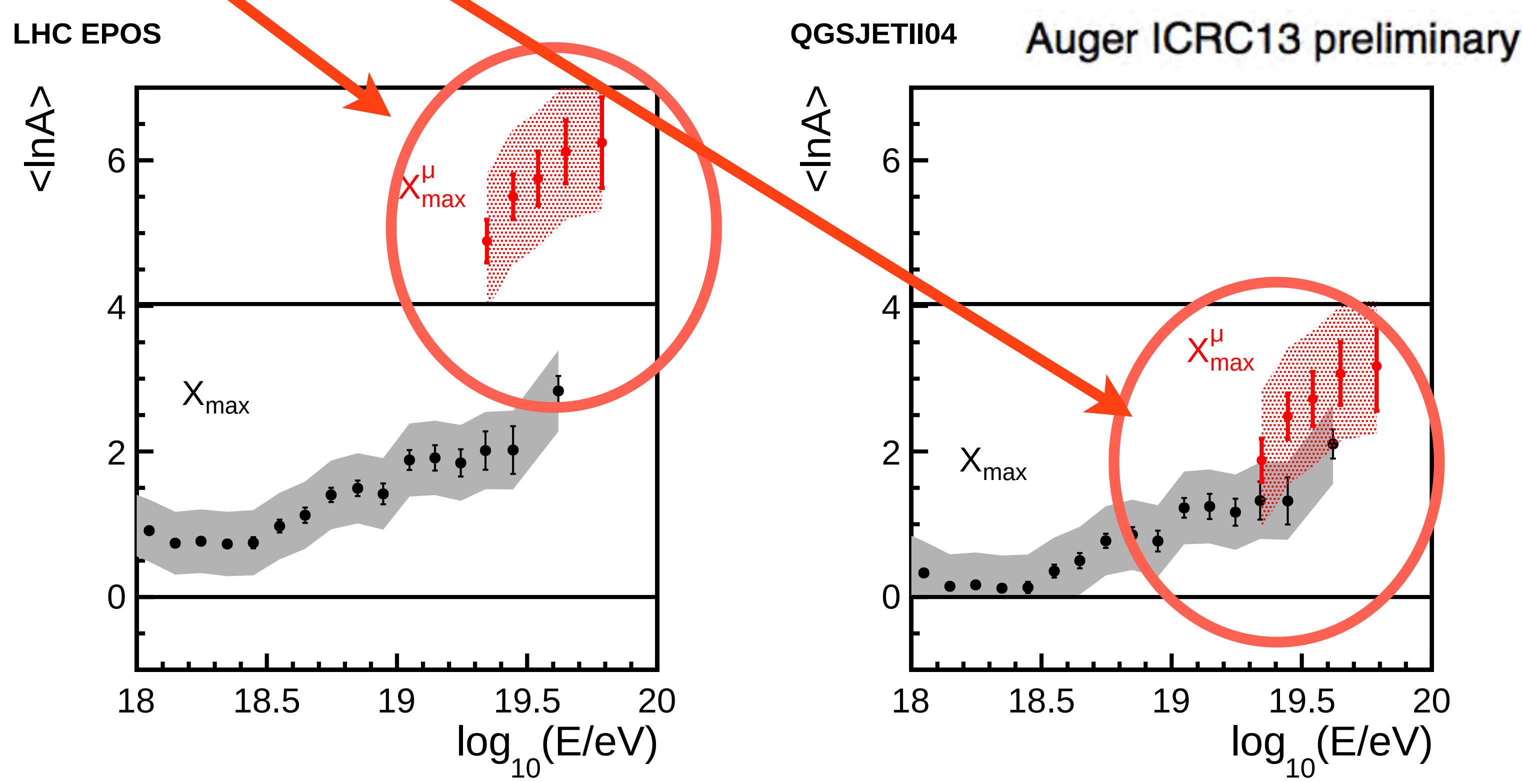

Summary and Conclusions

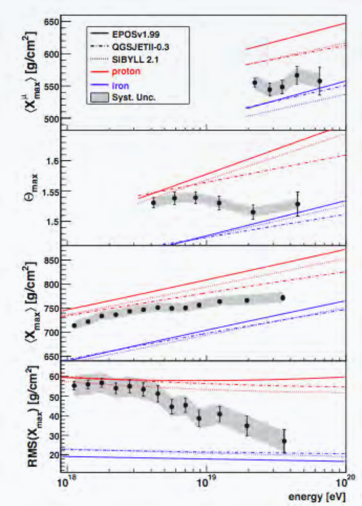

FD and SD

- X_{max} Results compatible with previous publications
- X_{max} distributions become narrower with increasing energy
- Direct FD composition measurements extended to higher energy by the SD measurements
- Direct and indirect independent composition variables

  yield compatible results with different systematics

Interpretation

- At low energy data is compatible with a significant fraction of protons
- Break on the elongation rate slope seems to indicate a change in composition towards a predominance of heavier nuclei at higher energies
- $< X_{max} >$ and RMS(X_{max}) show similar trends towards heavy-like showers at high energies, but exact values of several variables are difficult to explain with existing hadronic interaction models, for simple mass composition scenarios
- Results are model dependent. Any changes on the model

  predictions will affect our interpretation of primary mass

  composition

Old/New Hadronic Models Predictions

Tevatron $E = 10^{15}$eV

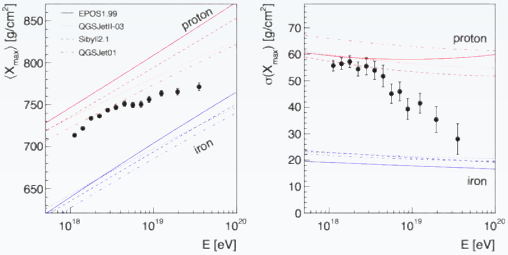

LHC $E = 10^{17}$eV